



저작자표시-비영리-변경금지 2.0 대한민국

이용자는 아래의 조건을 따르는 경우에 한하여 자유롭게

- 이 저작물을 복제, 배포, 전송, 전시, 공연 및 방송할 수 있습니다.

다음과 같은 조건을 따라야 합니다:



저작자표시. 귀하는 원저작자를 표시하여야 합니다.



비영리. 귀하는 이 저작물을 영리 목적으로 이용할 수 없습니다.



변경금지. 귀하는 이 저작물을 개작, 변형 또는 가공할 수 없습니다.

- 귀하는, 이 저작물의 재이용이나 배포의 경우, 이 저작물에 적용된 이용허락조건을 명확하게 나타내어야 합니다.
- 저작권자로부터 별도의 허가를 받으면 이러한 조건들은 적용되지 않습니다.

저작권법에 따른 이용자의 권리는 위의 내용에 의하여 영향을 받지 않습니다.

이것은 [이용허락규약\(Legal Code\)](#)을 이해하기 쉽게 요약한 것입니다.

[Disclaimer](#)

Doctoral Thesis

Carbon- and Binder- Free Cathode for Lithium
Oxygen Batteries

Sun Tai Kim

Department of Energy Engineering
(Battery Science and Technology)

Graduate School of UNIST

2016

Carbon- and Binder- Free Cathode for Lithium Oxygen Batteries

Sun Tai Kim

Department of Energy Engineering
(Battery Science and Technology)

Graduate School of UNIST

Carbon- and Binder- Free Cathode for Lithium Oxygen Batteries

A thesis/dissertation
submitted to the Graduate School of UNIST
in partial fulfillment of the
requirements for the degree of
Doctor of Philosophy

Sun Tai Kim

01. 13. 2016

Approved by



조재필

Advisor

Jaephil Cho

Carbon- and Binder- Free Cathode for Lithium Oxygen Batteries

Sun Tai Kim

This certifies that the thesis/dissertation of Sun Tai Kim is approved.

01. 13. 2016

signature
조재필

Advisor: Jaephil Cho

signature

Nam-Soon Choi

Nam-Soon Choi

signature

Youngsik Kim

Youngsik Kim

signature

Yoon Seok Jung

Yoon Seok Jung

signature

이태

Kyu Tae Lee

Contents

Abstract	i
List of Figures	iii
List of Tables	vii
Abbreviations	viii
1. Introduction	1
1.1. Energy Storage System	1
1.2. Lithium Ion Batteries	2
2. The Lithium Oxygen Batteries	3
2.1 ORR and OER	8
2.2 Review of catalysts for ORR and OER	15
2.3 The Zn-air battery	20
2.4 The Li-O ₂ battery	27
3. Experiment I	33
3.1 The Cell Setup	33

3.2 Optimization of Au nanoparticles-coated Ni nanowire substrate as a highly stable one bodied electrode for lithium-oxygen Batteries -----	36
3.2.1 Introduction -----	37
3.2.2 Experimental Section -----	39
3.2.3 Results and Discussion -----	41
3.2.4 Conclusion -----	66
4. Experiment II -----	67
4.1 A Possibility of Silver catalyst as a Carbon- and Binder-free Cathode material on Different Electrolytes for Lithium-oxygen Batteries -----	67
4.1.1 Introduction -----	68
4.1.2 Experimental Section -----	70
4.1.3 Results and Discussion -----	71
4.1.4 Conclusion -----	88
5. References -----	89
6. Acknowledgement -----	106

Abstract

Unstable oil prices and the effects of global warming have forced us to look for alternative energy storage and conversion systems. So battery industry especially lithium ion battery (LIB) have been developed so fast. A battery is usually made up of an anode on one side, a cathode on the other, and an electrolyte (and separator) in between. For a LIB, lithium ions move from the anode to the cathode through the electrolyte, creating a chemical reaction that allows electrons to be harvested along the way. And very recently portable electronic devices and electric vehicle (EV) have been developing at a rapid pace, and these progress demand much high energy and power density. So metal-air batteries have been shed light on due to their high energy density and extremely high power compared to those of other conventional batteries. A metal air battery is a battery that could use a metal — lithium, aluminum, iron, or zinc etc.— for the anode, air (technically oxygen) as the cathode and electrolyte. Many people have interests in the metal air batteries because oxygen is abundant in nature, free, and doesn't require a heavy casing to keep it inside a battery cell. Among metal-air batteries, metals such as Li, Al, Fe, and Zn, Zinc-air and Li-O₂ batteries in particular have potential for use as alternative energy storage devices. Although other metals like Al can show much high voltage and power, Zn has various advantages such as low cost, abundance, low equilibrium potential, environmental benignity. The theoretical specific energy density of Zn-air batteries is 1084 Wh · kg⁻¹. And Li-air (or Lithium Oxygen) battery; Although li metal is explosively reactive with water, the lithium Oxygen (Li-O₂) battery has attracted interest because of its extremely high theoretical energy density, 11,140 Wh · kg⁻¹ (excluding O₂) and power density is 3505 Wh · kg⁻¹, which is about eight times larger than that of conventional rechargeable lithium-ion batteries. The Zn-air and Li-O₂ battery, however, have many problems in the case of Zn air battery; ohmic loss, carbon dioxide absorption and zinc dendrite formation and in the case of Li-O₂ battery; a low current density, instability of nonaqueous electrolytes, and poor cycle ability etc. Moreover, carbon cathode can lead to the inevitable reactions between the discharge product Li₂O₂. In addition, several recent studies have reported about binders including PVDF which are necessary to make a carbon electrode also react with chemically generated LiO₂.

So in this PhD thesis, I studied on the problems of Li-O₂ battery. And the possibility of carbon- and binder free cathodes for the Li-O₂ battery has been studied.

Gold (Au) and Silver (Ag) nanoparticles coated Ni nanowire substrate were used as electrodes (Au/Ni, Ag/Ni electrode) for Li-O₂ battery. The Au/Ni electrode demonstrates improved capacity of ~ 600 mAh g⁻¹_{Au}. More importantly, it exhibited improved cyclability over 200 cycles at full discharge and charge condition between 2.3 V and 4.3 V. Meanwhile, since Ag is not electrochemically stable as much as Pt and Au at high voltages. It is needed to be found proper

electrolytes for Ag/Ni electrode. The stability and performance of different electrolyte solvents were investigated such as 1,2-dimethoxyethane (DME), diethylene glycol dimethyl ether (DEGDME), tetraethylene glycol dimethyl ether (TEGDME), dimethylformamide (DMA), dimethyl sulfoxide (DMSO) or N-methyl-2-pyrrolidone (NMP). It was found that the NMP based electrolyte exhibits superior electrochemical properties. The Ag/Ni electrode with NMP/1M LiTFSI delivers a capacity of $473 \text{ mAhg}^{-1}_{\text{Ag}}$ at $100 \text{ mA}^{-1}_{\text{Ag}}$ under between 2.3 V and 3.8 V and shows stable cycling performance until 35th with $300 \text{ mAhg}^{-1}_{\text{Ag}}$ cut off condition at $100 \text{ mA}^{-1}_{\text{Ag}}$.

List of figures

Figure 1-1. The past, present and future applications of Lithium-ion batteries according to power

Figure 2-1. Trends in oxygen reduction activity graphically plotted as a function of the oxygen binding energy.

Figure 2-2. A general Tafel plot an anodic process.

Figure 2-3. Volumetric and gravimetric energy density of many kinds of batteries.

Figure 2-4. Volumetric and gravimetric energy density of many kinds of batteries.

Figure 2-5. A schematic figure of reaction of Zn air battery.

Figure 2-6. Pictures of Zn air battery vehicle (LJB MANAGEMENT INC.) and military application (EMW Co.,Ltd.).

Figure 2-7. SEM image of different types of Zn. (a) Zn granule, (b) Zn powder, and (c) dendritic Zn.

Figure 2-8. The graph and table of theoretical and practical specific energy densities of many batteries.

Figure 2-9. The reaction way of Zn air and Li-O₂ battery. Zn air battery is one compartment cell meanwhile Li-O₂ battery is two compartment cell.

Figure 2-10. The four types of Li-O₂ batteries. (a) nonaqueous, (b) aqueous, (c) hybrid, and (d) solid state electrolyte type.

Figure 3-1. Schematic of the fabrication of Au nanoparticles deposited Ni nanowire substrate by electrodeposition method.

Figure 3-2. Preparation of Au/Ni Electrode and morphology of Au/Ni electrode with different Au quantity. (a) SEM image of AAO template, (b) SEM image of deposited Ni nanoparticles on AAO template by E-beam evaporator, (c) picture of 3 electrode electrodeposition homemade Teflon kit, (d) picture of Ni nanowire substrate, (d, f, g and h) SEM images of Ni nanowire substrate with different amounts of Au nanoparticles (d) 0.081 mg/cm^2 , (e) 0.4 mg/cm^2 (f) 1.8 mg/cm^2 , and (g) 4.5 mg/cm^2 .

Figure 3-3. Voltage profiles of (a) Ni plate electrode and (b) Ni nanowire substrate electrode. The dis/charge current at $2.5 \text{ mA g}^{-1}_{\text{Ni}}$. (c) Cyclic voltammogram of Ni nanowire substrate and Au/Ni electrode between $2.3 \text{ V} \sim 4.3 \text{ V}$ at a scan rate of 5 mV sec^{-1}

Figure 3-4. Cyclic voltammogram on voltage window between $2.3 \text{ V} \sim 4.3 \text{ V}$ during 1, 10, 25, and 50 cycles at 5 mV sec^{-1}

Figure 3-5. Electrochemical evaluation of Au/Ni electrode at discharge current of $500 \text{ mA g}^{-1}_{\text{Au}}$. Capacity were normalized by Au quantity. (All the cells were pre-conducted cyclic voltammogram using Ag/AgCl reference electrode between 2.3 and 4.3V for 50 cycles).

Figure 3-6. The morphology of Au/Ni electrode and EDX image. SEM images of the as-fabricated (a) Ni nanowire, (b) Au/Ni electrode, TEM images of (c) Ni nanowire, (d) Au/Ni electrode, and EDX images of (e) Ni, and (f) Au element, respectively.

Figure 3-7. SEM image of (a) front and (b) back sides of AAO membrane. The pore size of front and back sides are $\sim 20 \text{ nm}$ and $\sim 200 \text{ nm}$, respectively. Ni nanoparticle seeds are deposited on the front side and Ni nanowires grew through the back side of AAO membrane.

Figure 3-8. The EDX results of the Au/Ni electrode.

Figure 3-9. The morphology of nanoporous Au leaf. (a) SEM image of nanoporous Au leaf and (b) TEM image of nanoporous Au leaf.

Figure 3-10. Electrochemical evaluation of Au/Ni electrode and nanoporous Au leaf at different current. (a) voltage profiles of Au/Ni electrode at different currents of $300 \text{ mA g}^{-1}_{\text{Au}}$, $500 \text{ mA g}^{-1}_{\text{Au}}$

and $1000 \text{ mA g}^{-1}_{\text{Au}}$, (b) discharge capacity plot vs. cycle number of (a) with increasing current of $300 \text{ mA g}^{-1}_{\text{Au}}$ to $1000 \text{ mA g}^{-1}_{\text{Au}}$, (c) voltage profiles of nanoporous Au leaf at different currents of $300 \text{ mA g}^{-1}_{\text{Au}}$, $500 \text{ mA g}^{-1}_{\text{Au}}$ and $1000 \text{ mA g}^{-1}_{\text{Au}}$, and (d) discharge capacity plot vs. cycle number of (a) with increasing current of $300 \text{ mA g}^{-1}_{\text{Au}}$ to $1000 \text{ mA g}^{-1}_{\text{Au}}$

Figure 3-11. Capacity and cycle result of Au/Ni electrode at $500 \text{ mA g}^{-1}_{\text{Au}}$. (a) voltage profiles of Au/Ni electrode and (b) plot of discharge capacity vs. cycle number of (a).

Figure 3-12. XPS spectra of pristine, after 110th charged and discharged electrode. (a) Au 4f and (b) Ni 2p

Figure 3-13. SEM images of Au/Ni electrode (a) pristine, (b) after discharged 110th cycle and (c) after charged 110th cycle

Figure 3-14. XRD patterns of (a) pristine Au/Ni electrode, Li_2O_2 and the electrode after 1st discharge and charge, 110th discharge and 110th charge. (b) magnified peaks (a).

Figure 3-15. (a) Raman and (b) FT-IR spectra of Au/Ni electrode, Li_2O_2 , and Li_2CO_3 Both spectra, however, are too noisy to be assigned

Figure 3-16. XPS spectra of (a) Li 1s, (b) C 1s, and (c) O 1s. Pristine Au/Ni electrode, after 1st and 100th charge and discharge electrode. O 1s spectra of pristine sample at 531.7 eV are related with nickel oxide layer which is formed on nickel under normal conditions in air.

Figure 3-17. Morphology change of Li metal. (a) Fresh Li metal, (b) after 50th cycled Li, (c) after 110th cycled Li, and (d) cross sectional image of (c).

Figure 3-18. Capacity and cycle result of rebuilt cell. (a) voltage profiles of rebuilt cell, (b) cycle graph of (a), and (c) the summation cycle graph of the pristine and rebuilt cells. Figure 3S-1. SEM image and picture of Ni nanoparticles coated on the front side of AAO.

Figure 3-19. SEM image and picture of Ni nanoparticles coated on the front side of AAO.

Figure 3-20. SEM image and picture of Ni nanoparticles coated on the back side of AAO.

Figure 3-21. The blue print of a top part of homemade kit for electrodeposition. (Especially for

AAO template)

Figure 3-22. The blue print of a bottom part of homemade kit for electrodeposition. (Especially for AAO template)

Figure 3-23. The blue print of a cap part of homemade kit for electrodeposition. (Especially for AAO template)

Figure 3-24. The real picture of Ni nanowire current collector made by homemade electrodeposition kit.

Figure 4-1. The morphology of Ni nanowire substrate and Ag/Ni electrode and EDX image. SEM images of the as-fabricated (a) Ni nanowire, (b) Ag/Ni electrode, TEM images of (c) Ni nanowire substrate, (d) Ag/Ni electrode, and EDX images of (e) Ni, and (f) Ag element, respectively.

Figure 4-2. The first 2 cycles of voltage profiles using Ag/Ni electrode on different electrolytes at $100 \text{ mAg}^{-1}_{\text{Ag}}$. (a) Voltage profiles of Ether based electrolytes and (b) high donor number electrolytes.

Figure 4-3. SEM image of each Ag/Ni electrode and picture of each separator. (a) pristine Ag/Ni electrode, Ag/Ni electrode and picture of separator after 2 cycles in (b) DME, (c) DEGDME, (d) TEGDME, (e) DMF, (f) DMSO, and (g) NMP respectively.

Figure 4-4. XPS spectra of Ag/Ni electrodes after 2nd cycle. (a) Li, (b) C, (c) F, and (d) Ag.

Figure 4-5. XPS spectra of Ag/Ni electrodes after 2nd cycle.

Figure 4-6. XPS spectra of Ag/Ni electrodes after 2nd cycle.

Figure 4-7. ¹H-NMR spectra of Li metal in six electrolytes. (a) DME, (b) DEGDME, (c) TEGDME, (d) DMF, (e) DMSO, and (f) NMP respectively.

Figure 4-8. Capacity and cycle result of Ag/Ni electrode at $100 \text{ mAg}^{-1}_{\text{Ag}}$. (a) Voltage profiles of Ag/Ni electrode from 2.3 V to 3.8 V, (b) capacity cut off voltage profiles of Ag/Ni electrode with $300 \text{ mAhg}^{-1}_{\text{Ag}}$, and (c) plot of discharge capacity vs. cycle number of (b).

Figure 4-9. SEM images of Ag/Ni electrode (a) pristine, (b) after 6th cycle with full dis/charge condition from 2.3 V to 3.8 V and (c) after 36th cycle with 300 mAhg⁻¹_{Ag} capacity cut off condition.

Figure 4-10. The scheme of reactions for the decomposition of DMSO solvent.

List of tables

Table 1-1. The current employed lithium-ion batteries to the some EV.

Table 2-1. Thermodynamic electrode potentials of electrochemical O₂ reductions.

A, B: The thermodynamic potentials for the 1-electron reduction reaction to form a superoxide, and its further reduction to O₂²⁻, are not listed in here. Because the values are strongly dependent on the solvents.

Table 2-2. ORR exchange current densities on various electrode materials at different conditions.

Table 2-3. Discharge voltage and discharge capacities of 1st cycle with many different catalysts.

Table 3-1. Recent results of non-carbon based cathodes for Li-O₂ battery.

Table 4-1. The specific capacity of each electrolyte.

Table 4-2. The structure, donor number, dielectric constant values of each electrolyte

Abbreviations

AAO	Anodic aluminum oxide
CV	Cyclic Voltammetry.
DEGDME	Diethylene glycol dimethyl ether
DME	Dimethoxyethane
DMF	Dimethylformamide
DMSO	Dimethyl sulfoxide
ICP	Inductively coupled plasma
NMP	N-methyl-2-pyrrolidone
ORR	Oxygen reduction reaction
OER	Oxygen reduction reaction
SEM	Scanning Electron Microscopy
TEM	Transmission Electron Microscopy
TEGDME	Tetraethylene glycol dimethyl ether
XPS	X-ray Photoelectron Spectroscopy
XRD	X-ray diffraction analysis

1. Introduction

1.1 Energy Storage

The demands of developing renewable and new energy storage materials to reduce fossil fuel consumption has been continuously increasing during several decades. In 1990's, global warming was one of the most important issues. In 2000's, reducing CO₂ gas emission was also one of the chief concerns to protect the earth's ozone layer and minimize global warming. And it is believed that both issues (global warming and CO₂ gas emission) are closely related with fossil fuel combustion. So many people have struggled to invest renewable energies and new energy storage systems for replacing fossil fuels. Another critical factor of demands for the renewable and new energy devices is the instability of oil prices. The demand of crude oil for United States had grown an average of 1.76% per year from 1994 to 2006, with a high of 3.4% in from 2003 to 2004. World demand for oil is projected to increase 37% over 2006 by 2030.¹ And the oil demand is possibly divided by four broad sectors: 1. transportation, 2. residential, 3. commercial, and 4. industrial. And a large part to increases in demand from the transportation sector in recent decades. Therefore, to overcome the global warming and oil crisis, considering the issues coming from this huge consumption of fossil fuels and further developments are required for a future power. In such a development, advanced energy storage technologies such as wind, solar and hydro power have been developed. However, such power generation technologies need a power storage technologies so that energy storage system play a key role in the realization of the future power source. It is believed that the most efficient energy storage and the most realistic solution is the batteries. Among these various energy storage systems, batteries have many advantages compared to other storage systems such as pumped hydroelectric and compressed air energy storage (CAES) described below. Basically batteries does not have any limitations of geographical consideration and the size of batteries can be flexibly designed on the different applications. So we can use a different battery to a right objective application. A battery or an electrochemical cell is basically made of electrodes (Anode and Cathode) and electrolyte (since galvanic cell doesn't need a separator so it is not counted in here), which converts chemical energy into electrical energy. Many people believed that the first battery technology is attributed to the development in 1800 by Alessandro Volta of the voltaic pile.² Since then, hundreds of different chemical reactions have been utilized and thousands of different types of batteries have been commercialized including the development of lithium ion batteries in 1990s.³ And now, Li-ion batteries have become a very important technologies. Basically the Li-ion batteries show great possibilities as power sources that can lead us to the new era. Since lithium-ion batteries are featured by high energy density, high power density and long service life compared with other commonly used batteries and thus have wide application to many electronics. A battery works by directly converting chemical

energy to electrical energy by employing different chemical reactions. The many different combinations of anode, cathode and electrolyte materials to produce different cell chemical reactions thereby produces numerous types of batteries from the lead-acid, Li-ion to Li-S and metal air batteries.⁴ the LIBs have been used the most common type of batteries to portable electronic devices due to its excellent cycle ability and its relatively high energy density.⁵ And as people need a more powerful and much larger capacity battery as the development of new materials for Li-ion batteries have mainly focused on increasing a specific capacity and decreasing an overpotential during charge process.⁶

1.2 Lithium Ion Batteries

Li-ion batteries (LIBs) have been most widely used to many industries such as mobile devices like a smart watch, cell phone, a lap top computer, and at the present LIBs are growing in popularity for electric vehicle (EV), military equipment and even aerospace applications shown in Figure 1-1.

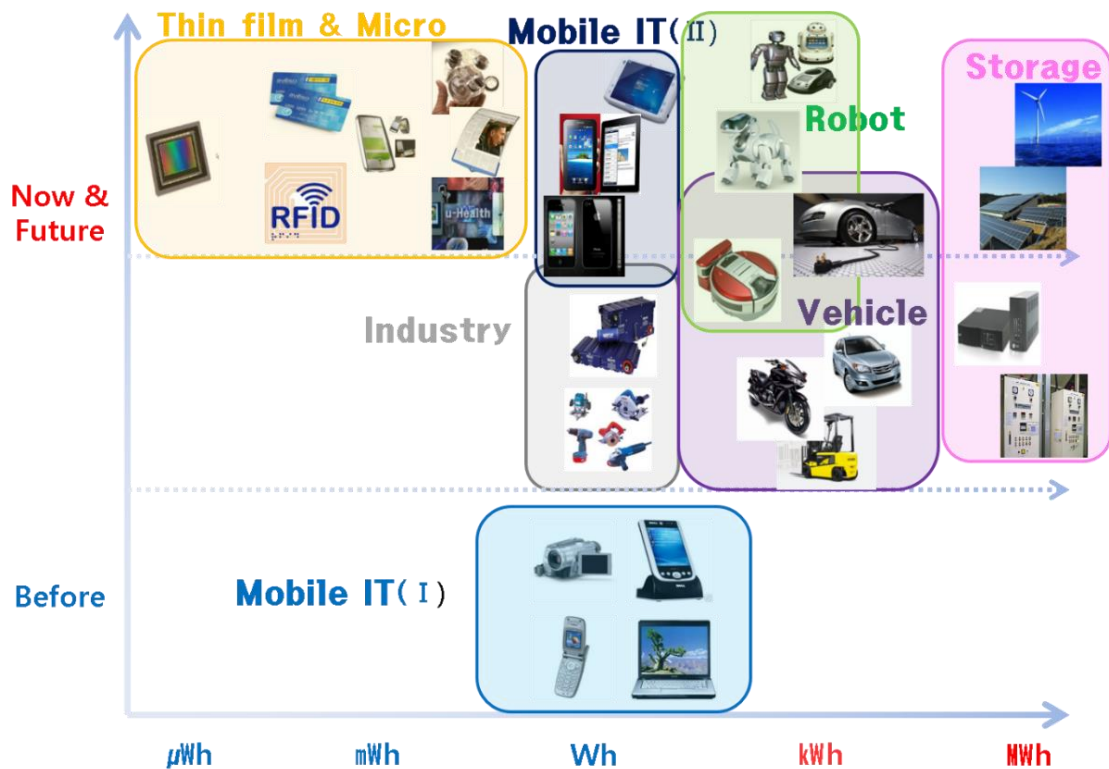
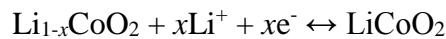


Figure 1-1. The past, present and future applications of Lithium-ion batteries according to power

They are one of the most popular types of rechargeable batteries because of a high energy density, small memory effect.⁷ (Batteries gradually lose their maximum energy capacity if they are repeatedly recharged after being only partially discharged. The battery appears to "memory" the smaller capacity).⁸ This battery system uses Li transitional metal oxides (usually LiCoO₂) as the cathodes, carbons as the anodes (usually graphite), and non-aqueous carbonated liquids as the electrolytes. The overall reactions are as following

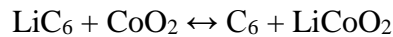
Positive electrode:



Negative electrode:



Overall reaction:



The lithium ions flow through the electrolyte whereas the electrons generated from the reaction, $\text{Li} = \text{Li}^+ + e^-$, go through the external circuit to make the electricity and this chemical reactions are reversible. Thus, the electrode system must allow for the flow of both lithium ions and electrons. That is, each electrode material (of course including a high capacity) and electrolyte must have a good ionic conductivity and an electronic conductivity. Briefly introduce the each part of LIBs.

Cathode.

Conventionally, advanced cathode materials are lithium metal oxides, such as, LiMn₂O₄, LiNi_xMn_yCo_(1-x-y)O₂ (Spinel structure), LiCoO₂, LiNiO₂, (Layered structure) and, LiFePO₄ (olivine structure). Among them, layered materials exhibit high permanence in the range of high voltage, however due to the high cost of cobalt and its toxicity to human body. Consequently, combinations of cobalt, manganese, and nickel are frequently favored. Olivine is nontoxic and shows thermal stability without a large capacity fading. However, its poor conductivity is a problem so that many coating methods have been applied to improve the low conductivity, but it leads cost increasing of the battery.⁹

Anode.

Anode materials are lithium metal, lithium-alloying materials, graphite, and silicon etc.¹⁰

Since the birth of lithium ion battery in the end of 1980s and early 1990s many kinds of anode materials have been studied. Lithium seems to be the most proper and stable anode, however it demonstrates drawbacks with cycleability and lithium dendrite formation that leads to short circuit problem.³ Alloy anodes exhibit high-energy capacity and safety characteristics. However, it shows low cycle life and high initial capacity loss. And in the case of silicon, although it has got a great interest for use as the anode material for lithium-ion batteries due to its high capacity, it still has many problems such as a large volume expansion during the lithiation process and the low diffusion rate of lithium in silicon so that fast capacity degradation occur especially at high current rate.¹¹ Meanwhile carbon material is the most widely used anode material despite its relatively low theoretical capacity ($\sim 370 \text{ mAh g}^{-1}$) compared to the other materials such as lithium metal ($\sim 3,860 \text{ mAh g}^{-1}$) and silicon ($\sim 3,500 \text{ mAh g}^{-1}$).¹² Because carbon material is cheap and huge abundance in Earth. As a result, it has been focused on the modification of carbon anode materials including research on mild oxidation of graphite, formation of composites with metals and metal oxides, coating by polymers and other kinds of carbons, and carbon nanotubes.¹³

Separators.

The separators are also one of the critical components in batteries, and are placed between the positive electrode and the negative electrode to prevent physical contact of the both electrodes and it enable ion transport and simultaneously isolate electron flow. It must be stable towards the electrolyte and electrode materials chemically and electrochemically, and should have mechanically high tension to withstand the unexpected reactions such as volume expansion and metallic dendrite formation during the battery operation. Structurally, the separator should have sufficient porosity to absorb electrolyte for the high ionic conductivity.¹⁴ Therefore, selection of a proper separator is critical to the battery performance, including energy density, power density, cycle life and safety. For better battery performances, the separator is more favored to be thinner and more porous and for battery safety, the separator should be able to shut the battery down when the battery is overheated, such as the short circuit, so that thermal runaway can be avoided. The shutdown function can be obtained through a multilayer design of the separators, in which at least one layer melts to close the pores below the thermal runaway temperature and the other layer provides mechanical strength to prevent physical contact of the electrodes.¹⁵ The separators of LIBs can be broadly divided by three types: (1) polymer type, (2) inorganic type, and lastly (3) non-woven fabric type.¹⁶ Generally the properties of polymer separators are characterized by their thickness, porosity, and thermal stability (in other words thermal shutdown properties). The nonwoven fabric separators have been well known to its high porosity and a low cost, meanwhile the polymer composite separators have excellent wettability and thermal stability. Among

numerous battery separators, the ceramic based separators have especially been interested because of its improved thermal stability and thermal shutdown property so the safety of LIBs is quite being enhanced by using it.¹⁷ The former separators consists of either a polyethylene–polypropylene multilayer structure or a blended polyethylene – polypropylene which increases safety by allowing meltdown of the polyethylene to close the pathways for ionic conduction at a temperature higher than that at which thermal runaway occurs. Whereas the latter comprises nano-size ceramic materials coated on both sides of a flexible and highly porous non-woven matrix which enhances the safety by retaining extremely stable dimensions even at high temperatures to prevent each electrode from contacting to each other.

Electrolytes

The electrolyte, which commonly refers to a solution comprising the solvents and salts, regarded as the third key component counted after cathode and anode. Although the role of electrolyte is often thought an insignificant thing but actually the choice of electrolyte is really critical. A safe and stable lithium ion battery requires a large range of voltage window.¹⁸ It is possible that the electrochemical stability window of electroactive materials is widened by the appropriate electrolytes. In addition, if there is “extremely” high power cathode material which working with a highly oxidizing potential ($> 5 \text{ V vs. Li/Li}^+$), it should be required a proper electrolyte which operate over their thermodynamic stability window. There are numerous liquid solvents available, each with different dielectric constants and viscosity so that we should select a specific solvent to consider the ionic conductivity of the electrolyte.¹⁹

The Li-ion battery system have many advantages such as it can operate relatively high voltage at $\sim 3.7 \text{ V}$ with exhibiting high specific energy densities of $\sim 150 \text{ Wh} \cdot \text{kg}^{-1}$ and $\sim 400 \text{ Wh} \cdot \text{l}^{-1}$,²⁰ exhibit a low self-discharge of below 8% per month, show a long cycle-life of greater than 1000 cycles, and wide operation temperature ranges ($-20 \sim 60 \text{ }^\circ\text{C}$ for charge / $-40 \sim 65 \text{ }^\circ\text{C}$ for discharge). So based on these advantages, many kinds of lithium-ion batteries are employed in electric vehicle (EV). Further development of Li-ion batteries focusses on increasing the specific energy (gravimetric and volumetric energy density) and to fulfill the increased consumer demands especially for electric vehicles. The most widely used as the cathode electrode materials of the power battery could be Spinel-based lithium-ion; normally LiMn_2O_4 (LMO), Lithium Iron Phosphate (LFP), Nickel Cobalt Manganese (NCM), Nickel Cobalt Aluminum (NCA), and as the anode materials usually are carbon and now the Lithium Titanium Oxide (LTO) to improve the battery durability and performance of fast charging.⁶ Some of the current EV and the employed batteries are listed in **Table 1-1**.

Vehicle	Battery supplier	Positive electrode	Negative electrode
Nissan Leaf EV	Automotive Energy Supply (Nissan NEC JV)	LMO	Carbon
Honda Fit EV	Toshiba Corporation	NCM	LTO
Chevrolet Volt	Compact Power (subsidiary of LG Chem)	LMO	Carbon
Renault Fluence	Automotive Energy Supply (Nissan NEC JV)	LMO	Carbon
Tesla Model S	Panasonic Energy	NCA	Carbon

Table 1-1. The current employed lithium-ion batteries to the some EV.⁶

However, the Li-ion battery for use in huge energy storage applications is limited by its high cost ($> \$1,000/\text{kWh}$) and as electric vehicles (EVs) are becoming more popular and more, LIBs show some limitations. For examples, 1. LIBs require protection circuit to maintain voltage and current within safe limits. 2. They also subjects to aging, even if not in use - storage in a cool place at 40% charge reduces the aging effect. 3. Transportation restrictions - shipment of larger quantities may be subject to regulatory control. 4. Expensive to manufacture - about 40 percent higher in cost than nickel-cadmium. 5. Not fully mature - metals and chemicals are changing on a continuing basis. In addition, LIBs for vehicles should have high capacity and large serial-parallel numbers, which, coupled with such problems as high cost, safety, durability (low temperature tolerance, the protective system for cell degradation, thermal runaway from electrolyte decomposition), and uniformity of cells. Among many problems, the biggest limitation of LIBs for the vehicle, is the safety control of battery.²¹ So, lithium-polymer batteries (LPBs) had been thought as an alternative thing because of its relatively improved safety than that of Li-ion battery due to the gelled electrolytes - more resistant to overcharge; less chance for electrolyte leakage. However, LPBs also have some limitations such as expensive to manufacture, lower energy density and decreased cycle count compared to lithium-ion, and higher cost-to-energy ratio than LIBs. Therefore, there are foreseen limits of LIBs technology. That will limit everything from driving range to how much we can decrease the package size, and the latter an important consideration when designing batteries for passenger cars. That is why some motor companies are researching next generation battery chemistries, such as zinc-air and lithium-air. As the improved performances are needed such as high acceleration rate and long driving distance from a single charging, as researchers focused on the post LIBs. That is also why IBM have focused into battery research especially lithium air battery. Lithium-air and zinc-air batteries generate

power by exposing metal and an electrolyte to oxygen, oxidizing the metal and releasing energy. Theoretically, lithium-air batteries could provide “at least” about 10 times the energy density - the amount of energy stored per kilogram – The current lithium ion batteries can exhibit roughly 200 kilowatts per kilogram.

2. The Lithium Oxygen Batteries

2.1 ORR and OER.

ORR.

Oxygen (O_2) is the one of the most important and abundant elements in the Earth. The oxygen reduction reaction (ORR) and oxygen evolution reaction (OER) are also the most important reactions in energy converting systems such as fuel cells, Zn-air cells and Li- O_2 cells. ORR in aqueous solutions occurs mainly by two pathways. One is the direct 4-electron pathway from O_2 to H_2O , and the other is 2-electron reduction pathway from O_2 to hydrogen peroxide (H_2O_2). In non-aqueous aprotic solvents, the 1-electron reduction pathway from O_2 to superoxide (O_2^-) can also occur.

ORR occurs at the cathode. And normally, the ORR kinetics is very sluggish. Thus researches have been focused on how to make the ORR kinetics fast to reach a practical usable level in a fuel cell or metal-air batteries. And many catalysts for a cathode to speed up the ORR have been studied such as Pt and Pt–Ru alloys.²² At the current stage in technology, platinum (Pt)-based materials are the most practical catalysts.²³ However, Pt or Pt-based alloy catalysts are too expensive for making commercially available air electrodes, extensive research over the past several decades has focused on developing alternative catalysts. These electrocatalysts include, carbon materials, and derivatives, transition metal compounds, non-noble metal catalysts and metal oxide catalysts such as MnO_2 , Co_3O_4 , La_2O_3 , $LaNiO_3$, $NiCo_2O_4$, $LaMnO_3$, $LaNiO_3$ etc.²⁴

Table 2-1 lists several typical ORR processes with their corresponding thermodynamic electrode potentials at standard conditions. The mechanism of the electrochemical O_2 reduction reaction is very complicated and involves many intermediates. And the reactions primarily depends on the natures of the catalyst materials, and electrolytes.

Electrolyte	ORR reactions	Thermodynamic electrode potential at standard conditions, V
Non-aqueous aprotic solvents	$O_2 + e^- \rightarrow O_2^-$ $O_2^- + e^- \rightarrow O_2^{2-}$	A B
Alkaline aqueous solution	$O_2 + H_2O + 4e^- \rightarrow 4OH^-$ $O_2 + H_2O + 2e^- \rightarrow HO_2^- + OH^-$ $HO_2^- + H_2O + 2e^- \rightarrow 3OH^-$	0.401 -0.065 0.867
Acidic aqueous solution	$O_2 + 4H^+ + 4e^- \rightarrow H^2O$ $O^2 + 2H^+ + 2e^- \rightarrow H^2O^2$ $H_2O_2 + 2H^+ + 2e^- \rightarrow 2H_2O$	1.229 0.70 1.76

Table 2-1. Thermodynamic electrode potentials of electrochemical O_2 reductions.²⁵

A, B: The thermodynamic potentials for the 1-electron reduction reaction to form a superoxide, and its further reduction to O_2^{2-} , are not listed in here. Because the values are strongly dependent on the solvents.

It is desirable to have the O_2 reduction reaction occurring at potentials as close as possible to the reversible electrode potential (thermodynamic electrode potential) with a satisfactory reaction rate. The current-overpotential is given in below Equation

$$I_c = i_{O_2}^o \left(e^{\frac{n_{ao}\alpha_o F \eta_c}{RT}} - e^{-\frac{n_{ao}(1-\alpha_o) F \eta_c}{RT}} \right)$$

where I_c is the oxygen reduction reaction current density, $i_{O_2}^o$ is the exchange current density, n_{ao} is the number of electrons transferred in the rate determining step, α_o is the transfer coefficient, η_c is the overpotential of ORR, F is the Faraday constant, R is the gas constant, and T is the temperature in Kelvin. To obtain high current at low overpotential, the exchange current density $i_{O_2}^o$ should be large and/or $\frac{RT}{\alpha_o n_{ao} F}$ should be small.²⁶

The exchange current density of an electrochemical reaction depends on the reaction and on the electrode surface where the electrochemical reaction occurs. For example, on a Pt electrode, the exchange current density of hydrogen oxidation is several orders larger than that of ORR. The O₂ reduction reaction shows a higher exchange current density on a Pt electrode than on an Au electrode. Therefore, electrode materials or catalysts have a strong effect on ORR kinetics. Different materials can give different exchange current densities. **Table 2-2** shows the ORR exchange current densities on various electrode materials.

Electrode material /catalyst	ORR exchange current density, A.cm⁻²	Electron transfer coefficient	Electron transfer number. in rate determining step	Measurement conditions
Pt	2.8 x 10⁻⁷	0.48	-	Pt/Nafion interface at 30 °C
PtO/Pt	1.7 x10⁻¹⁰	0.46	-	Pt/Nafion interface at 30 °C
FePc	1.3 x 10⁻⁷	-	-	In 0.5 M H₂SO₄ at 60 °C
PtFe/C	2.15	0.55	1	In 0.5 M H₂SO₄ at 25 °C
PtW₂C/C	4.7	0.45	2	In 0.5 M H₂SO₄ at 25 °C
Ru_xSe_y	2.22	0.52	1	In 0.5 M H₂SO₄ at 25 qC

Table 2-2. ORR exchange current densities on various electrode materials at different conditions.²⁷

Oxygen reduction reaction on other metals such as Au, Ir, Pd, Ag, Co, etc. has also been investigated.²⁸ However, these metals show lower ORR catalytic activity than that of Pt. Additionally, they are not electrochemically stable as much as Pt (therefore they are more easily oxidized than Pt). **Figure 2-1** shows the volcano plots which graphically show the Sabatier principle which states the interactions between the catalyst and the substrate. In the figure, for the x-axis, the heat of formation of the metal formate salt and for the y-axis, the temperature at which the reaction reaches a specific rate was used. At low values of ΔH_f , the reactions are slow (higher temperature required) because the rate of adsorption is slow. At high values of ΔH_f , desorption become the rate-limiting step. The maximum rate, observed for the platinum group metals in this case, requires intermediate values of ΔH_f , with the rate being a combination of the rate of adsorption and the rate of desorption.²⁹

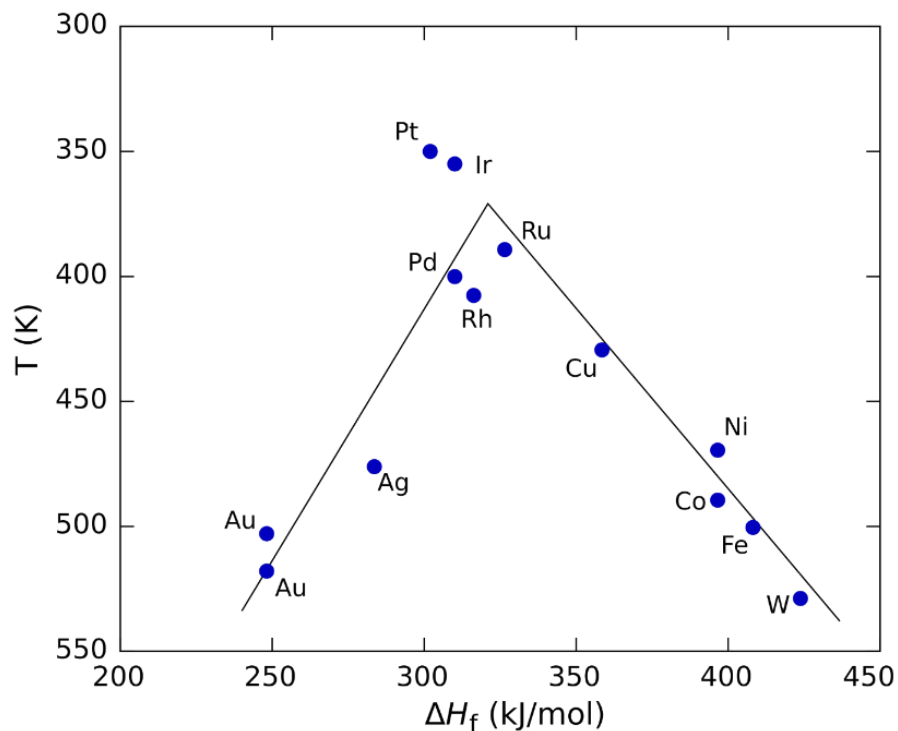


Figure 2-1. Trends in oxygen reduction activity graphically plotted as a function of the oxygen binding energy. (This figure is taken from wikipedia)

OER

The oxygen evolution reaction (OER) is also the most common and most important anodic process in electrolysis in various aqueous solutions. Although, the OER has been described as early as 1789, which detailed molecular insight into the relationship between catalyst surface

structure and OER reactivity has remained scarce. It has been reported that nickel and noble metals are regarded as the best anode materials in alkaline and acid solutions, respectively. The oxide layer is always formed at the surface in the potential region at which oxygen evolves, even if an inert metal electrode is used as the anode. Therefore, the oxide formed on the metal substrate always affects the reaction mechanism and electrocatalysis for the OER. It is generally believed in the use of an oxide anode, that the oxide is more stable than metal, since an oxide cannot be easily further oxidized.

In industrial electrochemical processes such as the water electrolysis for hydrogen production and metal electrowinning processes, etc., a stable anode material with low overvoltage in the OER is usually desirable. The main requisites of OER catalysts are normally high surface area, high electrical conductivity, good electrocatalytic behavior, minimization of the gas bubble problem, low cost, and safety. Among them, the electrocatalytic performance (or reactivity) is the most essential and most critical for the electrode reaction, and directly influences the overpotential of the OER. Therefore, a lot of fundamental and technological research about this property of the oxides has been studied.³⁰ The mechanism of the OER is quite complex than those of the hydrogen and chlorine evolution reactions, because many complex intermediate states exist in the oxygen evolution reaction steps. This means that there are many kinds of activation steps controlling the rate of the OER. A number of the OER mechanisms has been reported and discussed. And in all cases, the OER mechanisms have been usually deduced from the values of the observed Tafel slopes and of the reaction order under the assumption of Langmuir or Temkin conditions of adsorption.

-The Tafel equation is an equation in electrochemical kinetics relating the rate of an electrochemical reaction to the overpotential shown in Figure 2-2. The Tafel equation was first deduced experimentally and was later shown to have a theoretical justification. The equation is named after Swiss chemist Julius Tafel. The exchange current is at equilibrium, the exchange current density is the rate of reaction at the reversible potential. At the reversible potential, the reaction is in equilibrium meaning that the forward and reverse reactions progress at the same rates. This rate is the exchange current density.-

However, it is very difficult to deduce and justify the validity of the mechanism of the OER from the Tafel relation, especially regarding the potential distribution in the interface between the electrode and the electrolyte.^{30b} Thus, the discussion of the electrocatalysis of the mechanism which is deduced Tafel may be meaningless. However, the Tafel slope is still importantly related to the mechanism, and the adsorbed intermediates.³¹

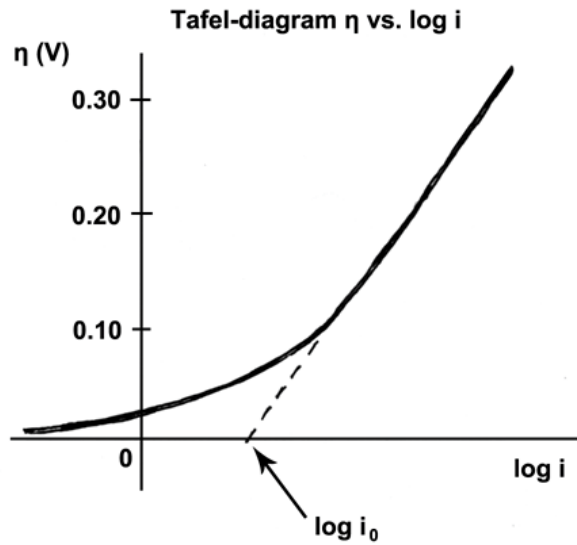


Figure 2-2. A general Tafel plot an anodic process. (This figure is taken from wikipedia)

On a single electrode the Tafel equation can be stated as,

$$\Delta V = A \times \ln \left(\frac{i}{i_0} \right)$$

Where,

- ✓ ΔV is the overpotential, V (note that the graph uses η for this quantity)
- ✓ A is the Tafel slope, V
- ✓ i is the current density, A/m² and
- ✓ i_0 is the exchange current density, A/m².

The Tafel equation can be also written as:

$$i = nFk \exp \left(\pm \alpha F \frac{\Delta V}{RT} \right)$$

Where,

- ✓ the + sign under the exponent refers to an anodic reaction, and a - sign to a cathodic reaction,
- ✓ k is the rate constant for the electrode reaction,
- ✓ R is the universal gas constant,
- ✓ F is the Faraday constant.

2.2 Review of catalysts for ORR and OER.

Like other battery technologies, Li–O₂ batteries also suffer from a series of scientific and technological problems such as low utilization efficiency and dendrite formation of the anode, electrolytes and salt decomposition, and sluggish kinetics of the cathode resulting in limited cell performance. To improve the cell performance, for the anode, normally Li metal is directly used as an anode so that the researches have not been focused on the anode. For the electrolytes which also critically affect the cell performances, many electrolytes which are strong to the O₂ radical, have large voltage window, low volatility, high oxygen solubility and robust during the cycling have been investigated.³² For the cathode, the main obstacles are the intrinsic slow reactions which are related with high overpotentials during the cycling. Thus in order to lower the overpotentials, numerous catalysts for ORR and OER have been investigated. Developing active, inexpensive catalysts is the always critical issue to many battery fields. It is necessary to find non-precious metal catalyst materials to replace currently widely used Pt-based catalysts. Several important kinds of precious metal catalysts with carbon supported or carbon free, transition metal oxide catalysts are briefly reviewed including nitrogen-doped catalysts in this thesis.

Precious metals and alloys.

In the Li-O₂ system, the ORR at cathode plays a key role in controlling the performance of cell, and efficient ORR electrocatalysts are essential for practical applications of the Li-O₂ battery. Thus many electrocatalysts have been intensively investigated. And the precious metal electrocatalysts also have been applied to the Li-O₂ battery. In Li-O₂ system, the O-O bond must be broken during oxygen reduction and reformed during oxygen evolution. These bond-breaking and bond-linking reactions may affect a considerable increasing and decreasing overpotential related to the ORR and OER in nonaqueous systems. It is reported that the most powerful ORR/OER catalysts are noble metals such as Pt and Au,³³ and bifunctional Pt/Au catalysts in mixed PC/ether electrolytes.³⁴ It is well known that the most effective ORR catalysts are those based on platinum (Pt) but Pt has only moderate activity for the OER in fuel cell and Zn-air cell field. However, Shao-Horn group reported interesting result that Au/C is more effective ORR catalyst in comparison to a Pt/C, and Pt/C is more effective OER catalyst for Li–O₂ cells.^{33c, 34} Interestingly, the next year, Bryan D. McCloskey also reported that Pt/C showed almost same ORR performance and exhibit better OER performance compared with Au.³⁵ I could infer based on above researches that of course the nature of the catalyst is a key factor controlling the performance of the oxygen electrode, especially the capacity, which is the primary reason for interest in the O₂ electrode, however, more importantly the cell performance and electrochemical behavior of electroactive materials can be changed or can be affected by different electrolytes.

Ruthenium (Ru) and iridium (Ir) are well known as the best OER catalysts, but they are not as active as Pt for ORR. Although, alloys of these compounds have shown a better bifunctional-catalytic performance, the development of bifunctional catalysts still represents a big challenge and the best catalytic materials are still precious metals.

Transition metal oxides

The transition-metal oxides have attracted extensive attention as alternative catalysts of precious metal catalysts in many fields such as fuel cell and metal air cell over the several decades,³⁶ due to its relatively high catalytic activity and low cost compared to precious metals and environmental friendliness. Various transition metal oxide catalysts have been examined for ORR and OER, including Co_3O_4 , MnO_2 , MnCo_2O_4 , NiCo_2O_4 , and nanowire $\alpha\text{-MnO}_2$.³⁷ They are usually supported with carbon materials, such as carbon black, ketjen black, and graphene, to improve the electrocatalyst activities for ORR/OER and to increase capacity in aqueous solutions and organic electrolytes. Among them, Co_3O_4 , Mn_3O_4 , and MnCo_2O_4 catalysts supported on carbon or graphene were reported to be promising bifunctional catalysts. Wang group reported the multiporous MnCo_2O_4 as a bifunctional catalyst which exhibited a capacity of 1000 mAh g^{-1} and stable cycles during 50th at 250 mA g^{-1} condition in LiTFSI /TEGDME electrolyte.³⁸ **Table 2-3** shows the discharge voltage and discharge capacities of many different catalysts including transition metal oxides, noble metal and bifunctional catalysts in 1 M LiPF_6 in propylene carbonate as the electrolyte. It is clear that the discharge voltage is not so much affected by the catalysts whereas the discharge capacity and its retention on cycling changes dramatically depending on the catalyst used.³⁹

Catalyst	Discharge Voltage (V)	Discharge capacity of 1 st cycle (mAhg ⁻¹)
Pt	2.55	470
Fe ₂ O ₃	2.6	750
Fe ₂ O ₃ – Carbon loaded	2.6	2700
NiO	2.6	2500
Fe ₃ O ₄	2.6	1600
Co ₃ O ₄	2.6	1200
La _{0.8} Sr _{0.2} MnO ₃	2.6	2000

Table 2-3. Discharge voltage and discharge capacities of 1st cycle with many different catalysts.

Cheng et al. reported CoMn₂O₄ nanoparticles having good ORR and OER catalytic activities. Since CoMn₂O₄ spinel is a semiconductor and good catalytic activity requires fast electron transport.⁴⁰ In addition, Although catalysts should affect discharge voltage which is believed to related with ORR and charge OER potentials, however, based on the above results shown in **Table 2-3**, it exhibits very similar discharge voltages around 2.6 V vs. Li with wide range of catalysts This could either be explained by assuming that the ORR in a Li-O₂ cathode is not a catalytically sensitive reaction or by assuming that the ORR activity of added carbon itself is sufficiently high to mask the ORR activity of catalysts of interest most Li-O₂ battery catalyst studies use cathodes with carbon.^{37a, 41} It is believed that the activity of ORR/OER catalysts has closely related with their morphology and surface area so that a porous nanostructured cathode can reduce the overpotential. Thus, it is key to develop a highly porous cathode for transition metal oxide catalyst for nonaqueous Li-O₂ batteries.

Carbon nano tubes and Graphene

The ORR at cathode of Li-O₂ plays a key role in controlling the performance of cell, and efficient ORR electrocatalysts are essential for practical applications of the Li-O₂ battery. Thus

precious metal and metal oxide catalysts have been intensively investigated. However, their intrinsic problems can not be overcome. For example, metal oxide electrocatalysts especially α - MnO_2 , it has low electron conductivity and insufficient activity and precious-metal-based catalysts, of course, exhibit improved ORR and OER activity but, the expensive prices of them prohibit and limit their widespread.⁴² Thus, carbon materials also have been studied as an ORR catalysts. It is reported that the different physical and chemical properties of carbon materials, such as morphology, crystal structure and defect of carbon, can significantly affect the ORR activity.⁴³ (Basically carbon materials are also good ORR catalysts⁴⁴) Jason group reported the exceptionally high capacity of 15000 mAh/g, using the hierarchically porous graphene.⁴⁵ Haoshen Zhou reported a novel thin-film electrode which are prepared by pencil-drawing on a ceramic state electrolyte.⁴⁶, it was a new and interesting electrode preparing a solid-state air electrode on the surface of a ceramic-state electrolyte. Recently, many heteroatom (O, N, S) modification of carbonaceous materials have been reported that they have a significant increased catalytic activity for ORR in organic solvent.⁴⁷ As a class of low-cost catalyst and support, nitrogen-doped carbons have been investigated extensively. However, they often require complicated synthesis procedures to obtain suitable microstructure in order to achieve high capacity. Although many researchers put efforts to develop a good catalysts using a carbon, carbon materials have good ORR activity and show large capacity but they are not effective for OER.⁴⁸ In addition, it is reported that the carbon reacts with Li_2O_2 on the charge (oxidation) cycle to produce an interfacial layer of Li_2CO_3 , which increases the charge overpotential.⁴⁹ During the discharge there is just little or no decomposition of the carbon. However, especially to the hydrophilic carbon, some decomposition occurs (Li_2CO_3 involved with electrolyte decomposition to form HCO_2Li and $\text{CH}_3\text{CO}_2\text{Li}$).⁵⁰ On the charge potential above 4 V vs. Li/Li^+ the lithium carboxylates undergo oxidative decomposition and simultaneously forms by decomposition of the electrolyte. So it is believed that the decomposition of carbon electrode cannot avoid due to the formation of Li_2CO_3 from electrolyte and electrode degradation during charging, and thus Li_2CO_3 accumulates on the carbon electrode, leading to rapid polarization, degradation and passivation of electrode and capacity fading on cycling.⁵¹

Non carbon materials

Almost all the Li- O_2 batteries reported, the catalysts were usually supported or loaded with carbon materials mentioned above, and then the specific capacities were normalized by the only mass of carbon materials, rather than all components of the electrode including the binders and catalysts. If the capacity was calculated by the total weight of the air electrode, the real values of capacity must be much lower than that of the reported values. Moreover, it is also believed that

the catalysts also could generate capacity (even it is not so much though). Furthermore, in the carbon-supported cathode or carbon cathode have been investigated as inefficient catalysts due to the instability of carbon. It is well known that carbon oxidizes above 4 V vs. Li/Li⁺.⁵² In addition, more importantly, carbon decomposes during oxidation of Li₂O₂ on charging due to attacked by intermediates of Li₂O₂ oxidation and it actively promotes electrolyte decomposition on charge. And much worse, the proportion of these side reactions from carbon increases on cycling. The Li₂CO₃, formed by the side reactions, deposits on the carbon cathode, leading to electrode passivation, electrolyte decomposition, resulting in severe polarization and eventually capacity fading and cell death.^{50, 53} So to reduce or eliminate the drawbacks from carbon, some researches about non carbon cathode for Li-O₂ battery have been reported. The alternative carbon cathodes should have a good conductive, large surface area, and most importantly stable in the extremely oxidative environment. The first attempt was reported by P.G. Bruce group. This showed good cycling stability with a DMSO-based electrolyte. However, the reported specific capacity was only around 320 mAh g⁻¹ and the fabrication process was difficult. Thus Bruce group reported TiC-based cathode which greatly reduced side reactions such as electrolyte decomposition and electrode degradation compared with carbon electrode. And they exhibit better cycles than that of carbon (TiC 98% capacity retention after 100 cycles, nanoporous gold 95% capacity retention after 100 cycles)^{33b, 54} Wen group also reported the free-standing type Co₃O₄ on Ni current collector without carbon and binder. The Co₃O₄ electrode exhibited about 4000 mAh g⁻¹.^{4c} Zhou group also reported interesting result that Ruthenium nanoparticles on indium tin oxide (ITO) as a cathode electrode exhibited quite reduced the charge overpotential and improve the cycling performance within a potential window between 2.3 V and 4.05 V for 50 cycles.⁵⁵ Recently Zhou group reported another carbon-free cathode (they call it an alternative cathode), which is Ru nanoparticles supported on Sb-doped tin oxide (STO) particles. It showed 750 mAhg⁻¹ at 0.1 mA cm⁻² for 50 cycles.⁵⁶ Very recently Park group reported carbon-free MnCo₂O₄ oxide as the oxygen electrode and they show the discharge capacity of 10520 mAh·g⁻¹ at the 6.8 mAh·cm⁻² condition.⁵⁷ Carbon-free and carbon alternative electrode for Li-O₂ batteries have been attempted to replace the carbon electrode and indeed, they exhibited good cycle ability and improved performances. However, although those carbon-free or alternative carbon cathode can effectively avoid carbon-involved side reactions, the stability of the electrolytes during the long term operation of Li-O₂ batteries and the relatively lower capacities compare to those of carbon cathode or carbon based cathode still remain challenges. The electrolyte decomposition should be overcome and improving the capacity is main issues for the carbon-free cathodes.⁵⁶

2.3 The Zinc-Air battery.

Leclanche developed the initial idea of metal–air battery with a MnO_2 /carbon cathode electrode. Metal–Air batteries or Metal-Air fuel cells used metal as an anode (negative) electrode such as Li, Mg, Al, Fe, and Zn and an oxygen in atmosphere as a cathode reactive material (positive). Thus the theoretical capacities and energy densities of metal air batteries are extremely higher than those of conventional batteries. **Figure 2-3** and **Figure 2-4** shows the volumetric and gravimetric energy densities of many batteries.

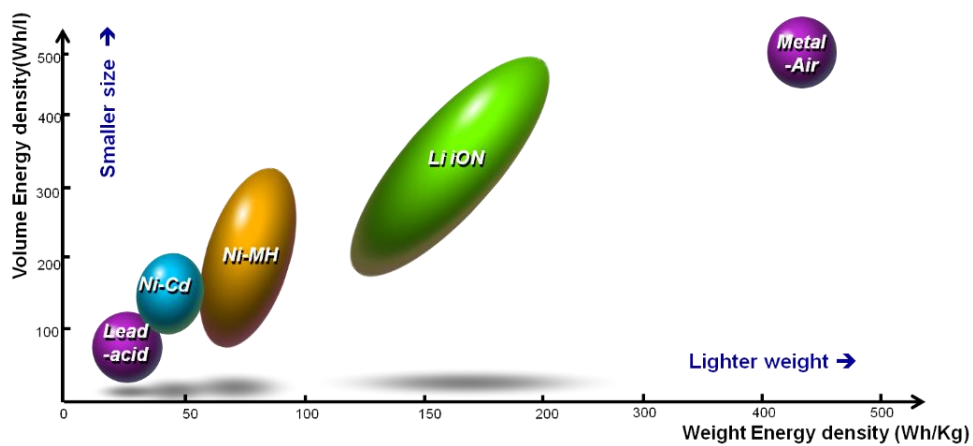


Figure 2-3. Volumetric and gravimetric energy density of many kinds of batteries.

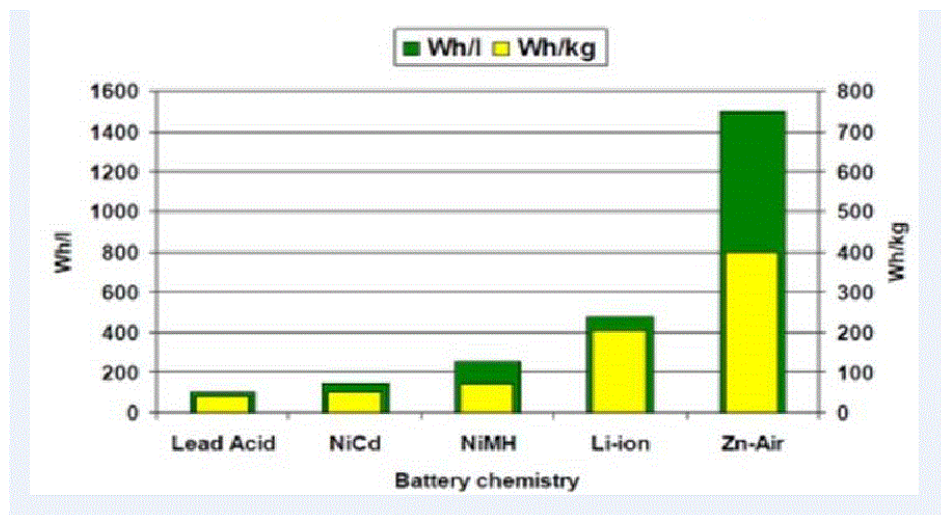


Figure 2-4. Volumetric and gravimetric energy density of many kinds of batteries.

Among many metal-air batteries, Zinc-air cell is the one of the more mature metal-air battery technologies due to its High energy density, abundancy, relatively low material cost (Zn : \$ 1.2 / kg, Mg : \$ 3 / kg, and Li : \$ 150 ~ 180 / kg) and its safety.⁵⁸ The typical Zinc-air cell design is given in **Figure 2-5**. Typical Zinc-air cell is comprised of an alkaline electrolyte (usually KOH), Zn powders (any types of zinc will do) at the anode, a carbon based air cathode, which usually consists of a non-precious metal catalyst, and a hydrophilic separator.

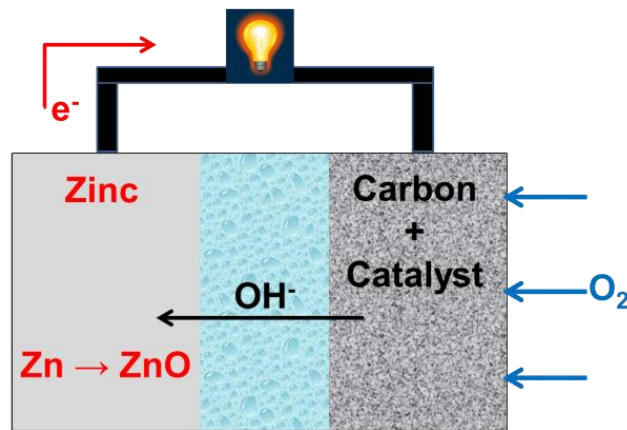
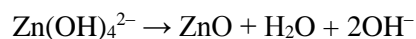
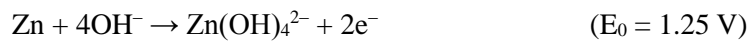


Figure 2-5. A schematic figure of reaction of Zn air battery.

The reactions of Zn air battery are as below,

Anode reaction



Cathode reaction



Overall reaction:



During discharge, oxygen from the air forms hydroxyl ions at the cathode. And the hydroxyl ions migrate into the zinc anode which is saturated with an alkaline electrolyte and form zincate ($\text{Zn}(\text{OH})_4^{2-}$). The $\text{Zn}(\text{OH})_4^{2-}$ decay to zinc oxide and water returns to the electrolyte. The water and hydroxyl from the anode are recycled at the cathode, so the water is not consumed.

Even though the theoretically potential of a Zn-air battery is 1.65 V and its real open circuit voltage is around 1.25 ~ 1.45 V, due to iR drop from the sluggish ORR reaction at cathode. Thus the iR drop can be minimized by using the electrodes with high electrical conductivity and the electrocatalysts and electrolyte with high ionic conductivity.⁵⁹ So many electrocatalysts (non precious metal) have been extensively studied so far.⁶⁰ Aqueous NaOH, KOH or LiOH is preferred as a good electrolyte and recently, KOH is usually used due to its better conductivity than the other electrolyte.⁶¹ The Zn-air cell requires refueling with new alkaline electrolyte and Zn supply as well as the removal of reaction products such as zinc oxide and potassium zincates.

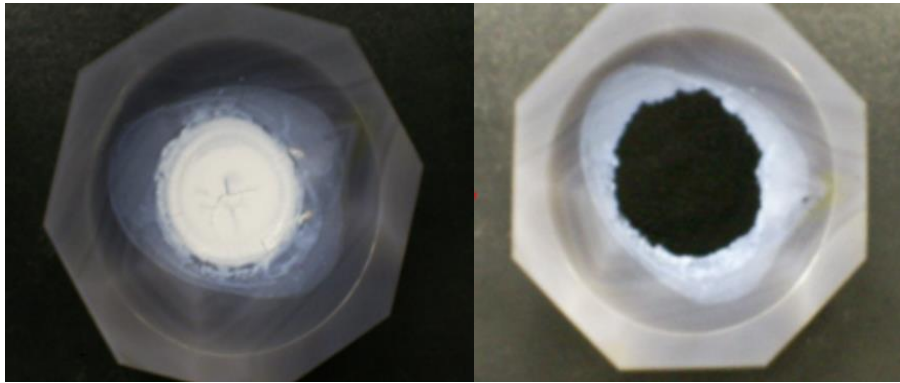
Due to its high specific energy, high power density, cheap cost and non-precious metals as catalysts, and most importantly its safety. The Zn-air cell is promising option for stationary and transportation. Zinc-air batteries are already in practice as a primary battery like hearing aids during several decades. And now hopefully, several companies are involved in development and commercialization of Zn- air battery for electric vehicles, indoor power generators, industrial facilities, and military purposes. However, few research groups and companies are working on the development of Zn-air systems so far throughout the world. Just a few companies have worked on a zinc-air battery system for electric vehicles, the primary and secondary batteries for military uses shown in **Figure 2-6**.



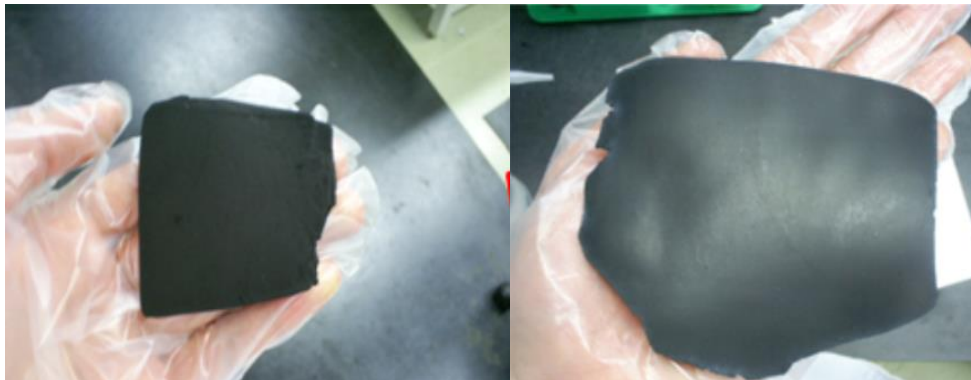
Figure 2-6. Pictures of Zn air battery vehicle (LJB MANAGEMENT INC.) and military application (EMW Co.,Ltd.).

The cathode

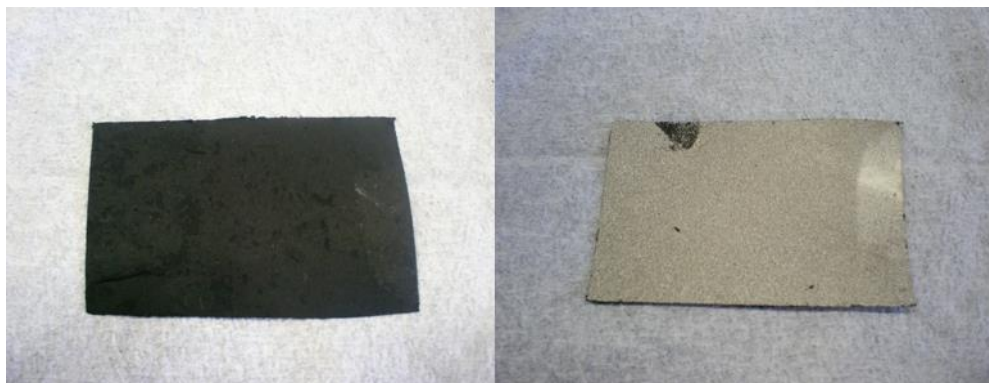
Zinc–air batteries have closely affected by the surrounding environment such as humidity; Too low humidity can lead the gradual drying-out of the electrolyte, or too high humidity can lead flooding of the air electrode. Thus balanced hydrophobicity and hydrophilicity are needed to the air electrode. Thus normally PTFE is used as a hydrophobic binder. The fabrication procedure of air electrode is as below.



1. Mix the carbon, catalyst and PTFE binder with isopropyl alcohol.



2. Knead the paste and roll press to make a proper thickness.



3. Press the paste on the Ni current collector.

In order to maximize the oxygen permeability, gas diffusion electrode (GDE) usually have to be as thin as possible. The thinner electrode exhibited improved rate and performance.⁶² The kinetics of the air electrode are also closely related with oxygen reduction reaction (ORR). ORR is quite sluggish reaction because of strong O=O bond (498 kJ mol^{-1}), which is extremely hard to break. So usually electrocatalysts are required to assist the bond activation and cleavage. ORR electrocatalysis has been a main topic of researches in the fields of metal–air batteries and fuel cells.⁶³ For Zn–air battery, ORR electrocatalysts have a critical role in battery performance including power density, energy efficiency and lifetime. Many efforts have been invested in finding proper electrocatalysts to reduce iR overpotential and enhance battery discharge performance.⁶⁴ ORR catalysts can be categorized by precious metals, metal oxides and carbonaceous materials. In the initial stage of zinc–air research, precious metal catalysts were widely used and platinum shows the best catalytic performance in first zinc–air battery due to its high activity.⁶⁵ Precious metal catalysts have high electrocatalytic activities. However, its cost is so expensive and its scarcity prohibit its widespread. Compared with precious metals, metal oxide catalysts are more desired to catalysts for air electrode. Perovskite and other metal oxide catalysts have been extensively investigated. Among them, manganese oxide (MnOx) have been a particularly interesting candidate due to its oxidation states so that MnO_2 is the most common ORR electrocatalyst in commercial zinc–air batteries.^{40, 66} Recently, carbon based electrocatalysts have been the subject of scrutiny. Basically pristine carbon materials have poor inherent ORR activity in alkaline media. So the researches have focused on increase the activity of carbon by chemical modification of the carbon surface or nitrogen-doped.⁶⁷ Despite all this progress, the performance of Zn-air battery is far from satisfactory (making it a secondary battery). Degradation usually starts from the catalyst materials, leading to deteriorating activities.^{40, 68} For example, even though MnOx is often thought to be the most popular catalyst, it has a strong propensity to get oxidized to MnO_4 at OER potentials. Carbon as the catalyst substrate material is also susceptible

to electrochemical corrosion. Therefore, continuous efforts are needed to find and design not only highly efficient bifunctional electrocatalysts, but also robust electrodes for electrically rechargeable zinc–air batteries.⁶⁹

The anode

Zinc has been the popular negative electrode material for many primary systems such as zinc–carbon, zinc–MnO₂, and zinc–air cell. Zn for the electrode materials are generally a gelled mixture of zinc granules or powders with alkaline electrolytes. The shape or morphology of the zinc granules has been found to be a critical factor to increase inter-particle contact and decrease internal electrical resistance in the negative electrode. In principle, high surface area zinc particles are preferred for better electrochemical performance. **Figure 2-7** shows different types of Zn.

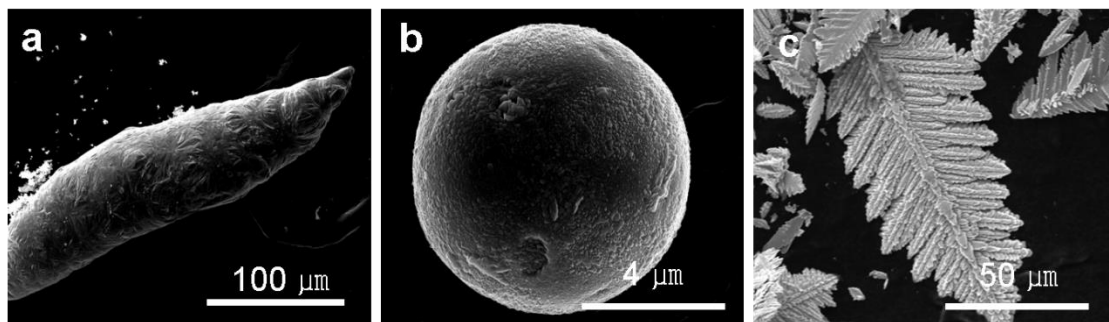


Figure 2-7. SEM image of different types of Zn. (a) Zn granule, (b) Zn powder, and (c) dendritic Zn.

It is reported that fine zinc morphologies had increased high-rate discharge performance.⁷⁰ In addition to powders, other types of high surface area zinc materials such as sphere type, flakes type, fiber type, dendrites and regenerated type of zinc foams have been investigated.⁷¹ However, it is noted that as the electrode surface area of Zn increases, the corrosion rate of it also significantly increases. So the balanced combination of coarse and fine particles are favored as a tradeoff between a performance and self-discharge rate.

The electrolytes

Mostly Zn-air battery operates in alkaline media, such as KOH and NaOH. And for a higher activity of the zinc and air electrode both, usually KOH is preferred to the NaOH because of its better ionic conductivity, lower viscosity and higher oxygen diffusion coefficients.⁷² Moreover,

its reaction products with atmospheric CO_2 – K_2CO_3 or KHCO_3 – have a higher solubility than their sodium counterparts, and can therefore alleviate the carbonate precipitation problem which is a serious challenge for zinc–air batteries. Most commonly, 6 M ~ 7 M KOH solution is employed for its maximum electric conductivity. And recently, the possibility of several aprotic electrolytes have been reported. Especially ionic liquids, for zinc–air batteries has been proposed and evaluated. These electrolytes are beneficial to the cycle ability of the zinc electrodes. By using them, dendrite formation of zinc can be somehow suppressed. They are also beneficial to suppress the self-corrosion of zinc anode, slow down the evaporation of the electrolyte and eliminate its carbonation. But the performances of Zn-air batteries using those aprotic electrolytes is not so good as much as that of the KOH electrolyte so far.⁷³

.

2.4 The Li-O₂ battery.

The Li-O₂ battery (often called Li-air or lithium-air battery) is the battery consuming oxygen from the ambient atmosphere like other Zn-air batteries. In addition, The Li-O₂ battery possesses a very high specific energy about 3700 mAh/g because lithium is the lightest metal, which is much larger than that of graphite or other commercially available anodes (of course including other metal air batteries). Thus it have been shed light on as a new energy generating system. **Figure 2-8** shows the theoretical and practical specific energy densities of many batteries including the Li-O₂ battery.

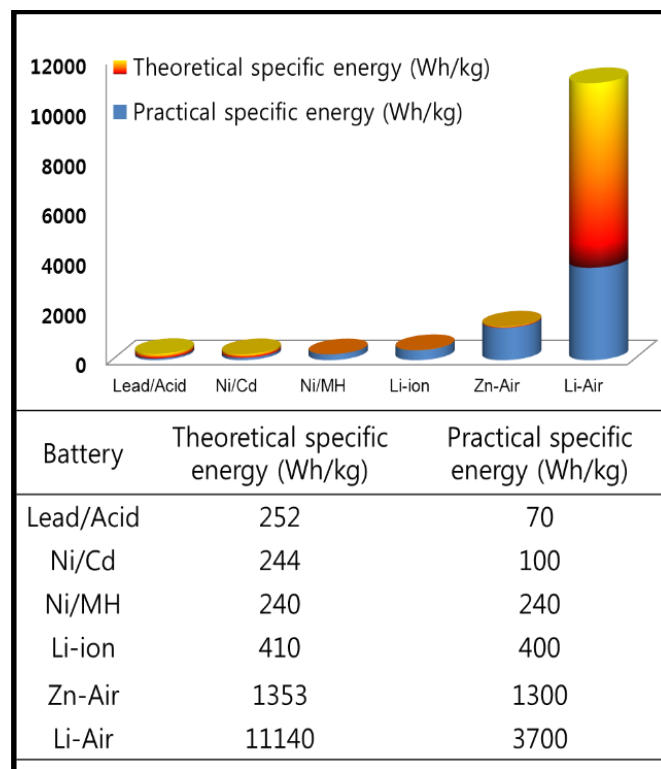


Figure 2-8. The graph and table of theoretical and practical specific energy densities of many batteries.⁷⁴

The common point that the Li-O₂ and Zn-air battery both react with reduced oxygen. Thus generally, people believed that Zn-air and Li-air are the almost same or at least similar to each other. However, it is technically different between Li-O₂ and Zn-air battery. **Figure 2-9** shows the different reaction way of Zn air and Li-O₂ battery.

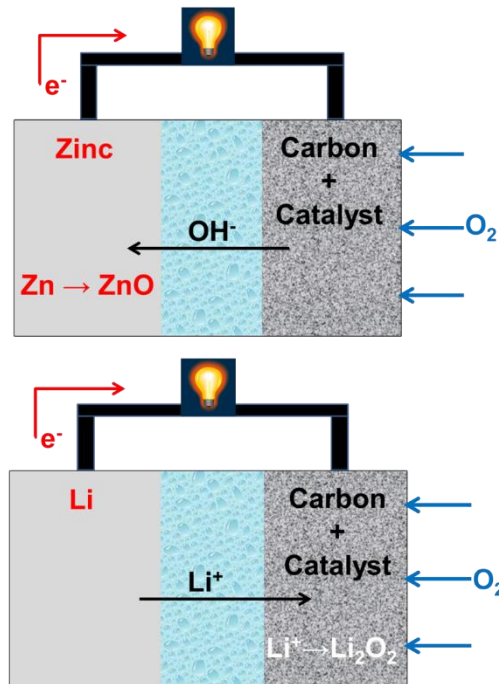


Figure 2-9. The reaction way of Zn air and Li-O₂ battery. Zn air battery is one compartment cell meanwhile Li-O₂ battery is two compartment cell.

And Li-O₂ battery need to exclude incoming moisture and nitrogen from the atmosphere to the battery, so sadly speaking, making a rechargeable real lithium-“air” battery is so difficult (I would not say it is impossible) with today’s knowledge and technologies. Therefore, the researches have been usually investigated by the Li-O₂ system so far using a pure oxygen gas.⁷⁵

In the Li-O₂ battery with a nonaqueous electrolyte (Li-O₂ battery can be divided to four types by electrolyte type shown in **Figure 2-10** but in this thesis, I focused on nonaqueous electrolyte system), reactions between reduced oxygen and lithium ions results in the formation of lithium peroxide (Li₂O₂) (or possibly lithium oxide (Li₂O)) as the final discharge reaction product on or in the cathode pores or surfaces. Since the capacity of Li-O₂ battery can be determined by total amount of Li that can be stored in Li₂O₂ or Li₂O in the cathode, the capacity of Li-O₂ battery is normalized by cathode weight and the porous materials are favored as the cathode.

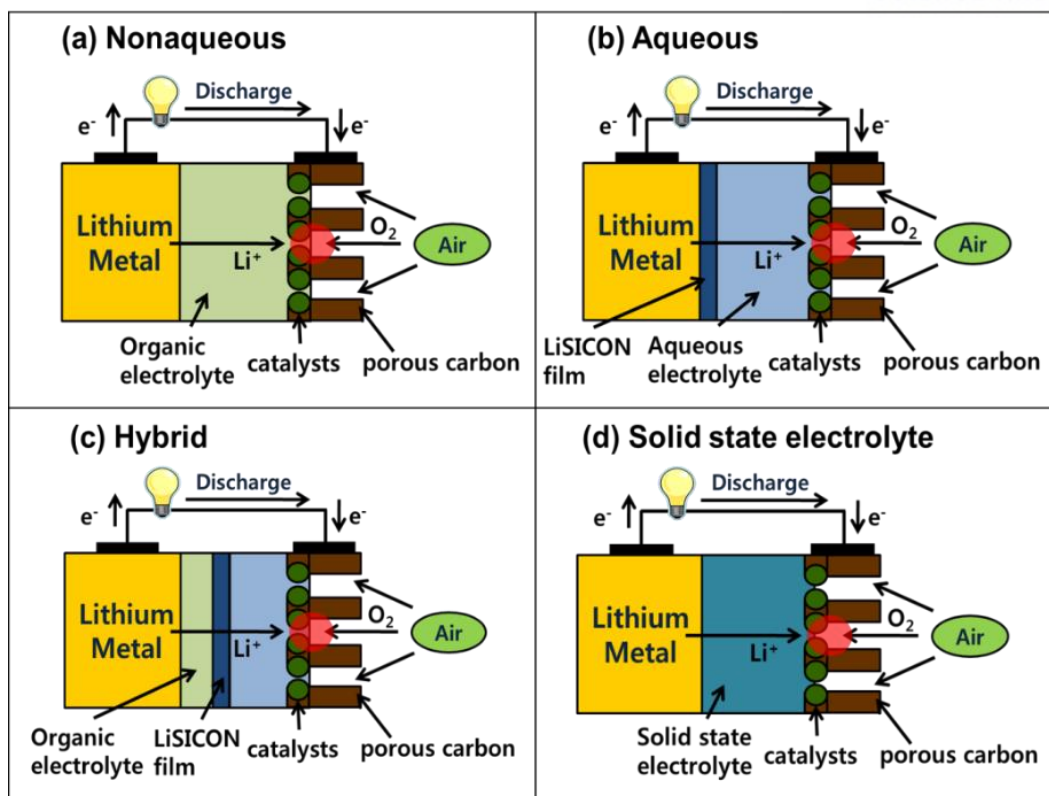


Figure 2-10. The four types of Li-O₂ batteries. (a) nonaqueous, (b) aqueous, (c) hybrid, and (d) solid state electrolyte type.⁷⁴

To achieve a truly rechargeable Li-O₂ battery, reversible oxygen reduction reaction (ORR) and oxygen evolution reaction (OER) resulting in the formation and oxidation of Li₂O₂, respectively, are the key point. The nonaqueous Li-O₂ battery was first reported by Abraham and Jiang in 1996.⁷⁶ Since then, there have been vast efforts to improve the performance of the Li-O₂ battery to enlarge the capacity and to extend cycle life. The reaction of Li-O₂ battery looks simple as below.⁷⁷

1. $\text{Li}^+ + \text{O}_2 + \text{e}^- \rightarrow \text{LiO}_2$ ($E_0 = 3.0 \text{ V vs. Li/Li}^+$)
2. $2\text{Li}^+ + \text{O}_2 + 2\text{e}^- \rightarrow \text{Li}_2\text{O}_2$ ($E_0 = 3.1 \text{ V vs. Li/Li}^+$)
3. $4\text{Li}^+ + \text{O}_2 + 4\text{e}^- \rightarrow 2\text{Li}_2\text{O}$ ($E_0 = 2.9 \text{ V vs. Li/Li}^+$)

The dissolved oxygen in the electrolyte reduces on the surface of a cathode via a one electron transfer process to a super oxide ion (O_2^-). This reduced oxygen ion reacts with Li^+ ions to form lithium superoxide (LiO_2) as the intermediate reaction product. LiO_2 can further chemically or electrochemically be converted to lithium peroxide (Li_2O_2) as the final discharge product. At the charge reaction, lithium peroxide (Li_2O_2) oxidizes as Li^+ ions and O_2 as below.



However, a real cell not works simply as like the reactions. We need to consider the reactions between Li^+ and reduced oxygen, the solubility of gaseous oxygen in the electrolyte, lithium dendrite formation, Li_2CO_3 formation and CO_2 gas evolution during cycling leading to increase the capacity, decrease the overpotential and improve the cycle ability. These have been considered as major research topics for Li- O_2 cell. Thus there have been extensively studies about catalysts and electrolytes to solve those problems.⁷⁸

The cathode

The cathode material for the Li- O_2 battery is usually a porous carbon which can store discharge products more. So the cell capacity is mainly limited by the cathode properties such as surface area, conductivity, pore volume, and pore size distribution. Basically the oxygen solubility and the diffusion coefficient of nonaqueous electrolytes are relatively small factors. (compared to factors from cathode) So the kinetics of the reactions rate, the amount of formed Li_2O_2 are strongly determined by cathode. Most of the cathodes used for Li- O_2 cells are made of carbon, binder, and possibly catalyst so far.⁷⁹The most common technique making a cathode for Li- O_2 battery is just mixing active materials (usually carbon) and catalysts with binder using a solvent to make a slurry, then cast the slurry onto a metal mesh or foam or carbon paper as a current collector. At the early stage of the Li- O_2 battery (around ~ 2010), several studies have been mainly focused on carbon and catalysts to increase the discharge capacity or to optimize the properties of the carbon cathode.^{33c, 80} Most of these studies were aiming at improving the formulation of the cathode to provide more space to store higher amounts of Li_2O_2 . However, after many studies have been reported, the surface area is not the only parameter affecting the cell performance. Many variable factors are connected to each other such as pore size distribution of carbon (PSD), pore volume, porosity, the electrode thickness, the loading density, cathode formulation, etc. affecting the discharge capacity and performance of the Li- O_2 battery.^{48a, 81}

After then, catalysts often used as a component of the cathode have been extensively studied because it is believed that catalysts can improve the kinetics of ORR and OER reactions. They can alleviate the charge overpotential in the cell. The effect of different catalysts including many metal oxides such as MnO_2 , Co_3O_4 , precious metals such as Au, Pt or composite, and nonprecious alloys on the performance of Li- O_2 cells have been studied.^{78a, 82} After such many efforts to improve the performance to solve the problems from the cathode, the discharge capacity and kinetics of the reactions have been improved indeed by catalysts. However, the cycle ability is

hampered by the carbon material itself. It is reported that Li_2O_2 can react with carbon cathode,^{63a, 83} forming Li_2CO_3 and evolving CO_2 gas. Recently, other designs like a binder-free cathode and carbon-free cathode have been reported.^{55, 57, 84}

The Anode

The Li- O_2 battery use a lithium metal directly. (sometimes, further treated metal used) So the formation and growth of dendrites on lithium metal has been the most common issue. In addition, basically lithium is one of the strongest reducing agent so that the contact between lithium and the aprotic electrolytes results in partial decomposition of the electrolyte on the lithium and formation of a surface layer so called the solid electrolyte interphase layer (SEI). The SEI layer can protect the electrolyte from further decomposition by the negative electrode. So to suppress the dendrite formation and electrolyte decomposition, additives and solid electrolytes have been studied.⁸⁵

The electrolyte

Lithium superoxide (LiO_2) and lithium peroxide (Li_2O_2) are very reactive. So the most of the known electrolytes are unstable in the Li- O_2 battery. Especially carbonate based electrolytes can be easily decompose during the cell cycling because of super oxide radical ($\text{O}_2^{\bullet-}$).^{10a, 86} Several different mechanisms have been proposed for the decomposition of carbonate based electrolytes. It has been believed that the super oxide radical ($\text{O}_2^{\bullet-}$) reacts via nucleophilic substitution with the C of the carbonyl group carbonate based electrolyte.⁸⁷ It has also been suggested that the super oxide radical attacks the ethereal carbon of the electrolytes. Several studies have recently reported that ether based electrolytes are relatively strong to the super oxide radical.^{32c, 88} However, further studies revealed that ether based electrolytes also cannot be avoided from degradation during the cell cycling.⁸⁹ Beside the instability of electrolyte solvents, degradation of lithium salts is also one of the main issues. Several lithium salts such as LiPF_6 , LiTFSI , LiBF_4 , LiClO_4 and LiCF_3SO_3 etc are decomposed during the cycling due to the reaction with Li_2O_2 .⁹⁰ Although already many different types of electrolytes and further improved electrolytes such as aprotic organic electrolytes, polymer electrolytes, ionic liquids, etc. have been investigated, the degradation of the electrolyte solvents and salts in the Li- O_2 battery is still one of the major challenges which should be overcome and elucidated.

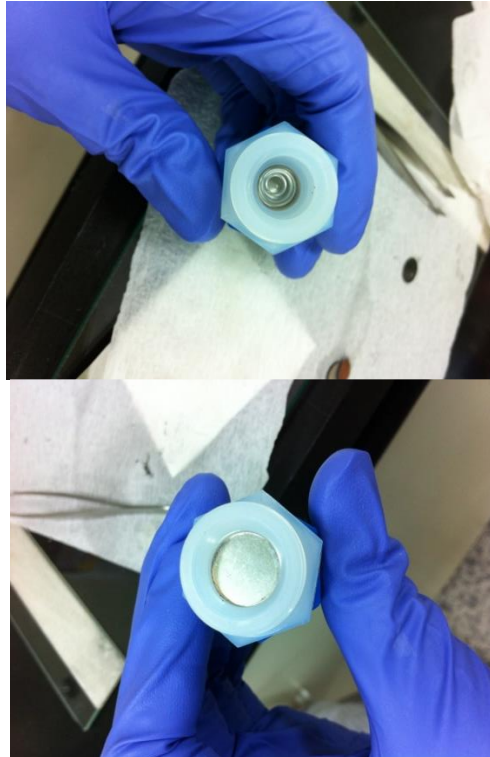
I mentioned the problems of carbon cathode and the decomposition or degradation of electrolytes and salts in Li-O₂ battery above. Therefore in this thesis, I tested carbon- and binder-free cathode for Li-O₂ battery.

3 Experiment I

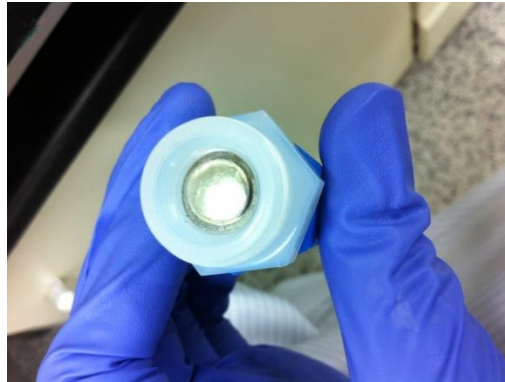
3.1 The Cell Set-up.

Li-O₂ cells were assembled using a modified Swagelok type cell design with an opening allowing oxygen access to the cathode. The cells were kept in specially designed air-tight containers with inlet and outlet valves for keeping the pressure of the oxygen gas. The details of the applied current and voltage, which were different as different studies, are described in the appended papers. The applied current and the capacities of the cells were calculated based on the amount of cathode materials in the electrodes. All the cells were tested using Wona tech Battery cyclor applying different current density. In this design, a stainless steel rod and a stainless steel hollow rod were used as the current collectors of the negative and positive electrodes, respectively. The cells were assembled in a dry room where the dew point is below 65°C using lithium foil as the negative electrode, glass fibers filter as a separator (Whatman), and a carbon- and binder- free cathode as the positive electrode. The details of the cathode preparations are presented in the each experiment section below.

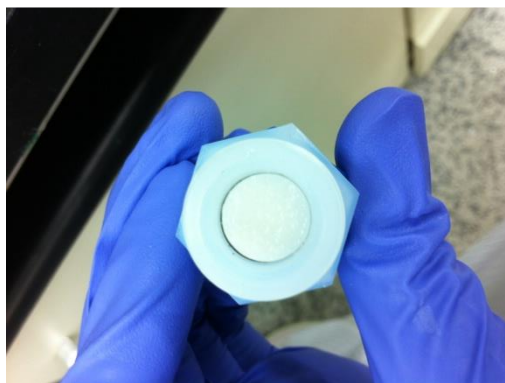
The assemble procedure of Swagelok type cells are as below.



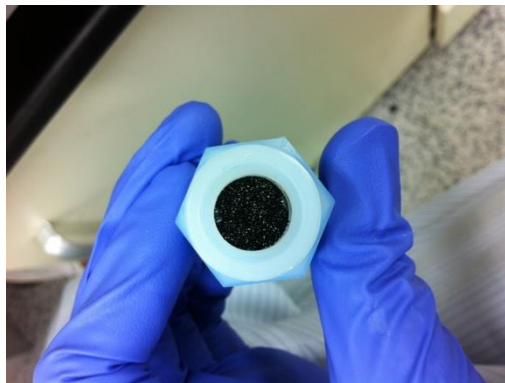
1. Put the stainless spacer on the spring



2. Put punched lithium metal on the spacer



3. Put punched glass fiber separator on the lithium metal and inject electrolyte



4. Put punched cathode electrode on the electrolyte wetted separator.



5. Close tightly the upper side of Swagelok cell.



6. The picture of assembled Swagelok cells.

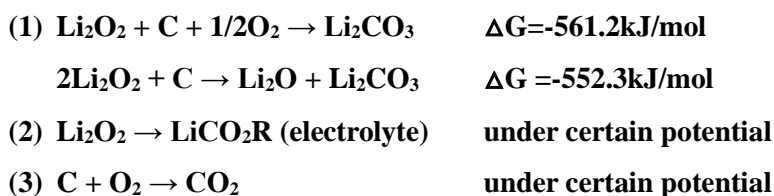
3.2 Optimization of Au nanoparticles-coated Ni nanowire substrate as a highly stable one bodied electrode for lithium-oxygen Batteries

Abstract

Au nanoparticles-coated Ni nanowire substrate without binder and carbon is used as an electrode (denoted as Au/Ni electrode) for Li-oxygen (Li-O₂) battery. Minimum amount of Au nanoparticles with sizes of < 30 nm on Ni nanowire substrate are coated by simple electrodeposition method to the extent that maximum capacity can be utilized. This optimized one bodied Au/Ni electrode shows a high capacity of 921 mAhg⁻¹_{Au}, 591 mAhg⁻¹_{Au}, and 359 mAhg⁻¹_{Au} was obtained at different current 300 mA g⁻¹_{Au}, 500 mA g⁻¹_{Au}, and 1000 mA g⁻¹_{Au} respectively. More importantly, the Au/Ni electrode exhibits excellent cycle ability over 200 cycles.

3.2.1 Introduction.

After introducing the non-aqueous Li-air battery,⁷⁶ it has been attracting many researchers because of its high theoretical energy density, 11,140 Whkg⁻¹ (excluding O₂) and power density is 3505 Whkg⁻¹, which is about eight times larger than that of conventional rechargeable lithium-ion batteries.⁷⁴ The Li-O₂ battery, however, has many problems which have to be elucidated and overcome, such as low current density, instability of nonaqueous electrolytes as like decomposition of electrolytes, even instability of salts, and poor cycle ability.^{35, 90a, 91} In order to solve these problems, it is urgent to find a proper electrolyte, but there is no ultimately stable electrolyte for non-aqueous Li-O₂ batteries at present, just ether-based electrolytes were found to be relatively robust to oxygen radicals.⁹² To achieve a stable electrolyte and to disclose details about relations with each battery component, we need to fix a cathode part, thus helping a search a favorite electrolyte. Consequently, to improve performance and stability of cathode, various catalysts, such as α -MnO₂, Co₃O₄, Mn₃O₄, Ru, and Pt/Au composite have been examined,^{34, 39, 77, 93} leading to improved performance of cathode. However, since those catalysts normally were used on carbon substrates, it did not solve the problem arising from the carbons. Carbon cathode can lead to the inevitable reactions between the discharge product Li₂O₂ and carbon favored by the negative Gibbs free energy according to following reactions.^{83a}



For these reasons, using any carbon cathode have not shown stable long cycle graph under the full discharge/charge condition (e.g. between 4.3V and 2.3V), such as carbon black, activated carbon, carbon nanotube (CNT), and graphene.⁹⁴ Although it has been reported significantly improved the cyclability of carbon-based cathode out to 900 cycles by a redox mediator, the cell operation condition was also limited by capacity cut-off.⁹⁵ In addition, several recent studies have reported about binders which are necessary to make a carbon electrode. The reactivity between chemically generated LiO₂ and PVDF binder in 1 M LiPF₆/TEGDME has been reported.⁹⁶ In addition to binder instability, several recent studies have shown that lithium salts and/or binder can be decomposed during cycling.^{50, 90a, 97} Therefore further controlled studies with carbon and binder-free electrodes will be critical to unambiguously probe the stability of electrolyte solvents and salts in the presence of Li₂O₂ and discharge intermediates.⁹⁸ To achieve carbon- and binder-

free cathode, it is critical to choose a source with a good catalytic surface and structure to facilitate a Li-O₂ reaction. Once a good source is identified, it is also important to maximize the capacity. Some recent research have suggested that possibility of carbon free electrodes have been reported and shown good results, such as Ru/ITO carbon free electrode with cycling to 50 cycles, nanoporous gold electrode and TiC-based electrode with stable cycling to 100.^{83a, 99} For instance, nanoporous Au electrode showed the quite reversible capacity of 300 mAhg⁻¹_{Au} between 4 and 2.3 V in the DMSO (dimethyl sulfoxide) electrolyte.

Among those, Au may not be a suitable material for the cathode due to its high mass and cost, however, its diverse synthetic methods can lead to many chances for further optimization for usage of the cathode materials. For instance, its morphology and quantity that contributes to the capacity and oxygen reduction and evolution (ORR/OER) reactions are easily controlled. In this study, we reported the optimized synthetic condition of Au nanoparticles-coated Ni nanowire substrate via a simple electrodeposition method for a highly efficient electrode for Li-O₂ battery

3.2.2 Experimental Section

Fabrication of Au/Ni electrode. In order to prepare Ni nanowire substrate, anodic aluminium oxide membrane (AAO, Whatman Anodisc 25) was used as a template. At first, Ni nanoparticles as seeds for Ni nanowire growth were densely deposited up to ~200 nm on the one side of AAO membrane templates with a pore size of ~ 20 nm (let's assume this side is a front side of AAO) placed on the silicon wafer by E-beam evaporator as shown in **Figure 3-19**, note that AAO template has different pore sizes on its front and back shown in **Figure 3-20**, so if Ni nanoparticles were deposited of back side of AAO (opposite side of front), the Ni nanoparticles can't fully cover the pores of AAO as shown in **Figure 3-19** and the blue print of home made electrodeposition kit shown in **Figure 3-21, 3-22, and 3-23** the real picture of Ni nanowire current collector is shown in **Figure 3-24**. Secondly, the deposited side by Ni nanoparticles of the template was attached on the current collector and covered by a 25 mm rubber O-ring, which are placed onto the open hole exposed to Ni plating solution in the home-made electroplating cell. The plating solution consisted of 0.3 M $\text{NiCl}_2 \cdot 6\text{H}_2\text{O}$ (Samchun chemical), 0.2 M H_3BO_3 (Samchun chemical), and 0.15 M NH_4Cl (Daejung chemical) in distilled water. Electroplating was performed at ambient temperature under pulse condition that voltage of -1.1V 15sec and then -0.9V 5sec (vs Ag/AgCl) were applied by turns for 3hr. Finally, the AAO template was dissolved using a 2 M NaOH (Daejung chemical) solution with gentle agitation at room temperature for 24h and then rinse it several times with distilled water. This Ni nanowire substrate was placed on a current collector again and covered by a 23 mm rubber O-ring in a homemade Teflon electroplating cell and put the plating solution consisting of 0.005 M $\text{HAuCl}_4 \cdot 3\text{H}_2\text{O}$ (Sigma Aldrich) and 2 M NH_4Cl (Daejung chemical) in solvent mixed 50 % of Methanol and 50 % of DI water. Electroplating was performed also under pulse condition that voltage of -X.0V(-1.0 V, -2.0 V, -3.0 V, and -4.0 V) 3 sec and then rest 15 sec were applied by turns for 6 minutes and thus actual depositing time is 60sec. After deposited, the disk was washed with distilled water several times and then dried. The loading quantity of Au was estimated via inductively coupled plasma (ICP) analysis and optimized. The amount of Au was 0.081 mg/cm², 0.4 mg/cm², 1.8 mg/cm², and 4.5 mg/cm² at applied voltage of -1.0 V, -2.0 V, -3.0 V, and -4.0 V, respectively. The disk of the Au/Ni electrode was directly used as a cathode.

Preparation of Au leaf electrode. Nanoporous Au leaf (Au>99.5%, Hanil gold, Korea) was purchased and used without further treatment. Au leaf was attached on Ni foam current collector by roll-press without binder. The loading amount of Au leaf was 0.1 ± 0.01 mg.

Assemblage of the Li-O₂ full-cell. For electrochemical test, Swagelok-type Li-O₂ cell consisting of Au/Ni electrode punched by 1.23 cm² (12.5pi), glass microfiber filter paper punched by 1.27 cm² (12.7pi) (Whatman grade GF/D), lithium foil punched by 1.23 cm² (12.5pi) without additional pretreatment, and 1.3M LiTFSI in TEGDME (tetraethylene glycol dimethyl ether) electrolyte solution was used. All cell assemblage were carried out in a dry room where the dew point is below 65.0°C.

Electrochemical characterization of the full-cell. For the electrochemical characterizations, the Au leaf electrode and Au/Ni electrode were cycled between 2.3 and 4.3 V at different current condition. (300 mA g⁻¹_{Au}, 500 mA g⁻¹_{Au}, and 1000 mA g⁻¹_{Au} under 1 atm O₂ blowing at 24°C, Wonatech Co. Ltd.)

Characterization of Au leaf and Au/Ni electrodes. Field Emission Scanning Electron Microscopy (FESEM) (FEI nano 230), normal transmission electron microscopy (TEM) (JEOL Inc.) operating at 200 kV, energy-dispersive spectroscopy (EDS, JEM-2100, JEOL Inc.) elemental mapping, X-ray diffractometer (XRD) (D/Max2000, Rigaku). X-ray photoelectron spectroscopy (XPS) (Thermo Scientific K α spectrometer, 1486.6 eV).

3.2.3 Results and Discussion

It has been reported that Au nanoparticles could enhance the discharge voltages of Li–O₂ cells¹⁰⁰ and Ni current collector is widely used in Li–O₂ battery.^{80a, 93a, 101} Therefore it is more beneficial to use nanostructured Ni current collector in which Au nanoparticles can be directly grown up on it to maximize Au utilization (**Figure 3-1**).

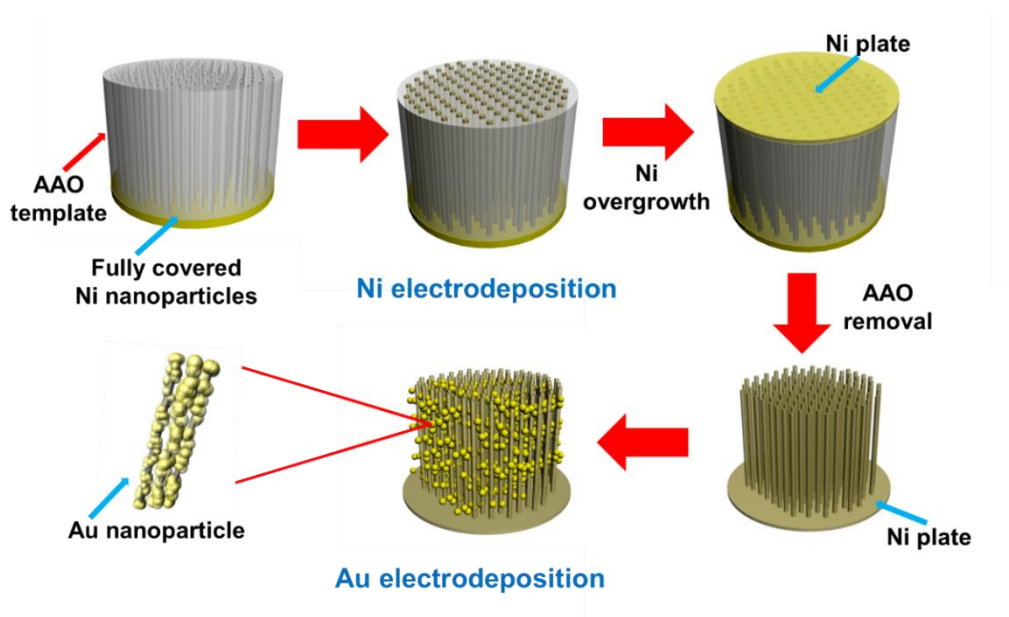


Figure 3-1. Schematic of the fabrication of Au nanoparticles deposited Ni nanowire substrate by electrodeposition method.

To do so, Ni nanoparticles as seeds for Ni nanowire growth were densely deposited on the side of anodic aluminium oxide (AAO) membrane template on the side with a pores size of ~ 20 nm after loading on the silicon wafer by using E-beam evaporator. Secondly, the deposited side of the template was then attached to the current collector in the open hole of home-made electroplating cell. Finally, after filling the Ni plating solution into the holes and subsequent applying voltage to overgrow Ni nanowire substrate from the AAO templates, Ni nanowires with a diameter of ~ 200 nm could be obtained. For Au nanoparticles deposition, Ni nanowire substrate was immersed in the plating solution consisting of H₂AuCl₄·3H₂O and NH₄Cl and was subsequently applied voltage (for details see the experimental section). By means of this unique method, we effectively coated minimum amount of Au nanoparticles on Ni nanowire substrate to the extent that maximum capacity can be utilized. **Figure 3-2a** and **b** shows SEM images of AAO template to prepare Ni nanowire substrate and **Figure 3-2c** and **d** show real picture of homemade Teflon kit and Ni nanowire substrate (for details in Experimental section). **Figure 3-2e, f, g,** and

h show SEM images of Au/Ni electrode on which different amounts of Au (0.081 mg/cm^2 , 0.4 mg/cm^2 , 1.8 mg/cm^2 , and 4.5 mg/cm^2) is deposited. When the Au amount was 4.5 mg/cm^2 , reformation of porous structure is can be seen due to overgrown Au nanoparticles on the Ni substrate (**Fig. 3-2h**).

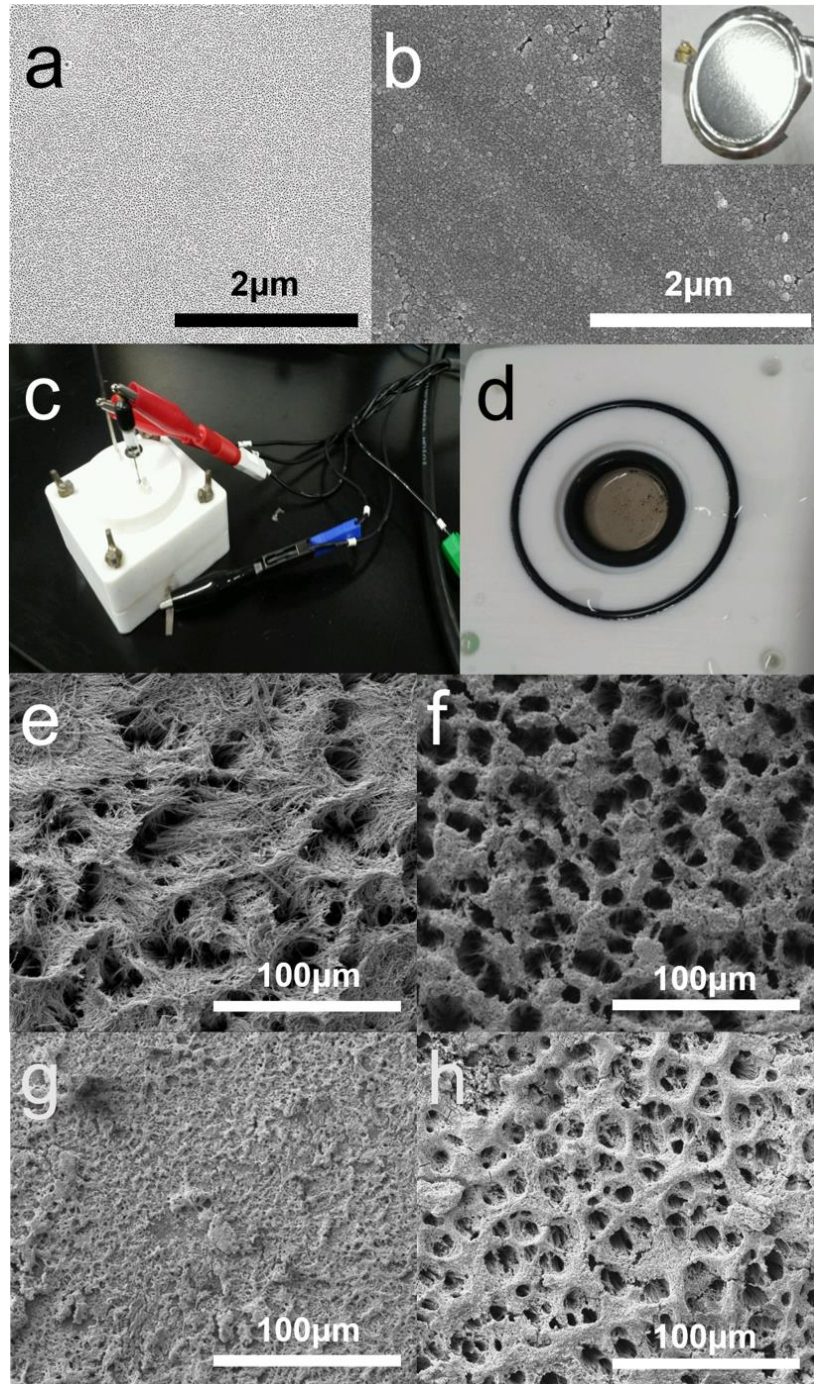


Figure 3-2. Preparation of Au/Ni Electrode and morphology of Au/Ni electrode with different Au quantity. (a) SEM image of AAO template, (b) SEM image of deposited Ni nanoparticles on AAO template by E-beam evaporator, (c) picture of 3 electrode electrodeposition homemade Teflon kit, (d) picture of Ni nanowire substrate, (d, f, g and h) SEM images of Ni nanowire substrate with different amounts of Au nanoparticles (d) 0.081 mg/cm², (e) 0.4 mg/cm² (f) 1.8 mg/cm², and (g) 4.5 mg/cm².

At first, we conducted cyclic voltammogram test of Ni nanowire substrate to figure out the catalytic reaction. The oxygen reduction reaction (ORR) and oxygen evolution reaction (OER) of Ni substrate was observed to be negligible (**Figure 3-3**). This result can also support the full cell result, indicating that Ni nanowire did not contribute to the capacity (**Figure 3-3**). Accordingly, Ni functioned merely as a current collector. Therefore no need to normalize the capacitance by both mass of Ni and Au. Before electrochemical full cell test using Au/Ni electrode, we confirmed a stability of Au/Ni electrode by cyclic voltammetry (CV) test. The ORR and OER currents were observed to be stabilized over 50 cycles in the examined potential window from 2.3 to 4.3 V. (**Figure 3-4**).

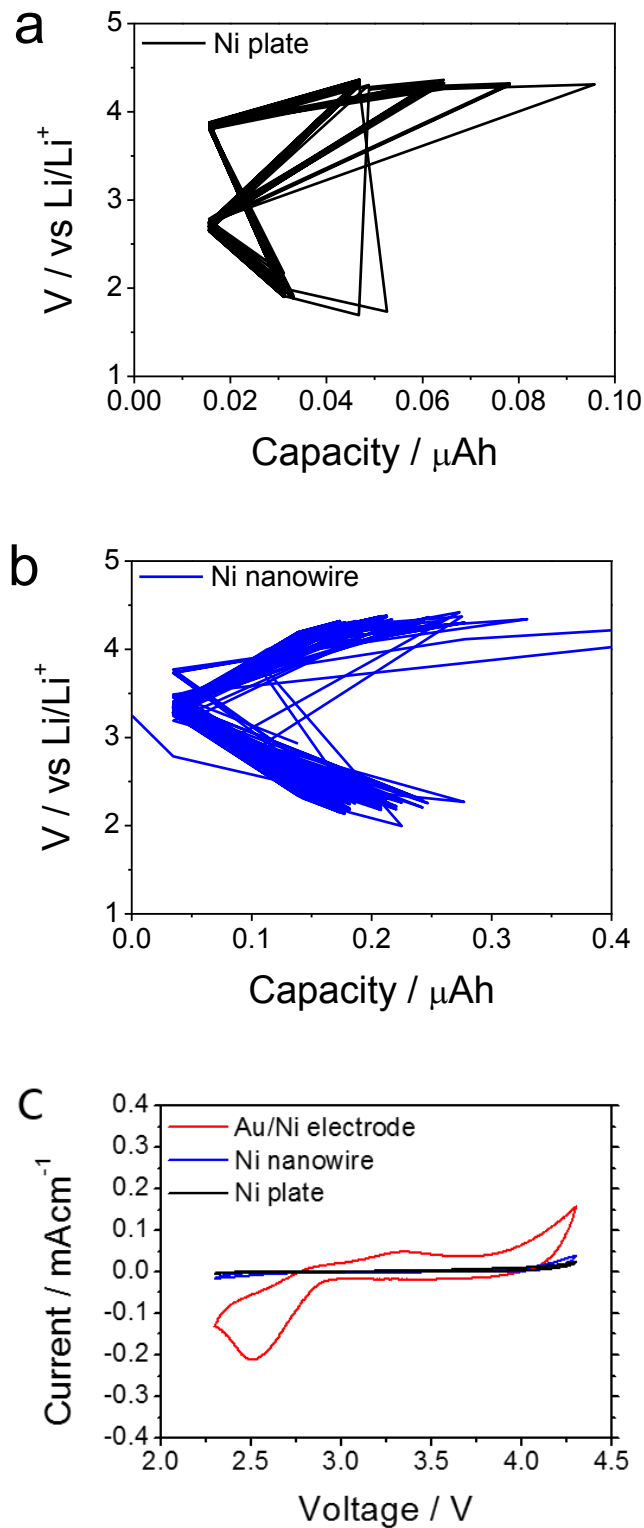


Figure 3-3. Voltage profiles of (a) Ni plate electrode and (b) Ni nanowire substrate electrode. The dis/charge current at $2.5 \text{ mA g}^{-1} \text{ Ni}$. (c) Cyclic voltammogram of Ni nanowire substrate and Au/Ni electrode between 2.3 V~4.3 V at a scan rate of 5 mV sec^{-1}

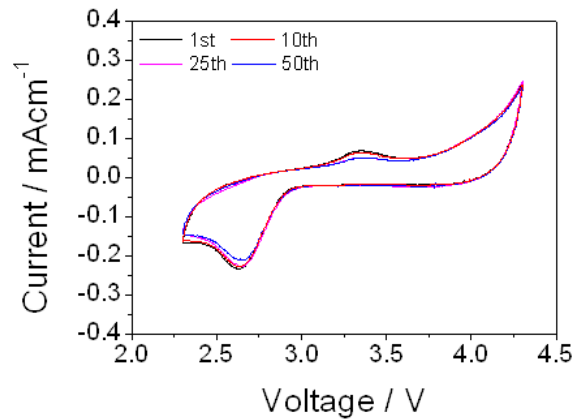


Figure 3-4. Cyclic voltammogram on voltage window between 2.3 V~4.3 V during 1, 10, 25, and 50 cycles at 5 mVsec⁻¹

The full cell test of Au/Ni electrode with a different Au amount was conducted at current rate of 500 mA_{g⁻¹Au} in 1.3M LiTFSI in TEGDME (tetraethylene glycol dimethyl ether) electrolyte under 1 atm O₂ blowing at 24°C. Due to the high reactivity of DMSO solvent to Li metal, Li metal have to be pretreated before applying DMSO.^{99a} In order to avoid such a pretreatment, TEGDME electrolyte was used in this study. **Figure 3-5** displays the voltage profiles of Au/Ni electrode. The electrode with the lowest amount of Au (0.081 mg/cm²) shows the highest discharge capacity of 591 mA_hg⁻¹_{Au}.

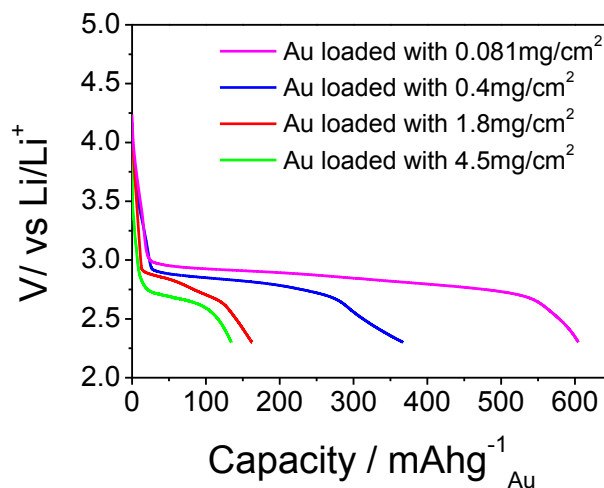


Figure 3-5. Electrochemical evaluation of Au/Ni electrode at discharge current of 500 mA_{g⁻¹Au}. Capacity were normalized by Au quantity. (All the cells were pre-conducted cyclic voltammogram using Ag/AgCl reference electrode between 2.3 and 4.3V for 50 cycles).

In order to maximize the Au active sites participating in ORR and OER reactions, Au nanoparticles should be coated on the surface of Ni nanowire substrate as possible, which is the way to maximize capacity. As shown in **Figure 2f, g, and h**, when the Au nanoparticles were deposited more than the required amount, it causes the capacity decrease due to loss of active sites. The other sample, shown in **Figure 2e**, needed further analysis so that **Figure 3-6** displays SEM and TEM image of Ni nanowire substrate on which Au amount of 0.081 mg/cm^2 was deposited (**3-6b and d**) (Note that the different diameter of the Ni nanowires, shown in **Figure 3-6 c and d**, could be originated from a different pore size distribution of AAO membrane. See **Figure 3-7**). Au nanoparticles were observed to be efficiently deposited on Ni nanowire substrate with an average Au nanoparticle size with $< 30 \text{ nm}$. Energy dispersive X-ray spectroscopy (EDX) confirmed the formation of Au (**Figure 3-6e and 6f** and **Figure 3-8**).

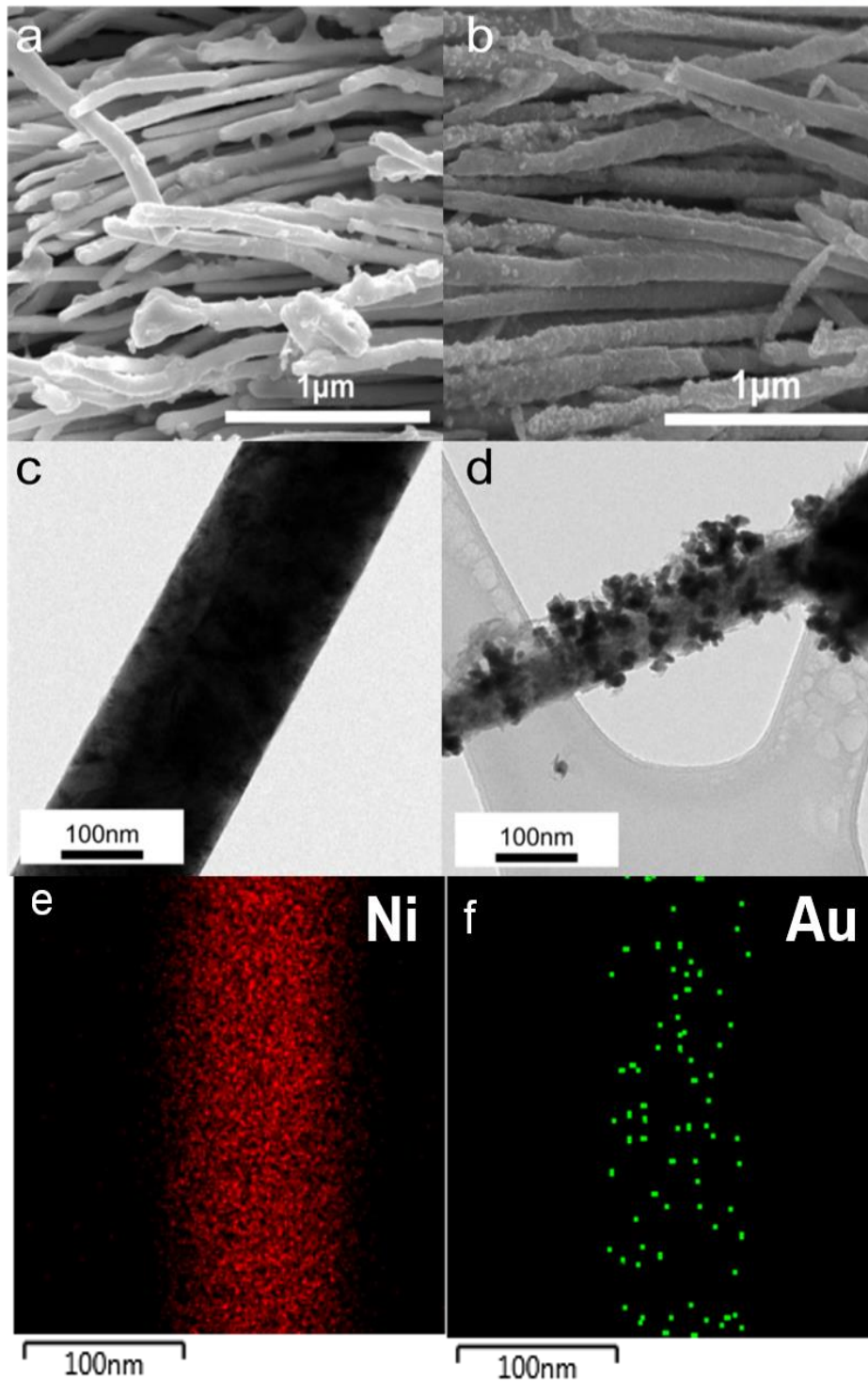


Figure 3-6. The morphology of Au/Ni electrode and EDX image. SEM images of the as-fabricated (a) Ni nanowire, (b) Au/Ni electrode, TEM images of (c) Ni nanowire, (d) Au/Ni electrode, and EDX images of (e) Ni, and (f) Au element, respectively.

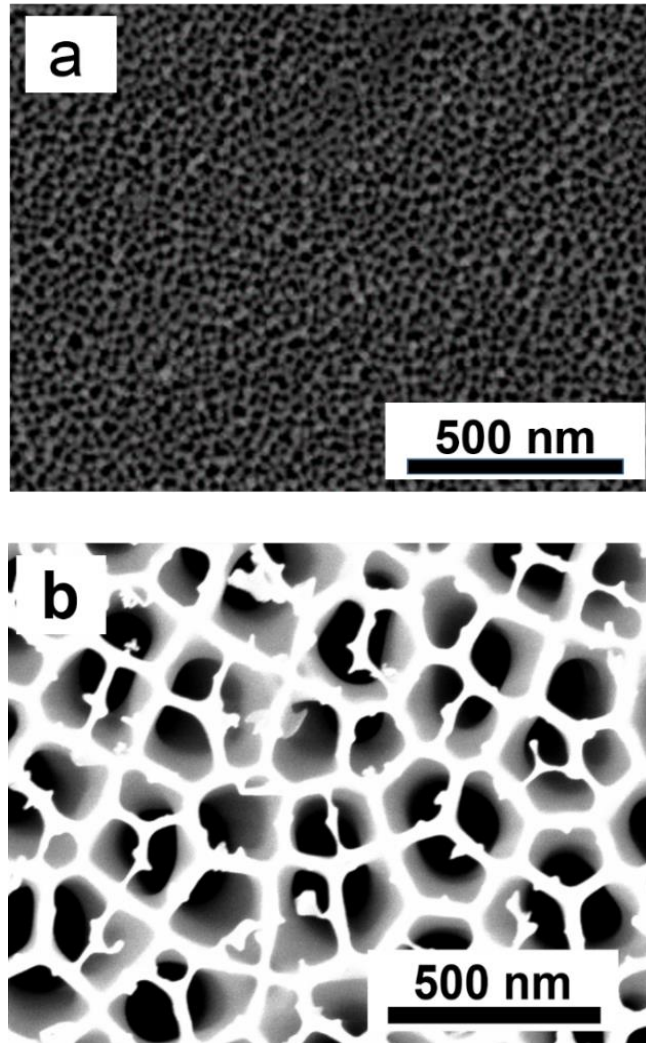


Figure 3-7. SEM image of (a) front and (b) back sides of AAO membrane. The pore size of front and back sides are ~ 20 nm and ~ 200 nm, respectively. Ni nanoparticle seeds are deposited on the front side and Ni nanowires grew through the back side of AAO membrane.

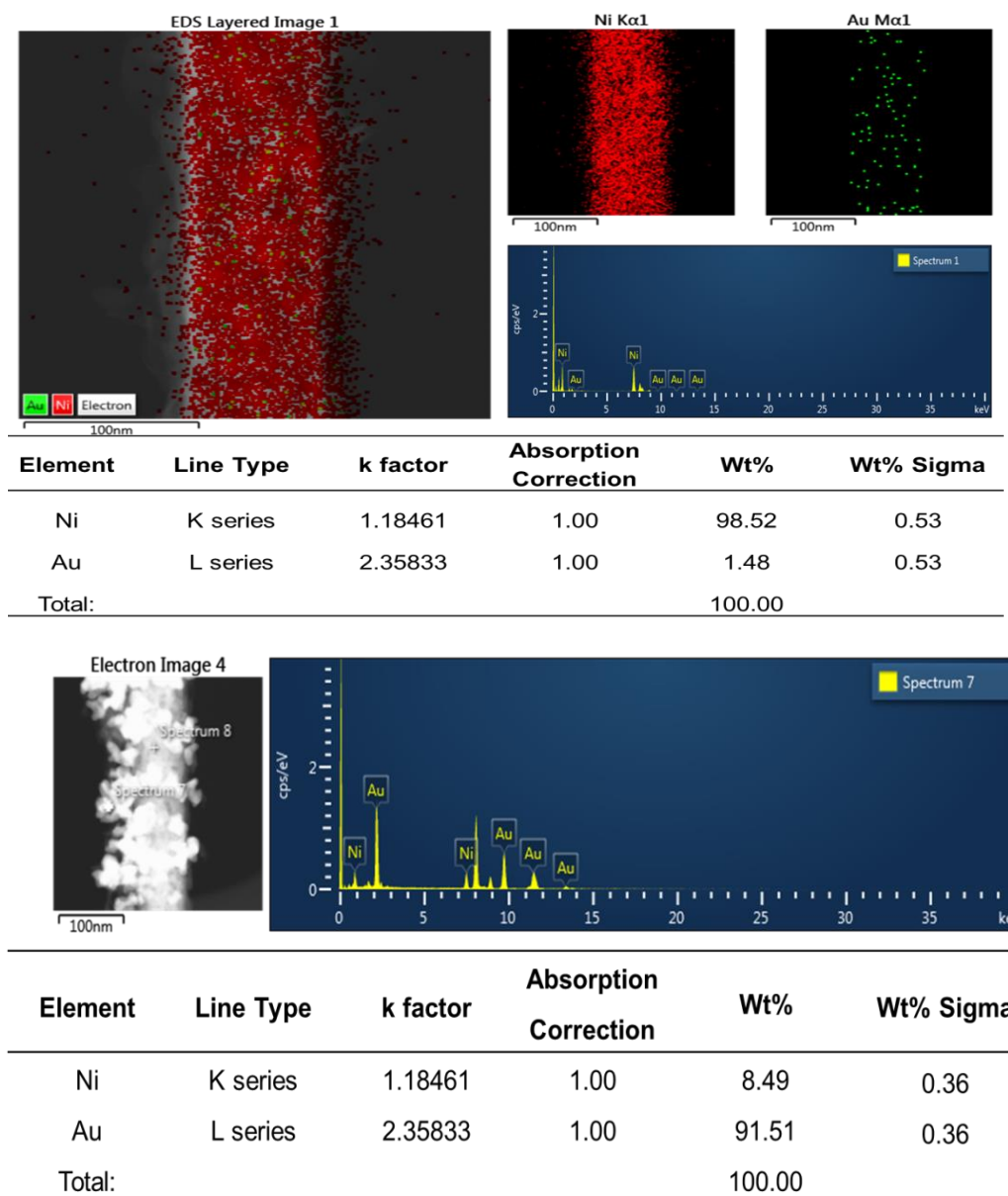


Figure 3-8. The EDX results of the Au/Ni electrode.

Since the Au nanoparticles were relatively well deposited on Ni nanowires, we expect the improved utilization, compared with other nanostructured counterparts. Accordingly, Au leaf with a nanopores with > 30 nm (**Figure 3-9**) was compared with the optimized sample.

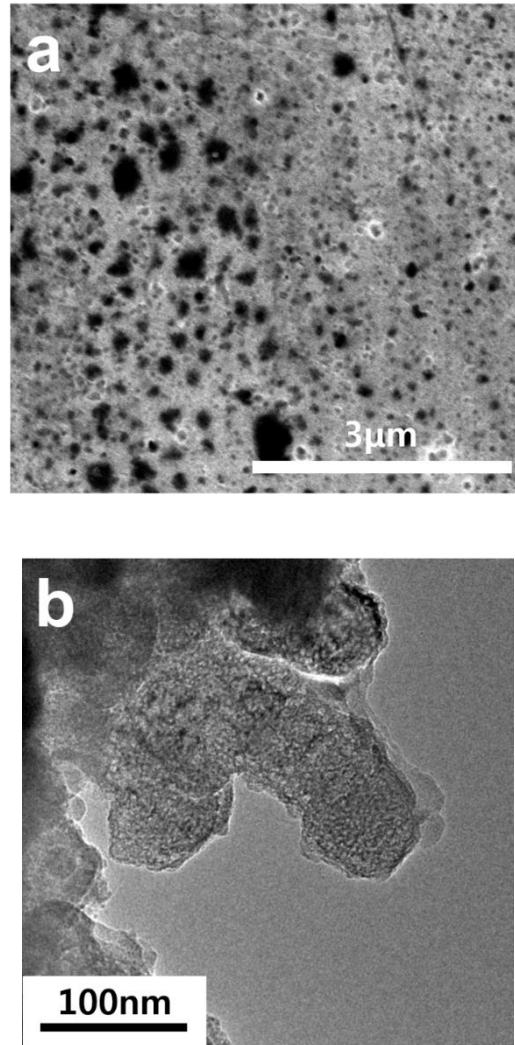


Figure 3-9. The morphology of nanoporous Au leaf. (a) SEM image of nanoporous Au leaf and (b) TEM image of nanoporous Au leaf.

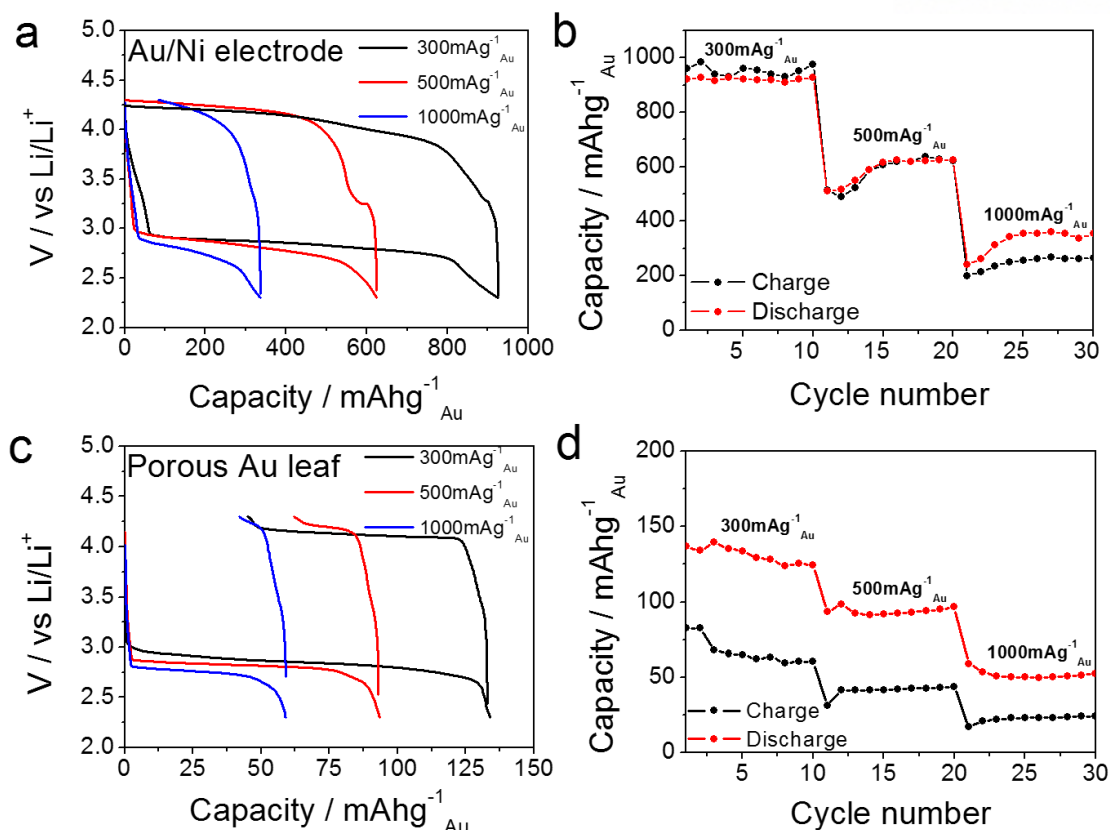


Figure 3-10. Electrochemical evaluation of Au/Ni electrode and nanoporous Au leaf at different current. (a) voltage profiles of Au/Ni electrode at different currents of 300 mAg⁻¹_{Au}, 500 mAg⁻¹_{Au} and 1000 mAg⁻¹_{Au}, (b) discharge capacity plot vs. cycle number of (a) with increasing current of 300 mAg⁻¹_{Au} to 1000 mAg⁻¹_{Au}, (c) voltage profiles of nanoporous Au leaf at different currents of 300 mAg⁻¹_{Au}, 500 mAg⁻¹_{Au} and 1000 mAg⁻¹_{Au}, and (d) discharge capacity plot vs. cycle number of (a) with increasing current of 300 mAg⁻¹_{Au} to 1000 mAg⁻¹_{Au}

A full cell test was conducted with a current of 300 mAg⁻¹_{Au}, 500 mAg⁻¹_{Au} and 1000 mAg⁻¹_{Au} between 2.3 and 4.3 V under 1 atm O₂ blowing at 24°C, as shown **Figure 3-10**. Discharge capacities of the Au/Ni electrode is far superior to those of Au leaf at different currents and for instance, discharge capacity of the Au/Ni was 921 mAhg⁻¹_{Au}, while that of the Au leaf was 134 mAhg⁻¹_{Au}. This result is also competitive to other carbon-free cathodes (**Table 3-1**).

Table 3-1. Recent results of non-carbon based cathodes for Li-O₂ battery (2014.07).

Journal	Title	capacity	Electrolyte and test condition	Capacity retention
Nano Lett., 2013, 13, 4702	Ru/ITO: A Carbon-Free Cathode for Nonaqueous Li-O ₂ Battery	1.81mAh/cm ²	Triglyme 0.15mA/cm ²	98% after 50 cycles
Chem. Commun., 2013, 49, 5984	Carbon-free cobalt oxide cathodes with tunable nanoarchitectures for rechargeable lithium-oxygen batteries	2280mAh/g	TEGDME 20mA/g (based on the Co ₃ O ₄ weight)	No information
		500mAh/g	TEGDME 100mA/g (based on the Co ₃ O ₄ weight)	100% after 50cycles with a limited capacity of 500mAh/g
J. Power Sources, 2014, 248, 1270	Carbon and binder free rechargeable Li-O ₂ battery cathode with Pt/Co ₃ O ₄ flake arrays as catalyst	930mAh/g	TEGDME 100mA/g	No information
		500mAh/g	TEGDME 200mA/g	75% after 30 cycles
Nat. Mater., 2013, 12,1050	A stable cathode for the aprotic Li-O ₂ battery	350mAh/g _{TiC}	DMSO 1mA/cm ²	98% after 100 cycles
		530mAh/g _{TiC}	TEGDME 0.5mA/cm ²	97% after 25 cycles
Science, 2012, 337, 563	A Reversible and Higher-Rate Li-O ₂ Battery	300mAh/g _{Au}	DMSO 500mA/g (based on the Au weight)	95% after 100 cycles

This work	Optimization of Au nanoparticles-coated Ni nanowire substrate as a highly stable one bodied electrode for lithium-oxygen Batteries	1563mAh/g _{Au}	TEGDME 100mA/g (based on the Au weight)	No cycling test
		591mAh/g _{Au}	TEGDME 500mA/g (based on the Au weight)	98% after 100 cycles
		359mAh/g _{Au}	TEGDME 1000mA/g (based on the Au weight)	No cycling test
		371mAh/g _{Au}	DMA 500mA/g (based on the Au weight)	99% after 50 cycles

Further, cycling performance of the Au/Ni electrode was carried out over 100 cycles, and the capacity of Au/Ni electrode was $591 \text{ mAhg}^{-1}_{\text{Au}}$ and $580 \text{ mAhg}^{-1}_{\text{Au}}$ after 1st and 100th cycle at $500 \text{ mA g}^{-1}_{\text{Au}}$. This corresponds to 98.1% capacity retention shown in **Figure 3-11a** and **b**. However, after around 100 cycle, gradual capacity fade occurs.

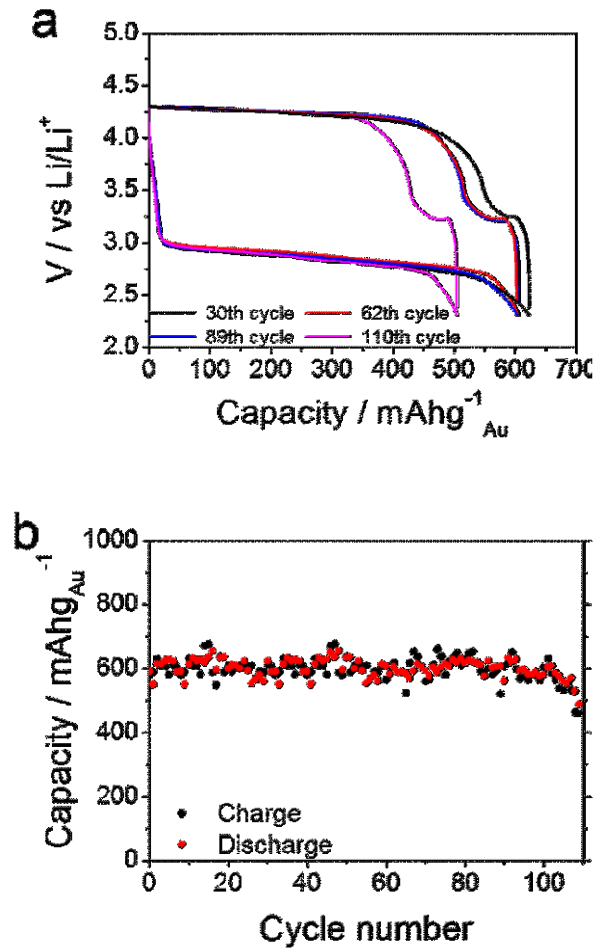


Figure 3-11. Capacity and cycle result of Au/Ni electrode at $500 \text{ mA g}^{-1}_{\text{Au}}$. (a) voltage profiles of Au/Ni electrode and (b) plot of discharge capacity vs. cycle number of (a).

To investigate the stability of elements and surface morphological change of Au/Ni electrode, XPS (**Figure 3-12**), SEM (**Figure 3-13**) and XRD (**Figure 3-14**) were examined.

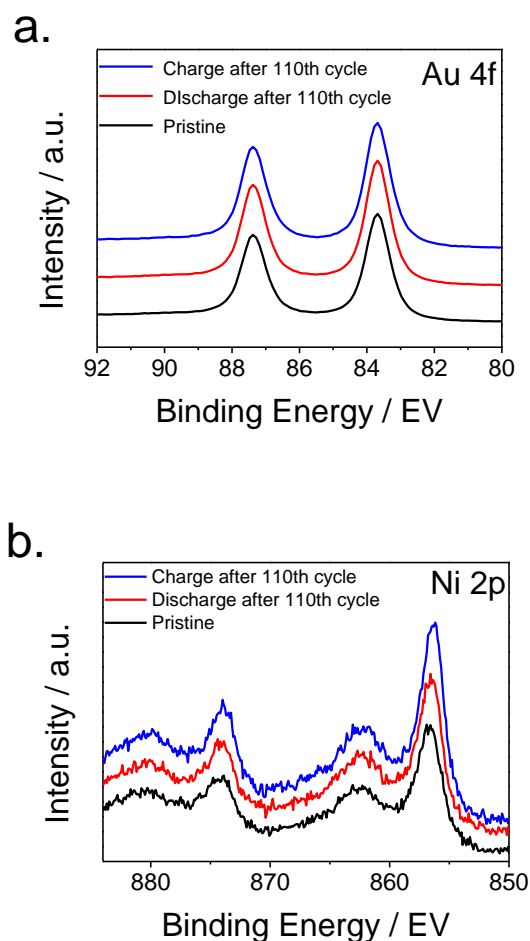


Figure 3-12. XPS spectra of pristine, after 110th charged and discharged electrode. (a) Au 4f and (b) Ni 2p

XPS does not show change the spectra of Au and Ni element during the long cycles. SEM images show that Li_2O_2 was covered with the pores of Au/Ni electrode upon fully discharge but the clogged pores was almost recovered after charge. The morphology of Au/Ni electrode almost has not been changed compared to the pristine one shown in **Figure 3-13**. XRD patterns of the cycled Au/Ni electrode were also not changed compared to the pristine one. Crystalline Li_2O_2 peaks are clearly visible after 1st discharge but its peak intensity significantly decreased after 110th cycle. It is reported that the accumulated Li_2CO_3 and lithium carboxylates on the cathode surface hinder the nucleation and crystallization of Li_2O_2 during the subsequent discharge, leading to the formation of amorphous Li_2O_2 .¹⁰² It has been already reported that formation of Li_2CO_3 occurred through ether-based electrolytes decomposition during the cycles.^{53a} Li_2CO_3 formed from TEGDME, however, generally are non-crystalline therefore not sensitive to XRD method.

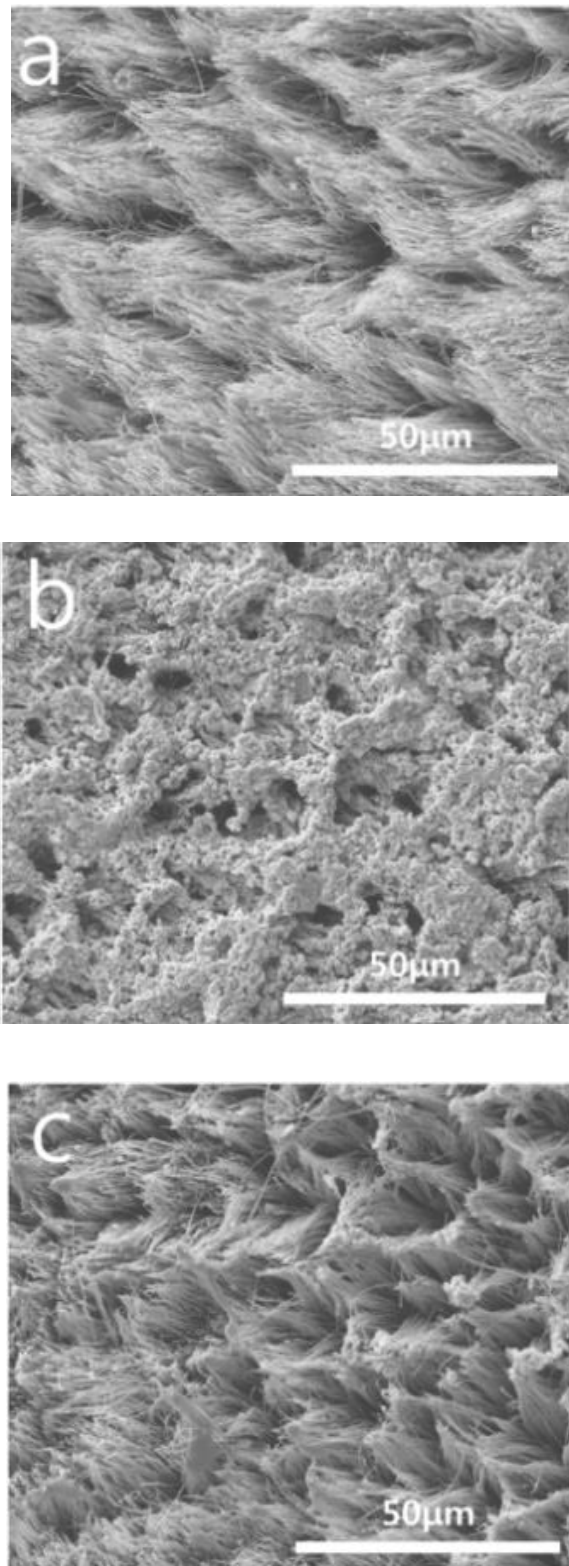


Figure 3-13. SEM images of Au/Ni electrode (a) pristine, (b) after discharged 110th cycle and (c) after charged 110th cycle

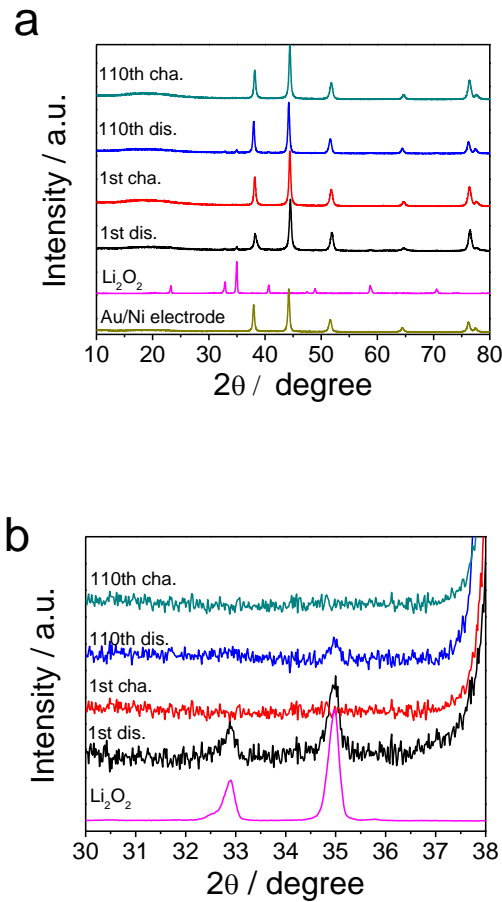


Figure 3-14. XRD patterns of (a) pristine Au/Ni electrode, Li₂O₂ and the electrode after 1st discharge and charge, 110th discharge and 110th charge. (b) magnified peaks (a).

To confirm the presence of Li₂CO₃, FT-IR, Raman and XPS were conducted (**Figure 3-15** and **3-16**). However, unfortunately the spectra from FT-IR and Raman were too noisy to be assigned. Only XPS displayed that Li₂O₂ was formed and decomposed, and that Li₂CO₃ has been accumulated during cycles, which is related to electrolyte decomposition.

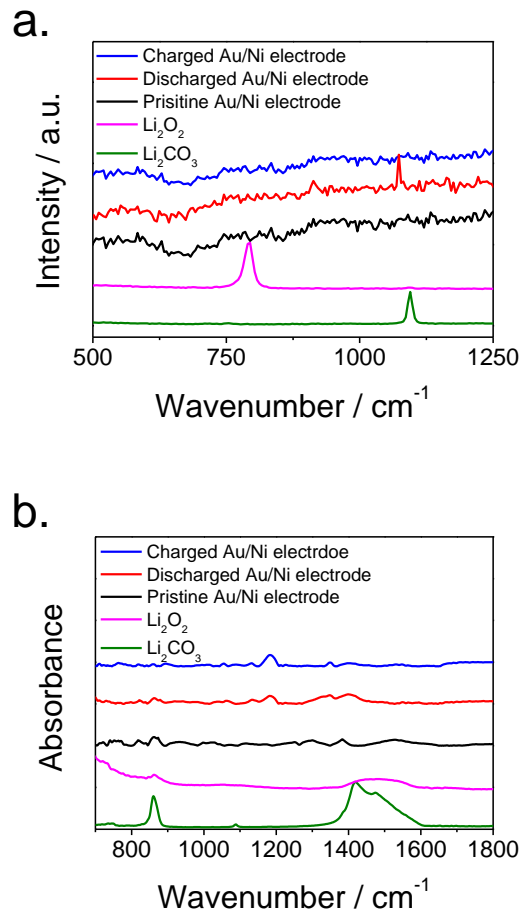


Figure 3-15. (a) Raman and (b) FT-IR spectra of Au/Ni electrode, Li_2O_2 , and Li_2CO_3 . Both spectra, however, are too noisy to be assigned.

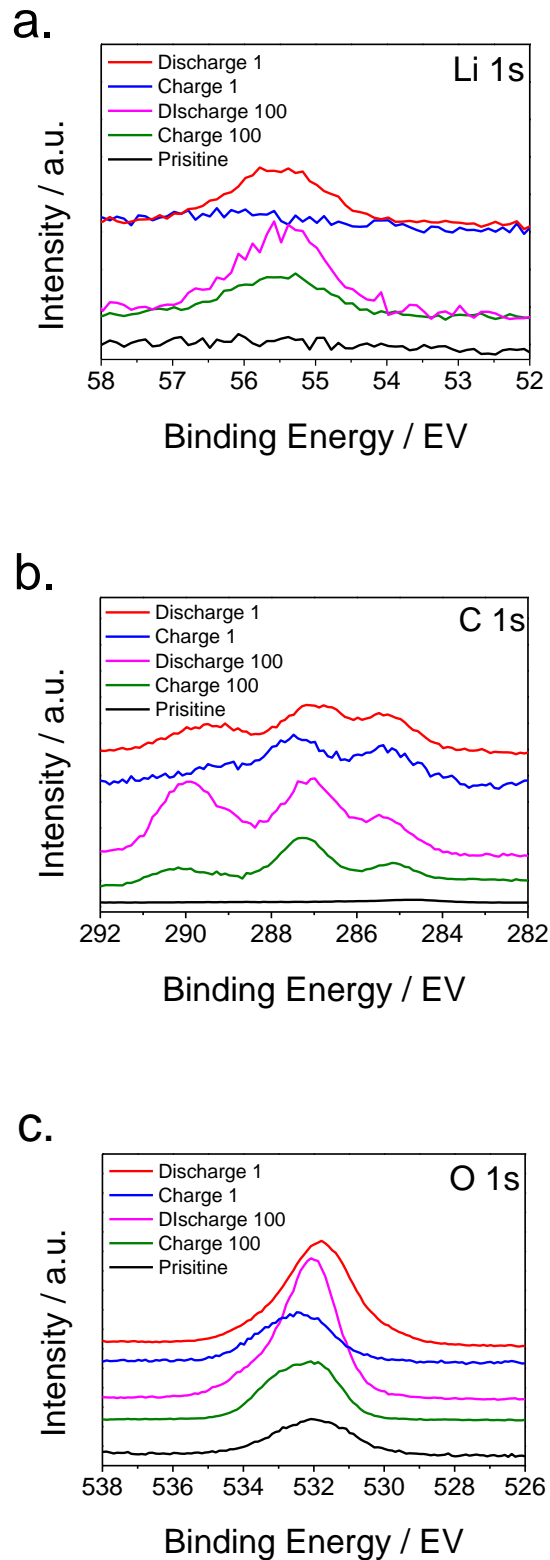


Figure 3-16. XPS spectra of (a) Li 1s, (b) C 1s, and (c) O 1s. Pristine Au/Ni electrode, after 1st and 100th charge and discharge electrode. O 1s spectra of pristine sample at 531.7 eV are related with nickel oxide layer which is formed on nickel under normal conditions in air.

Therefore we could infer that the gradual capacity fade is related with the electrolyte decomposition, but it was found Au/Ni electrode still wetted with the electrolyte, when the cell was disassembled. Thus electrolyte exhaustion was not the direct cause of the capacity fading. The Li anode, on the other hand, was covered with a dark black layer at its interface with the separator, whereas shiny metallic Li was still found on the current collector side. Once the dark surface was scratched, the area under the dark surface kept still shiny silver. A clue to the origin of the capacity fading can be further explained by examining SEM images of the Li metal (**Figure 3-17**). To investigate the surface of Li metal, SEM was conducted after 50th and 110th cycle. After 110th cycle, vividly developed black layer was observed, indicating that the capacity fading is not because of Au/Ni electrode but of Li anode.

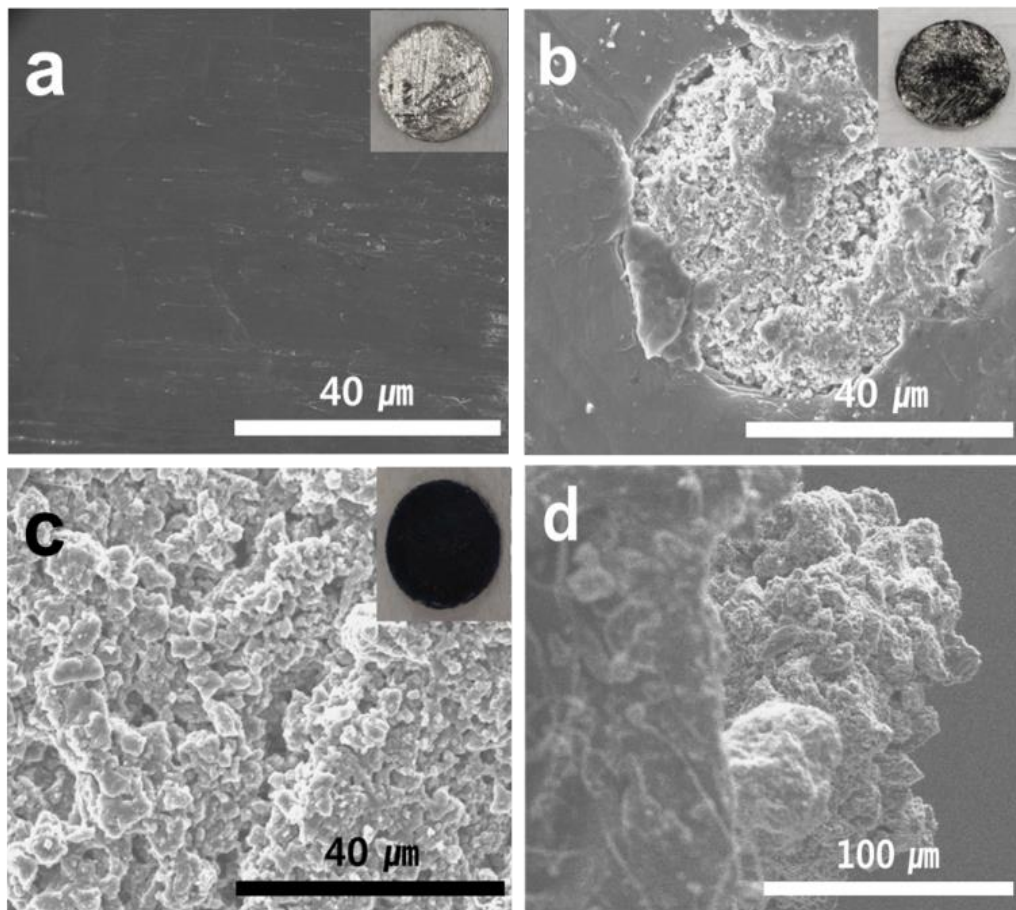


Figure 3-17. Morphology change of Li metal. (a) Fresh Li metal, (b) after 50th cycled Li, (c) after 110th cycled Li, and (d) cross sectional image of (c).

To prove this, another identical cell was rebuilt by using the used Au/Ni electrode but with a new Li metal, separator and fresh electrolyte. In **Figure 3-18a** and **b**, the rebuilt cell exhibited almost same voltage profile as shown in the **Figure 3-11a** and **b**. **Figure 3-18c** shows the summation of cycle result. Interestingly, the capacity fading occurred again around 100 cycles and also the Li anode showed a similar appearance to that observed in the first 110th cycled electrode. Recently, it is reported that the reaction of Li anode with H₂O was formed through electrolyte decomposition (TEGDME).¹⁰³ The Li metal is found to have limited reversibility, whereas the thickness of LiOH layer increases steadily as the cycling progressed possibly resulting from the reaction of Li with H₂O. We believe that the capacity fading is because of the passivation of Li anode that underwent an irreversible phase transformation during the cycling by influence of H₂O.

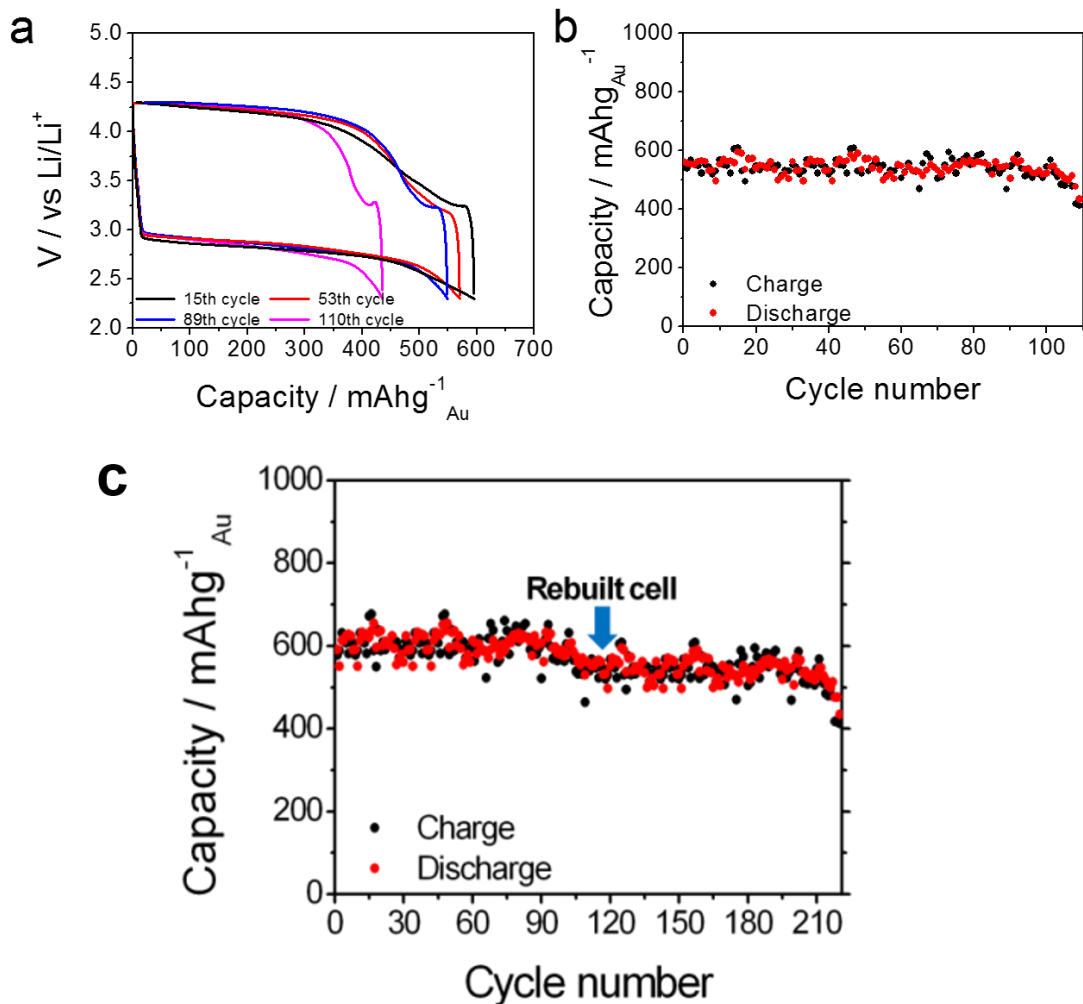


Figure 3-18. Capacity and cycle result of rebuilt cell. (a) voltage profiles of rebuilt cell, (b) cycle graph of (a), and (c) the summation cycle graph of the pristine and rebuilt cells.

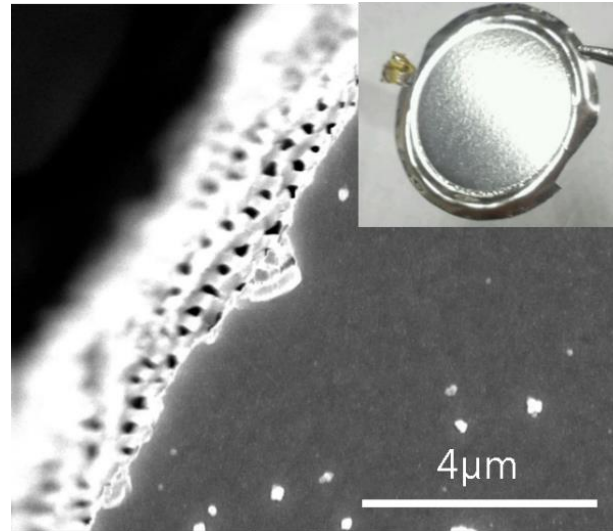


Figure 3-19. SEM image and picture of Ni nanoparticles coated on the front side of AAO.

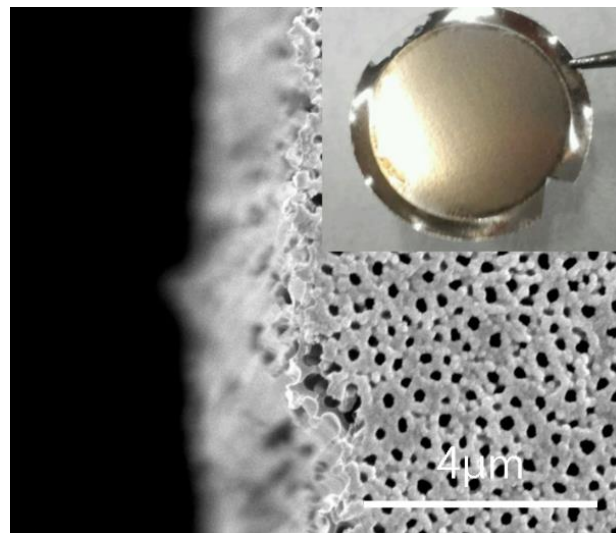


Figure 3-20. SEM image and picture of Ni nanoparticles coated on the back side of AAO.

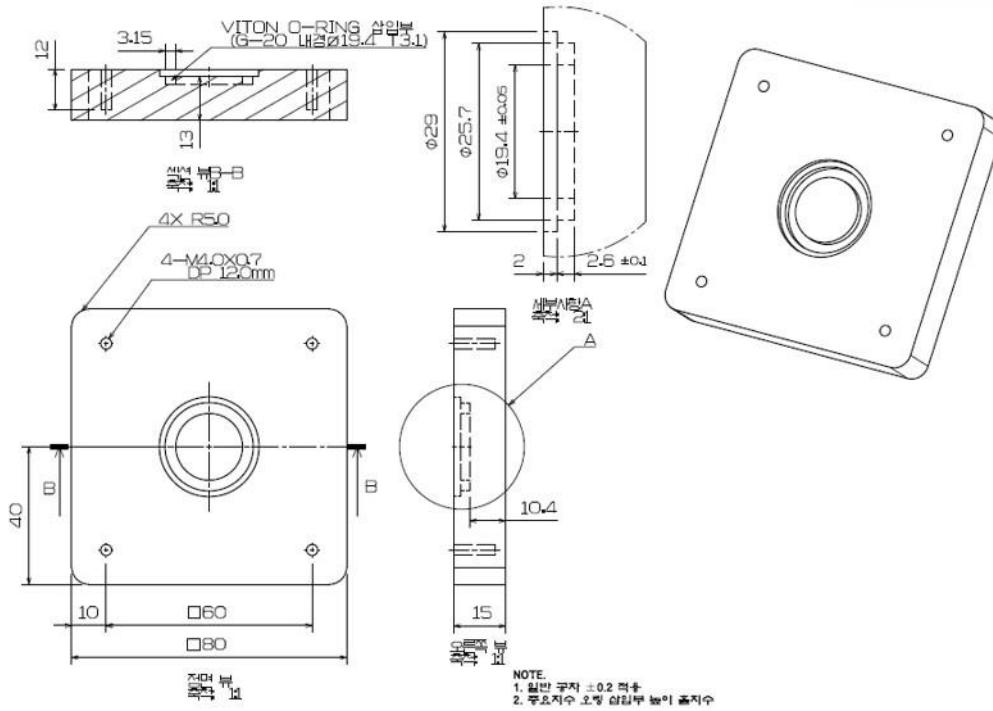


Figure 3-21. The blue print of a bottom part of homemade kit for electrodeposition. (Especially for AAO template)

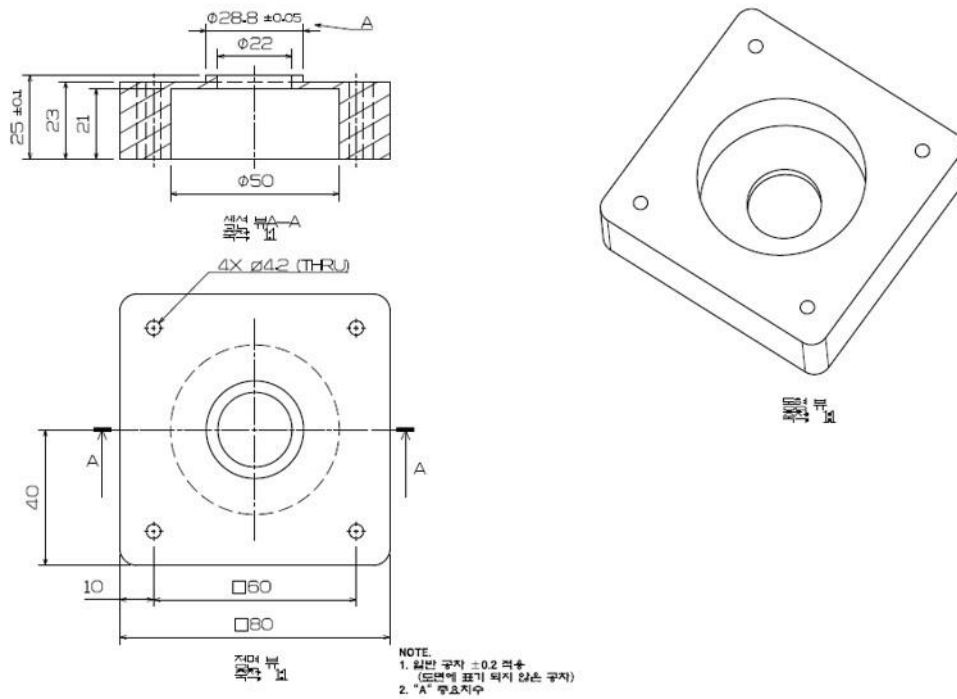


Figure 3-22. The blue print of a top part of homemade kit for electrodeposition. (Especially for AAO template)

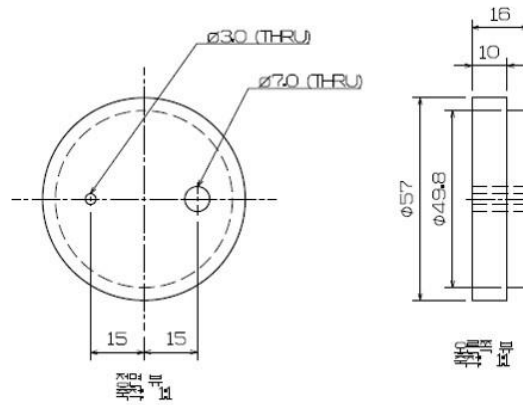


Figure 3-23. The blue print of a cap part of homemade kit for electrodeposition. (Especially for AAO template)



Figure 3-24. The real picture of Ni nanowire current collector made by homemade electrodeposition kit.

3.2.4 Conclusion

We have designed a highly efficient Au/Ni electrode by simple electrodeposition method for Li-O₂ battery, resulting in improved cycle stability and enhanced capacity compared with nanoporous Au leaf. It was shown that Au nanoparticles which were effectively fabricated on Ni nanowire substrate with minimizing quantity simultaneously maximizing active sites can show much larger capacity than that of nanoporous Au leaf electrode. In addition, Li-O₂ cell composed of the Au/Ni electrode can sustain excellent reversible cycling over 200 cycles (including rebuilt cell test). These results far exceeded the stability obtained at carbon cathodes. We confirm that the capacity fading was because Li metal passivation due to the electrolyte decomposition (TEGDME), not the Au/Ni electrode. This study indicates that it should further motivate the development of a decomposition-free electrolyte that could alleviate the Li anode.

4. Experiment II

4.1 A Possibility of Silver catalyst as a Carbon- and Binder-free Cathode material on Different Electrolytes for Lithium-oxygen Batteries

Abstract

Silver (Ag), which has not so many been used to a catalyst for lithium-oxygen (Li-O₂) battery because of its instability at high voltages, is utilized as an oxygen reduction reaction (ORR) catalyst. The positive limit of gold and platinum is approximately 4.5 V ~ 5.0 V vs. Li/Li⁺, meanwhile the limit of silver is around 3.6 V ~ 3.8 V vs. Li/Li⁺ in propylene carbonate (PC), dimethoxyethane (DME) and tetrahydrofuran (THF) solution.¹⁰⁴ However, since the electrochemical behavior of an electroactive material is substantially affected by the electrolytes, we examine the electrochemical performance of Ag catalyst in a family of etheral solvents (1,2-dimethoxyethane (DME), diethylene glycol dimethyl ether (DEGDME), tetraethylene glycol dimethyl ether (TEGDME), dimethylformamide (DMF), dimethyl sulfoxide (DMSO), and *N*-methyl-2-pyrrolidone (NMP) with 1M lithium bis-trifluoromethylsulfonylimide (LiTFSI) to find proper electrolytes on Ag catalyst for Li-O₂ batteries. To maximize active sites of Ag catalyst and to clarify its innate performance, Ag is used as an electrode (denoted as Ag/Ni electrode). Our investigation reveals that the NMP-based electrolyte exhibits superior electrochemical properties. The Ag/Ni electrode with NMP/1M LiTFSI delivers a capacity of 473 mAhg⁻¹_{Ag} at 100 mA_g⁻¹_{Ag} under between 2.3 V and 3.8 V and shows stable cycling performance until 35th with 300 mAhg⁻¹_{Ag} cut off condition at 100 mA_g⁻¹_{Ag}.

4.1.1 Introduction.

The aprotic lithium-oxygen (Li-O₂) batteries have been attracting many researchers because of its possibility and high theoretical specific energy density of about 3,500 Wh kg⁻¹, which significantly exceeds most other conventional electrochemical batteries.^{74, 76} The capacity of Li-O₂ battery is based on a simple electrochemical reaction, which is formation of Li₂O₂ during discharge based on oxygen reduction reaction (ORR) and decomposition of the Li₂O₂ during charge based on oxygen evolution reaction (OER) according to this reaction: $2\text{Li}^+ + 2\text{e}^- + \text{O}_2 \leftrightarrow \text{Li}_2\text{O}_2$ ($E_0 = 2.96 \text{ V vs Li/Li}^+$).³⁴ Although the electrochemical reaction seems so easy, it is still difficult for Li-O₂ batteries to be practical application because there are many problems which have to be elucidated and solved, such as high over-potential that associated with sluggish charge transfer kinetics,^{92a, 105} instability of electrolytes during dis/charge processes,^{91b, 106} and instability of carbon electrode during charge process.^{51a} Among these problems, regarding the carbon cathode which is the most commonly used to oxygen electrode to store the discharge products (Li₂O₂),⁹⁴ it is reported that Li₂O₂ can react with carbon cathode,⁸³ and that chemically generated LiO₂ can react with PVDF binder which is also common binder to make a carbon electrode.⁹⁶ From these reasons, many carbon free cathodes have been reported to further controlled studies.^{33b, 51a, 54-55, 84b, 107} And indeed they exhibit quite impressive results, such as stable cycles more than 100 cycles, however, most of the results were attributed by expensive noble metals such as platinum and gold (Pt and Au).^{33b, 84b, 107a} In the case of such noble metals, there are difficulties in practical application because of a scarcity and a price of the resources. So it is important and meaningful to find another possible candidate for the carbon- and binder- free cathodes, which is inexpensive compared to Pt and Au, has good ORR and/or OER activity, and good electrical conductivity as possible. From these conditions, we employed silver (Ag) as the candidate for the cathode in Li-O₂ batteries by simple electrodeposition method same as our previous work.^{107a} It is believed that Ag mostly satisfies above conditions; Not only is the cost of Ag about 60 ~ 70 times lower than Pt and Au, but also Ag has good catalytic property for ORR and good electrical conductivity.¹⁰⁸ Although Ag has such good benefits above, it is not perfect. The Aurbach group has reported the electrochemical stability window of Ag, Pt and Au by cyclic voltammetry test on different electrolytes such as propylene carbonate (PC), dimethoxyethane (DME) and tetrahydrofuran (THF) solutions with LiClO₄, LiAsF₆, LiSO₃CF₃, and Bu₄NClO₄ salt.¹⁰⁴ Since Ag is not electrochemically stable as much as Pt and Au at high voltages, Ag has been usually used to alkaline media batteries, which have relatively lower voltage range than that of Li-O₂ battery.^{108c, 109} Very recently, Ag-MnO₂, Ag-RGO composite catalysts in nonaqueous have been reported.¹¹⁰ However, those researches have neither been conducted by only Ag catalyst, nor been

concerned with solvent species in electrolytes, which can change the electrochemical behavior and stability of an electroactive material.⁸²

In this study, we synthesized Ag/Ni electrodes, that Ag nanoparticles are deposited on Ni nanowire current collector by simple electrodeposition method, to evaluate the innate performance of Ag catalyst and design suitable electrolyte systems in order to apply Ag catalyst to the aprotic Li-O₂ battery system. We evaluated the electrochemical performance of Ag/Ni electrodes with six different electrolytes, which are 1,2-dimethoxyethane (DME), diethylene glycol dimethyl ether (DEGDME), tetraethylene glycol dimethyl ether (TEGDME), dimethylformamide (DMA), dimethyl sulfoxide (DMSO) or *N*-methyl-2-pyrrolidone (NMP), to figure out the impact of solvent species on electrochemical properties of Ag catalyst in Li-O₂ batteries

4.1.2 Experimental Section.

Fabrication of Ag/Ni electrode. A Preparation of Ni nanowire substrate is described in detail in our previous work,^{107a} This prepared Ni substrate was placed on a Ni foil current collector again and covered by a 23 mm rubber O-ring in a homemade Teflon electroplating cell and put the plating electrolyte consisting of 0.02 M AgCH₃CO₂ (Sigma Aldrich), 1.5 M KSCN (potassium thiocyanate) (Sigma Aldrich) and 2 M NH₄Cl (Daejung chemical) in DI water. Electroplating was performed under pulse condition that voltage of -2.0V 2 sec and then rest 10 sec were applied by turns for 3 minutes and thus actual depositing time is 30 sec. After deposited, the disk was washed with DI water several times and then dried in vacuum oven. The loading quantity of Ag was estimated via inductively coupled plasma (ICP) analysis. The amount of Ag was 65 μg/cm².

Fabrication of electrolytes. All chemicals; 1,2-dimethoxyethane (DME), diethylene glycol dimethyl ether (DEGDME), tetraethylene glycol dimethyl ether (TEGDME), dimethylformamide (DMF), dimethyl sulfoxide (DMSO), and *N*-methyl-2-pyrrolidone (NMP) and lithium bis-trifluoromethylsulfonylimide (LiTFSI) salt; were purchased from Sigma Aldrich and were used as received. The concentration of LiTFSI salt in all solvents was a 1.0 M. All electrolytes were prepared in an argon-filled glove box.

Assemblage of the Li-O₂ full-cell. For electrochemical full cell test, Swagelok-type Li-O₂ cell consisting of Ag/Ni electrode punched by 1.23 cm² (12.5pi), glass microfiber filter punched by 1.27 cm² (12.7pi) (Whatman grade GF/D), lithium foil punched by 1.23 cm² (12.5pi) without additional pretreatment, and 200 μL of electrolyte. The assemblage of all cells was carried out in a dry room where a dew point is below 65.0 °C.

Electrochemical characterization of the full-cell. For the electrochemical characterizations, the Ag/Ni electrode was cycled by 2 different ways that one is full dis/charge condition from 2.3 V to 3.8 V and the other is capacity cut off condition with 300 mAhg⁻¹_{Ag} (at 100 mA g⁻¹_{Ag} current condition. under 1atm O₂ blowing at 24°C, Wonatech Co. Ltd.)

Characterization of Ag/Ni electrodes. Field Emission Scanning Electron Microscopy (FESEM) (FEI nano 230), normal transmission electron microscopy (TEM) (JEOL Inc.) operating at 200 kV, energy-dispersive spectroscopy (EDS, JEM-2100, JEOL Inc.) elemental mapping, X-ray diffractometer (XRD) (D/Max2000, Rigaku). X-ray photoelectron spectroscopy (XPS) (Thermo Scientific Kα spectrometer, 1486.6eV).

4.1.3 Results and Discussion.

Ag nanoparticles were directly grown up on Ni nanowire substrate to maximize Ag utilization by simple electrodeposition method details in our previous work.^{107a} By means of this unique method, we effectively coated minimum amount of Ag nanoparticles on Ni nanowire substrate to the extent that maximum capacity can be utilized. **Figure 4-1** displays SEM, TEM images of Ni nanowire substrate (**4-1a** and **c**) and Ag/Ni electrode on which Ag amount of $65 \mu\text{g cm}^{-2}$ was deposited (**4-1b** and **d**). Energy dispersive X-ray spectroscopy (EDX) confirmed the elements of Ag/Ni electrode (**4-1e** and **f**).

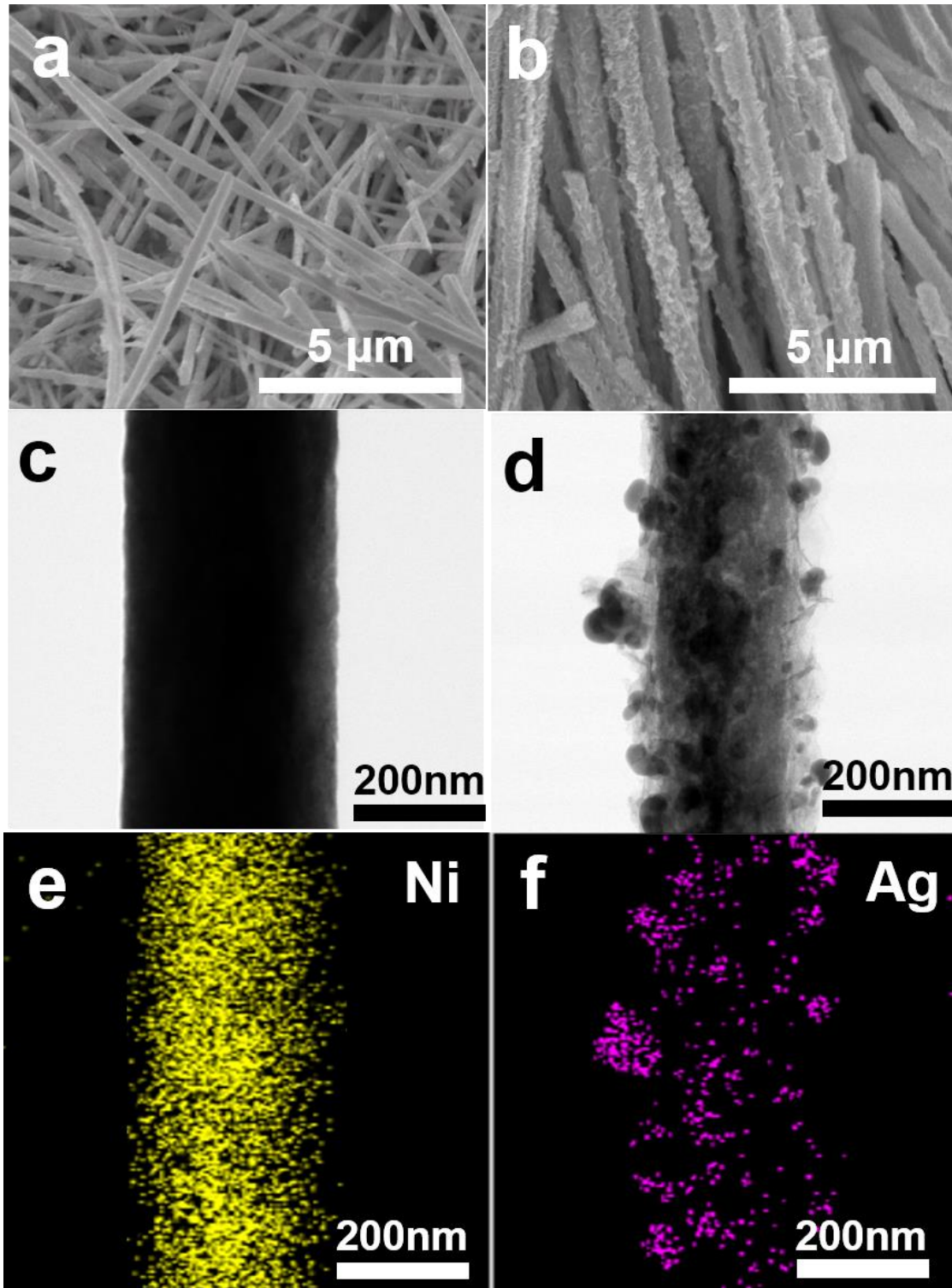


Figure 4-1. The morphology of Ni nanowire substrate and Ag/Ni electrode and EDX image. SEM images of the as-fabricated (a) Ni nanowire, (b) Ag/Ni electrode, TEM images of (c) Ni nanowire substrate, (d) Ag/Ni electrode, and EDX images of (e) Ni, and (f) Ag element, respectively.

The full cell tests of Ag/Ni electrode with six different electrolytes were conducted at current rate of $100 \text{ mA g}^{-1}_{\text{Ag}}$ in 1.0 M LiTFSI in each electrolyte with DME, DEGDME, TEGDME, DMF, DMSO or NMP solvent under 1 atm O_2 blowing at 24°C . Criteria of designing the suitable electrolyte system were following. 1) avoiding carbonate solvents, which were known to produce undesirable Li_2CO_3 or LiRCO_3 during discharging and CO_2 during charging,^{32c, 91b} 2) choosing the general solvents which have been reported many times to easily understand the properties of those,^{77, 106, 111} and 3) picking the solvents, which have the stability toward superoxide radicals and provide stable $[\text{Li}^+(\text{solvent})-\text{O}_2^-]$ complexes.⁷⁷ **Figure 4-2** shows voltage profiles of cells during the first 2 cycles in six different electrolytes and **Table 4-1** shows the specific capacities of them. Discharge capacities and cycling performance of the Ag/Ni electrode were greatly affected by the electrolytes. The discharge capacities of 1st cycle in each electrolyte were $224 \text{ mAh g}^{-1}_{\text{Ag}}$ (DME-based), $94 \text{ mAh g}^{-1}_{\text{Ag}}$ (DEGDME-based), $85 \text{ mAh g}^{-1}_{\text{Ag}}$ (TEGDME-based), $672 \text{ mAh g}^{-1}_{\text{Ag}}$ (DMF-based), $693 \text{ mAh g}^{-1}_{\text{Ag}}$ (DMSO-based), and $473 \text{ mAh g}^{-1}_{\text{Ag}}$ (NMP-based), respectively. Interestingly, the 2nd discharge capacities of DMF- and DMSO-based electrolytes, which showed high capacities at 1st cycle, were dramatically decreased to $30 \text{ mAh g}^{-1}_{\text{Ag}}$ and $102 \text{ mAh g}^{-1}_{\text{Ag}}$, respectively. Note that only NMP-based electrolyte maintains the reversible capacity, as shown in **Figure 4-2** and **Table 4-1**.

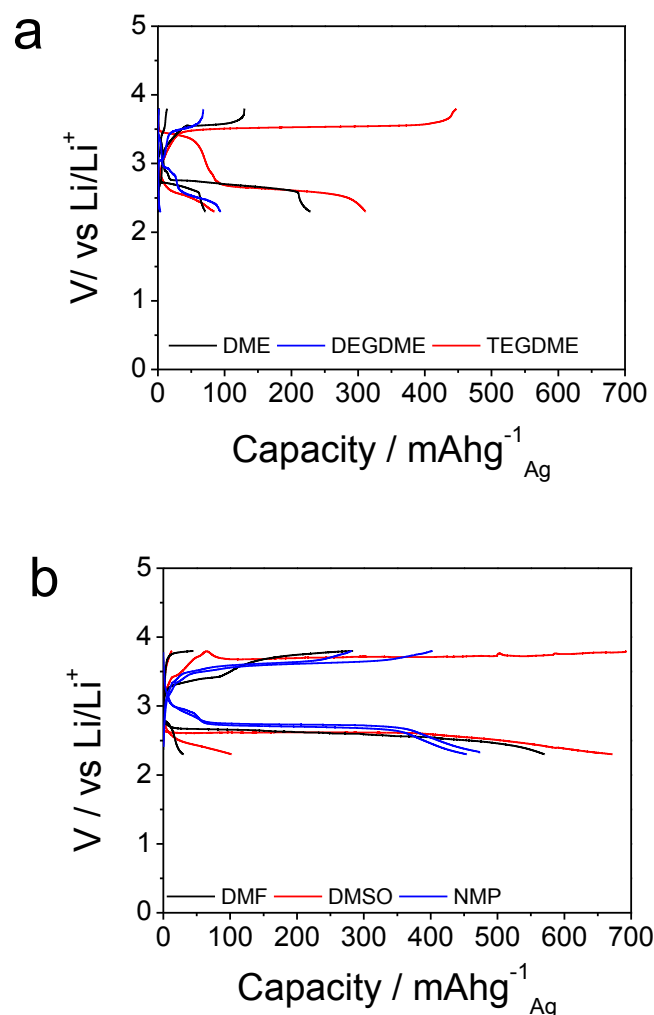


Figure 4-2. The first 2 cycles of voltage profiles using Ag/Ni electrode on different electrolytes at 100 mA g⁻¹ Ag. (a) Voltage profiles of Ether based electrolytes and (b) high donor number electrolytes.

	1,2-Dimethoxyethane (DME)	Diethylene glycol dimethyl ether (DEGDME)	Tetraethylene glycol dimethyl ether (TEGDME)	Dimethyl formamide (DMF)	Dimethyl sulfoxide (DMSO)	N-methyl-2-pyrrolidone (NMP)
1 st cycle (mAhg ⁻¹ Ag)	224	94	85	672	693	473
2 nd cycle (mAhg ⁻¹ Ag)	71	13	311	30	102	454

Table 4-1. The specific capacity of each electrolyte.

To figure out the different cycling properties of electrolytes, we disassembled the cells after 2nd cycle and found severely discolored separators except for that cycled in the NMP-based electrolyte. To investigate the origin of the discoloration of separators, the Ag/Ni electrodes were

examined by SEM (**Figure 4-3**) and XPS (**Figure 4-4**) measurements. The SEM images revealed that a severe passivation layer covered all the pores of Ag/Ni electrode only after 2 cycles between 2.3 V and 3.8 V. However, in the case of NMP/1M LiTFSI electrolyte, just some clogged pores were observed. The morphology of Ag/Ni electrode in NMP/1M LiTFSI also almost has not been changed compared to the pristine one, as shown in **Figure 4-3**.

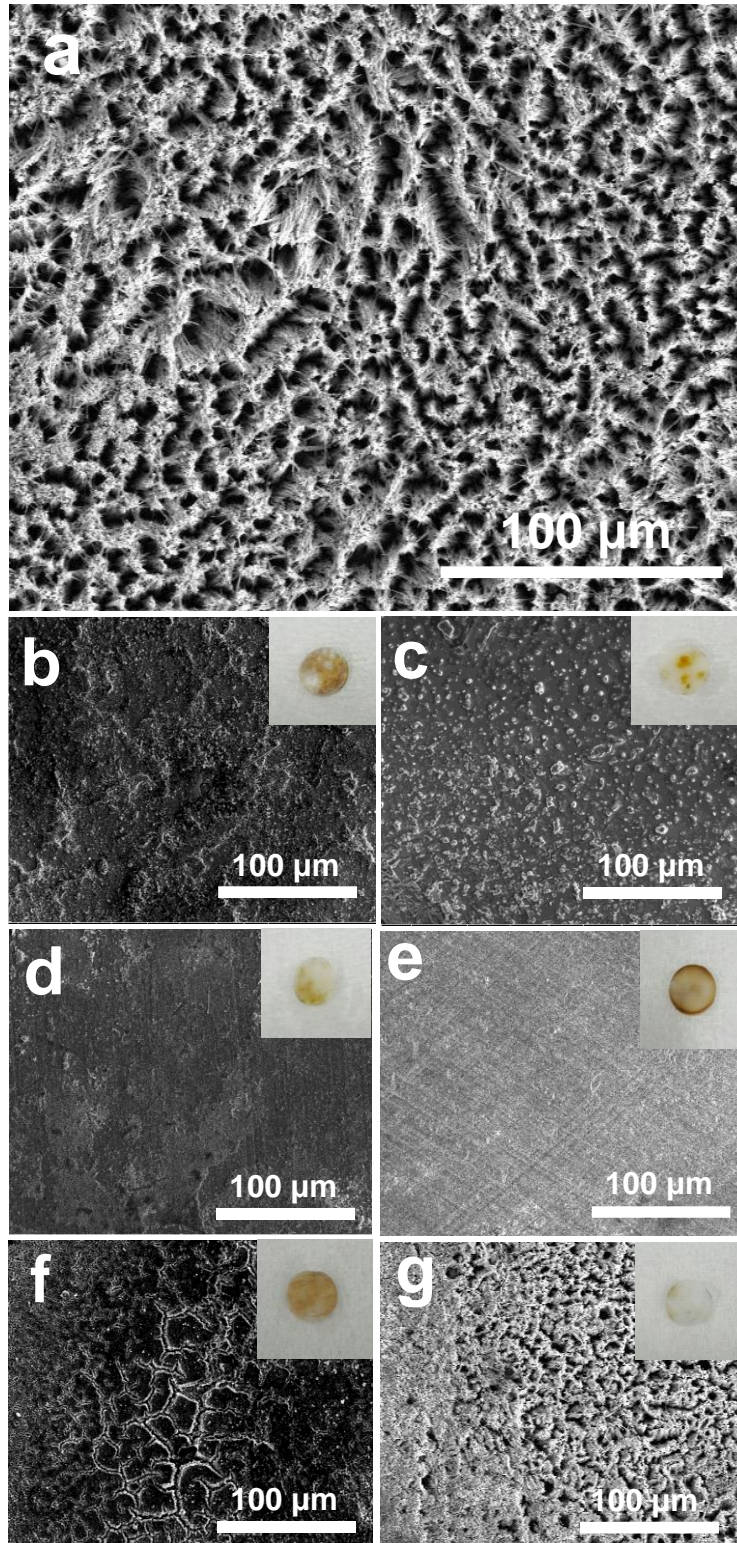
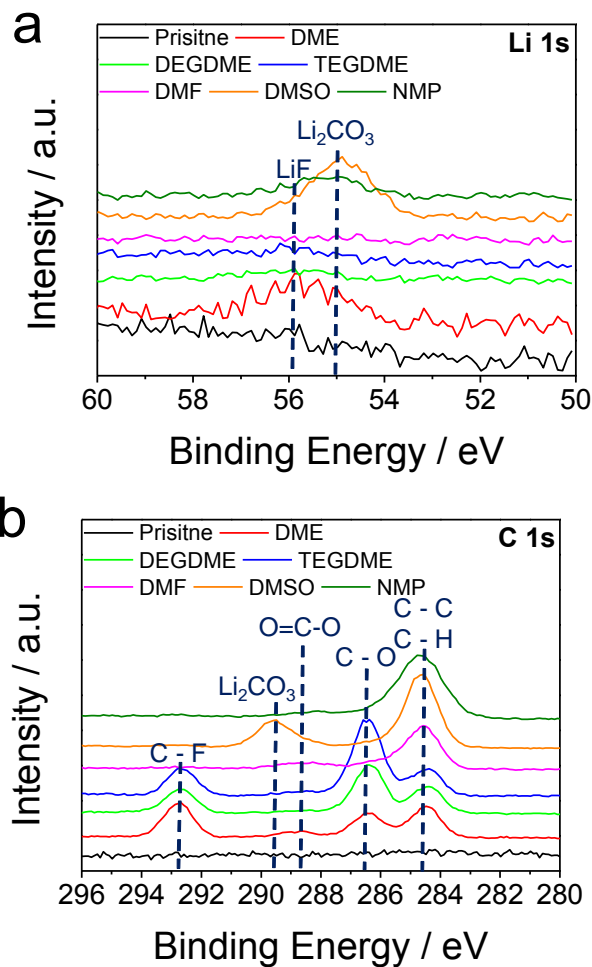


Figure 4-3. SEM image of each Ag/Ni electrode and picture of each separator. (a) pristine Ag/Ni electrode, Ag/Ni electrode and picture of separator after 2 cycles in (b) DME, (c) DEGDME, (d) TEGDME, (e) DMF, (f) DMSO, and (g) NMP respectively.

The effects of organic solvents on the surface chemistry of Ag/Ni electrodes were confirmed by a comparison of the Li 1s, C 1s, F 1s, and Ag 3d XPS spectra for the electrodes cycled in DME, DEGDME, TEGDME, DMF, DMSO and NMP with 1M LiTFSI. The DME-based electrolyte severely evaporated out of a cell during cycling because of its high volatility and electrochemically decomposed at the Ag/Ni electrode. Although less volatile ether solvent (DEGDME and TEGDME)-containing electrolytes exhibited no significant evaporation, they electrochemically decomposed at the Ag/Ni electrode and delivered very low discharge capacity of $94 \text{ mAh g}^{-1}_{\text{Ag}}$ and $85 \text{ mAh g}^{-1}_{\text{Ag}}$ at 1st cycle as shown in **Table 1**. Evidence of the electrolyte decomposition on the Ag/Ni electrodes is given in **Figure 4-4**.



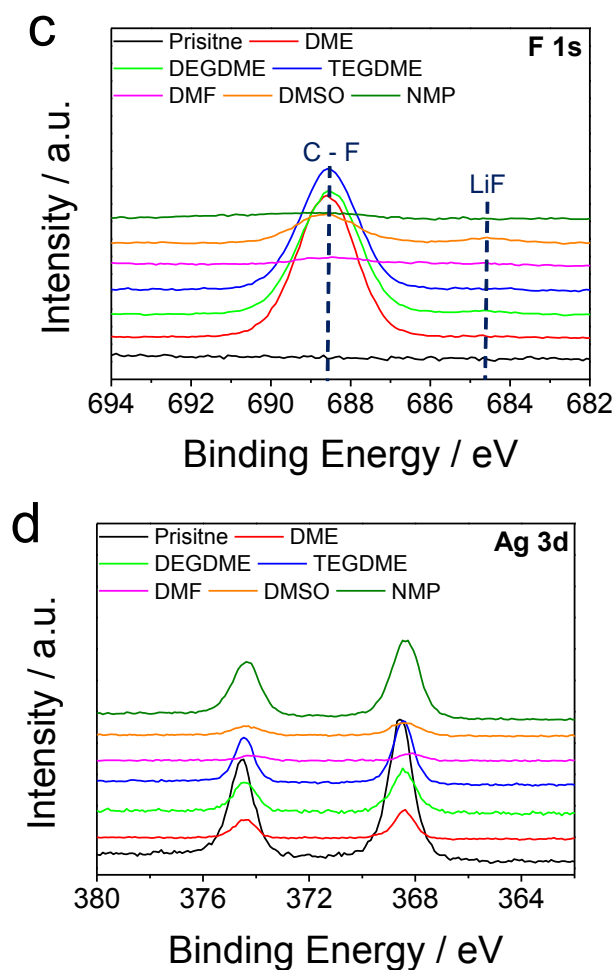


Figure 4-4. XPS spectra of Ag/Ni electrodes after 2nd cycle. (a) Li, (b) C, (c) F, and (d) Ag.

The C 1s XPS spectra (**Figure 4b**) obtained from the Ag/Ni electrodes cycled in DME, DEGDME or TEGDME with 1M LiTFSI show four types of carbon : carbon bonded to hydrogen (CH_x ; 284.8 eV), carbon singly bonded to oxygen (C-O-C; 286.8 eV), carbon double bonded to oxygen (C=O-C; 288.4 eV), carbon bonded to fluorine (C-F; 292.9 eV). These peaks may be originated from the decomposition of LiTFSI salt and ether solvents. The Li 1s, F 1s (**Figure 4-4a** and **c**) and S 2p (**Figure 4-5**) XPS spectra further confirmed that the LiTFSI salt and ether solvents undergo the electrochemical decomposition at the Ag/Ni electrode.

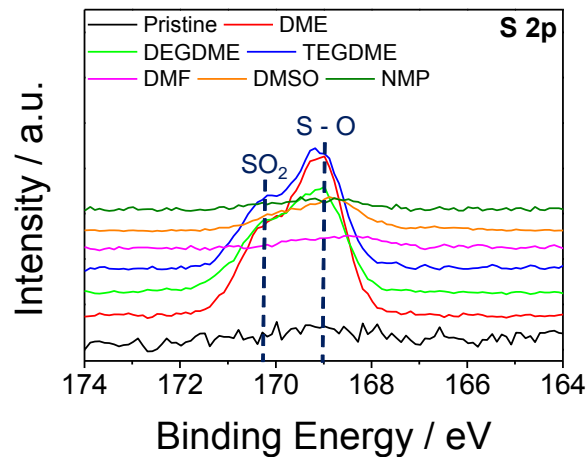
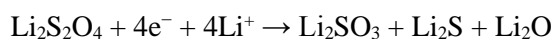
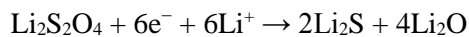
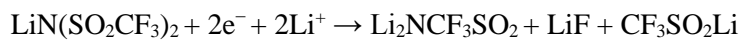
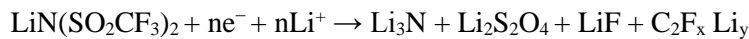


Figure 4-5. XPS spectra of Ag/Ni electrodes after 2nd cycle.

The peak at 55.8 eV in **Figure 4-4a** and 684.8 eV in **Figure 4-4c** can be ascribed to the LiF and 688.4 eV in **Figure 4-4c** can be assigned to the C-F bond originated from the LiTFSI decomposition upon discharge.¹¹² The broad peak at 169 eV and 170.2 eV of S 2p in **Figure 4-5** greatly increased compared to pristine Ag/Ni electrode. The Aurbach group has proposed the reductive decomposition of LiTFSI as follows.¹¹³



The XPS results are in accordance with the above reaction and suggest that the ether-based electrolytes with LiTFSI salt can readily decomposed at the Ag/Ni electrode and the surface of Ag/Ni electrode is mainly covered with the decomposition products of LiTFSI salt. Accordingly, the peak intensity corresponding to Ag decreased after 2 cycles (**Figure 4-4d**). Meanwhile, the DMF and DMSO/1M LiTFSI electrolytes showed the different results. The decomposition of DMF/1M LiTFSI can be explained by the N 1s XPS spectra of **Figure 4-6**.

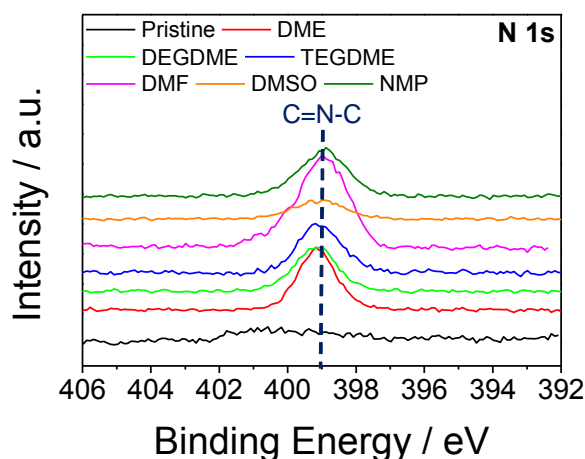


Figure 4-6. XPS spectra of Ag/Ni electrodes after 2nd cycle.

Since the XPS results presented no evidences related to the LiTFSI decomposition, it can be thought that the decomposition of DMF predominately occurs rather than that of the LiTFSI salt. The Bruce group reported about the reaction between the DMF solvent and reduced O_2 species.¹⁰⁶ The O_2^- either can react with Li^+ ions or attack the CO group resulting in formation of LiO_2 and carbon radical so that they attack on the DMF molecule yielding HCO_2Li , CO_2 , H_2O and NO . Ag/Ni electrodes cycled in DMSO/1M LiTFSI clearly show the peak corresponding to lithium carbonate (Li_2CO_3) at 289.5 eV, which was not observed for other electrolytes (**Figure 4-4b**). Recently, the Younesi group demonstrated that Li_2O_2 reacts with DMSO solvent resulting in the formation of carbonates species such as Li_2CO_3 .¹¹⁴ They explained that the weak acidic methyl groups in DMSO can react with a strong base Li_2O_2 , forming hydroperoxy radical.¹¹⁵ In addition, very recently M. Marinaro reported that Li_2O might react with the DMSO.¹¹⁶ Once the O_2 molecules which are dissolved in the electrolyte reach the Li surface, Li_2O can be easily formed and the Li_2O might further react with the DMSO molecules through an acid–base reaction. Thus, we could deduce that the solvent decomposition mainly occur in DMSO electrolytes, not the LiTFSI salt. (The decomposition mechanism is shown in **Figure 4-10**)

From their study, it is obvious that the decomposition of the DMSO solvent cannot be avoided at the Ag/Ni electrode. In addition, the clear peak of Li 1s XPS spectra of **Figure 4-4a** can be assigned to lithium carbonate (Li_2CO_3), rather than Li_2O_2 or $LiOH$.^{115, 117} The Li 1s and C 1s XPS spectra in **Figure 4-4a, b** and S 2p XPS spectra in **Figure 4-6** manifest that the surface layer formed on the Ag/Ni electrode mainly consists of the sulfur and carbonate-containing compounds produced by the solvent decomposition. From the XPS studies for the cycled Ag/Ni electrodes, we could confirm that the severe capacity fading of the Ag/Ni electrode with DMF and DMSO/1M LiTFSI closely linked to a thick surface layer generated not by the salt decomposition

but by the decomposition of DMF and DMSO solvents. This thick surface layer blocks the Ag signal of the Ag/Ni electrode and thereby the Ag peak intensity in **Figure 4-4d** was extremely lower than that of pristine Ag/Ni electrode. However, the peaks ascribed to the significant decomposition of NMP solvent and LiTFSI salt was not observed, as displayed in the XPS spectra of Li 1s, C 1s, F 1s in **Figure 4-4** and S 2p in **Figure 4-5** and N 1s in **Figure 4-6**. Moreover, the Ag peak intensity in **Figure 4-4d** was comparable with that of pristine Ag/Ni electrode unlike the results of the other electrolytes. We could deduce from the SEM images in **Figure 4-3** and XPS data in **Figure 4-4** that the NMP/1M LiTFSI has relatively superior stability compared to other electrolytes in Li-O₂ cells with the Ag/Ni electrode. Superior electrochemical stability of the NMP-based electrolyte can be explained by the chemical structure and stability toward the Li metal anode of NMP solvent. As shown in **Table 4-2**,^{32b}

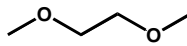
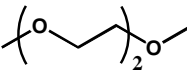
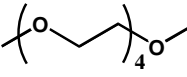
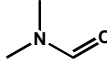
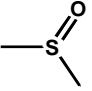
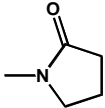
	1,2-Dimethoxyethane (DME)	Diethylene glycol dimethyl ether (DEGDME)	Tetraethylene glycol dimethyl ether (TEGDME)	Dimethyl formamide (DMF)	Dimethyl sulfoxide (DMSO)	N-methyl-2-pyrrolidone (NMP)
Structure						
Donor Number	20.0	19.5	16.6	26.6	29.8	27.3
Dielectric Constant (25°C)	7.20	7.23	7.79	36.7	46.7	32.2

Table 4-2. The structure, donor number, dielectric constant values of each electrolyte

Only NMP solvent has a cyclic structure. It was reported that the linear structured solvents have relatively low dissociation ability for Li salts, because they have more open and more flexible structure resulting in the mutual cancellation of molecular dipoles.⁸² Meanwhile, the cyclic structured solvents have attributed to the intramolecular strain of the structures so that the conformation of molecular dipoles can be aligned better. Therefore, it is likely that NMP, which has partially positive charged part, N⁺, can interact with the solvated TFSI⁻ anions, and mitigates the anion decomposition at the Ag/Ni electrode. Additionally, the ¹H-NMR spectra (**Figure 4-7**) revealed that the ether-based electrolytes (DME, DEGDME, and TEGDME) and NMP-based electrolyte have better stability toward the Li metal anode, compared to DMF- and DMSO-based electrolytes. However, as mentioned above, the decomposition of LiTFSI salt cannot be avoided in ether-based electrolytes in Li-O₂ cells with the Ag/Ni electrode. From these results, it is believed that the NMP/1M LiTFSI electrolyte is suitable for the Ag/Ni electrode in Li-O₂ battery.

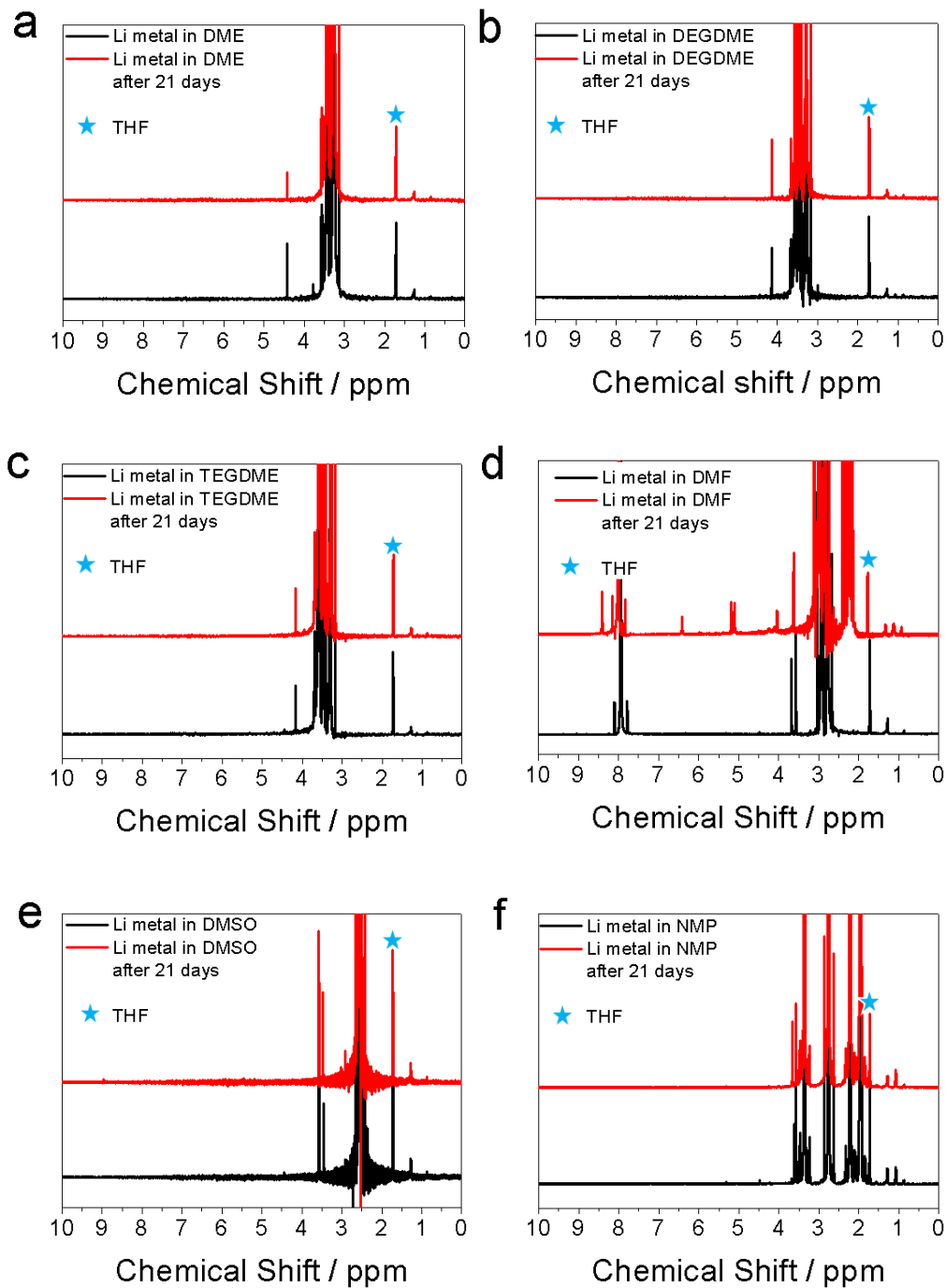


Figure 4-7. ^1H -NMR spectra of Li metal in six electrolytes. (a) DME, (b)DEGDME, (c) TEGDME, (d) DMF, (e) DMSO, and (f) NMP respectively.

Consequently, to verify further performance of Ag/Ni electrode with NMP, we conducted more cycle tests shown in **Figure 4-8**. **Figure 4-8a** exhibits the result of discharged/charged from 3.8 V to 2.3 V and **Figure 4-8b** displays the cycle performance with limited capacity of $300 \text{ mAhg}^{-1}_{\text{Ag}}$. The reason we choose the capacity of $300 \text{ mAhg}^{-1}_{\text{Ag}}$ is that the specific capacity of $300 \text{ mAhg}^{-1}_{\text{Ag}}$

1A_g is a near maximum capacity on which the discharge and charge plateau were nearly unchanged at 1st cycle in **Figure 4-8a**. Since a meaning of changing the plateau is that some reactions occur during charge and discharge processes, more improved cycling performance is expected when we conducted the cycling test under the limited capacity condition. As shown in **Figure 4-8a**, the capacity fade gradually occurs and in the case of capacity cut-off condition (**Figure 4-8b**) slight voltage degradation is observed after 35 cycles.

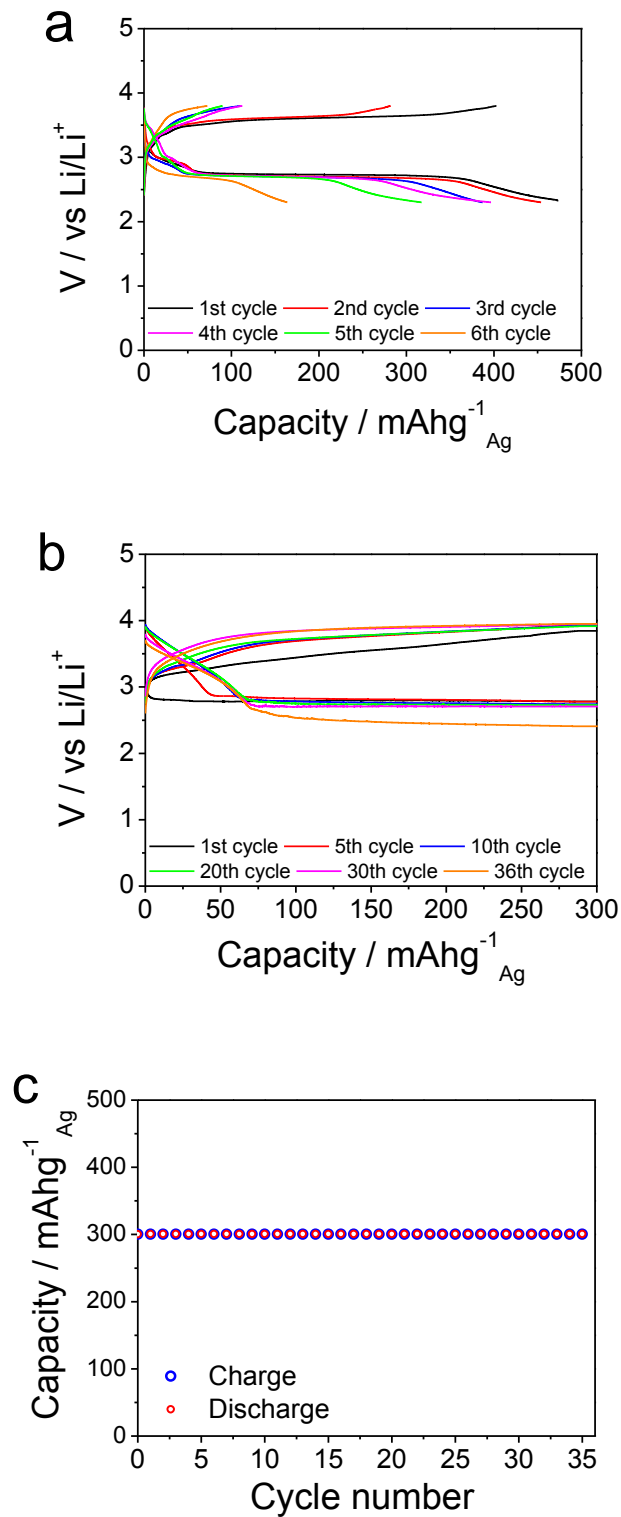


Figure 4-8. Capacity and cycle result of Ag/Ni electrode at 100 mA g⁻¹_{Ag}. (a) Voltage profiles of Ag/Ni electrode from 2.3 V to 3.8 V, (b) capacity cut off voltage profiles of Ag/Ni electrode with 300 mA h g⁻¹_{Ag}, and (c) plot of discharge capacity vs. cycle number of (b).

As confirmed by the SEM analyses shown in **Figure 4-9**, the surfaces of each cell were covered with the decomposition products. This indicates that the Ag/Ni electrode with NMP/1M LiTFSI electrolyte has reasonably good cycling stability at the initial cycles, but eventually the decomposition of NMP solvent takes place upon prolonged cycling. It has reported that the O_2^- can attack the ring CH_2 of NMP structure forming carbon radicals and these radicals result in formation of H_2O , CO_2 and NO_x .¹¹⁸ Generated H_2O , CO_2 and NO_x further react with Li_2O_2 to form Li_2CO_3 and $LiNO_x$ on the surface of the air electrodes.^{32a}

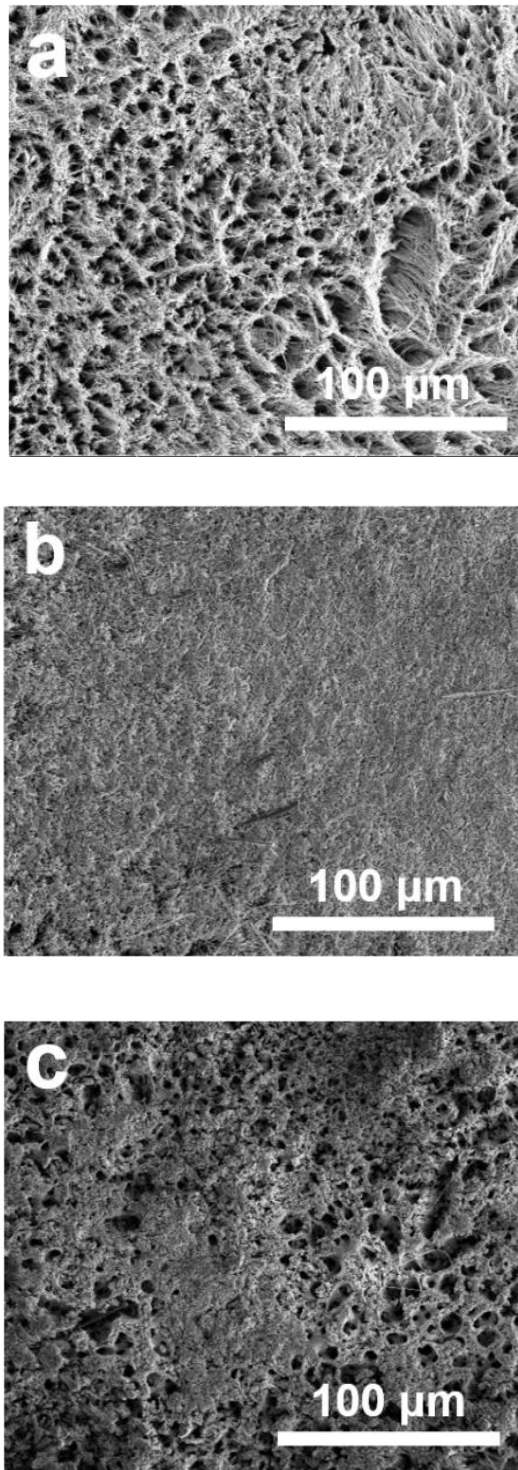


Figure 4-9. SEM images of Ag/Ni electrode (a) pristine, (b) after 6th cycle with full dis/charge condition from 2.3 V to 3.8 V and (c) after 36th cycle with 300 mAhg⁻¹ Ag capacity cut off condition.

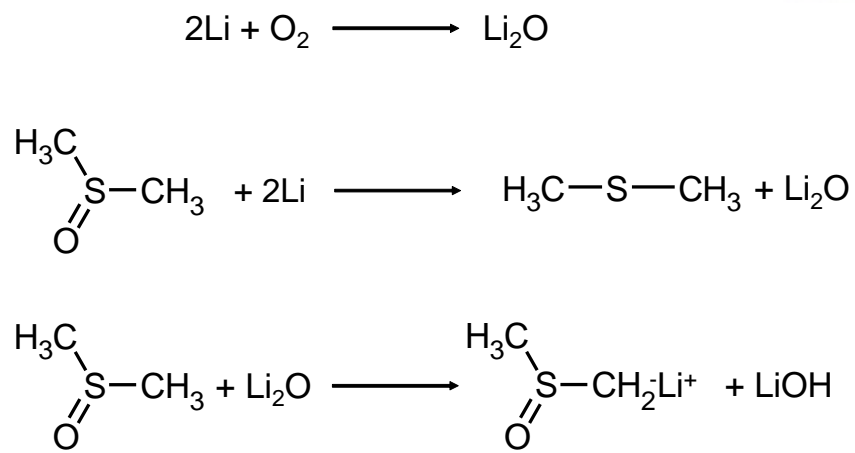


Figure 4-10. The scheme of reactions for the decomposition of DMSO solvent.

4.1.4 Conclusion.

We have designed the Ag nanoparticles effectively fabricated on Ni nanowire substrate (Ag/Ni electrode) by the electrodeposition method which is the one of the simplest metal deposition methods and simultaneously applicable method to a large scale production. By using it, we conducted full cell test with the six different electrolytes (DME, DEGDME, TEGDME, DMF, DMSO, and NMP) for Li-O₂ battery. It was shown that the poor performances were mainly caused by the decomposition of salt anions in ether-based solvent (DME, DEGDME, and TEGDME), and by the decomposition of solvents in DMF and DMSO during the discharge and charge processes using the Ag/Ni electrode. Only NMP shows the best performance among above electrolytes, which is 35 stable cycles with 300 mAhg⁻¹_{Ag} capacity cut off condition. We confirm that its cyclic structure and its stability toward Li metal anode are the reasons why NMP is more stable among the electrolytes. This study indicates that Ag with a proper electrolyte could be a potential candidate for carbon- and binder- free cathode for Li-O₂ battery. Therefore, further studies are needed to search for new and more stable solvents and lithium salts to make long-term cycling of rechargeable Li-O₂ batteries.

5. References

1. Klare, M. T., *Blood and oil : the dangers and consequences of America's growing petroleum dependency*. 1st ed.; Metropolitan Books/Henry Holt & Co.: New York, 2004; p xvi, 265 p.
2. Palacin, M. R., Recent advances in rechargeable battery materials: a chemist's perspective. *Chemical Society Reviews* **2009**, *38* (9), 2565-2575.
3. Etacheri, V.; Marom, R.; Elazari, R.; Salitra, G.; Aurbach, D., Challenges in the development of advanced Li-ion batteries: a review. *Energy & Environmental Science* **2011**, *4* (9), 3243-3262.
4. (a) Tsubota, M.; Yonezu, K.; Suematsu, K., History and Technology of the Lead-Acid-Battery in Japan. *Journal of the Electrochemical Society* **1987**, *134* (3), C107-C107; (b) Aurbach, D.; Gofer, Y.; Lu, Z.; Schechter, A.; Chusid, O.; Gizbar, H.; Cohen, Y.; Ashkenazi, V.; Moshkovich, M.; Turgeman, R.; Levi, E., A short review on the comparison between Li battery systems and rechargeable magnesium battery technology. *Journal of Power Sources* **2001**, *97-8*, 28-32; (c) Rosenman, A.; Markevich, E.; Salitra, G.; Aurbach, D.; Garsuch, A.; Chesneau, F. F., Review on Li-Sulfur Battery Systems: an Integral Perspective. *Advanced Energy Materials* **2015**, *5* (16); (d) Rahman, M. A.; Wang, X. J.; Wen, C. E., High Energy Density Metal-Air Batteries: A Review. *Journal of the Electrochemical Society* **2013**, *160* (10), A1759-A1771.
5. Tarascon, J. M.; Armand, M., Issues and challenges facing rechargeable lithium batteries. *Nature* **2001**, *414* (6861), 359-367.
6. Lu, L. G.; Han, X. B.; Li, J. Q.; Hua, J. F.; Ouyang, M. G., A review on the key issues for lithium-ion battery management in electric vehicles. *Journal of Power Sources* **2013**, *226*, 272-288.
7. Sasaki, T.; Ukyo, Y.; Novak, P., Memory effect in a lithium-ion battery. *Nature Materials* **2013**, *12* (6), 569-575.
8. Linden, D.; Reddy, T. B., *Handbook of batteries*. 3rd ed.; McGraw-Hill: New York, 2002.
9. (a) Park, O. K.; Cho, Y.; Lee, S.; Yoo, H. C.; Song, H. K.; Cho, J., Who will drive electric vehicles, olivine or spinel? *Energy & Environmental Science* **2011**, *4* (5), 1621-1633; (b) Belharouak, I.; Johnson, C.; Amine, K., Synthesis and electrochemical analysis of vapor-deposited carbon-coated LiFePO₄. *Electrochemistry Communications* **2005**, *7* (10), 983-988.
10. (a) Zhang, W. J., A review of the electrochemical performance of alloy anodes for lithium-ion batteries. *Journal of Power Sources* **2011**, *196* (1), 13-24; (b) Wu, Y. P.; Rahm,

E.; Holze, R., Carbon anode materials for lithium ion batteries. *Journal of Power Sources* **2003**, *114* (2), 228-236.

11. Ge, M.; Fang, X.; Rong, J.; Zhou, C., Review of porous silicon preparation and its application for lithium-ion battery anodes. *Nanotechnology* **2013**, *24* (42).

12. Ji, L. W.; Lin, Z.; Alcoutlabi, M.; Zhang, X. W., Recent developments in nanostructured anode materials for rechargeable lithium-ion batteries. *Energy & Environmental Science* **2011**, *4* (8), 2682-2699.

13. (a) Wu, Y. P.; Jiang, C.; Wan, C.; Holze, R., Anode materials for lithium ion batteries by oxidative treatment of common natural graphite. *Solid State Ionics* **2003**, *156* (3), 283-290;

(b) Endo, E.; Kihira, T.; Yamada, S.; Imoto, H.; Sekai, K., Surface treatment of carbon electrodes by electron beam irradiation. *Journal of Power Sources* **2001**, *93* (1-2), 215-223.

14. Shi, J. L.; Xia, Y. G.; Yuan, Z. Z.; Hu, H. S.; Li, X. F.; Zhang, H. M.; Liu, Z. P., Porous membrane with high curvature, three-dimensional heat-resistance skeleton: a new and practical separator candidate for high safety lithium ion battery. *Scientific Reports* **2015**, *5*.

15. (a) Luo, X.; Pan, W.; Liu, H. G.; Gong, J. H.; Wu, H., Glass fiber fabric mat as the separator for lithium-ion battery with high safety performance. *Ionics* **2015**, *21* (11), 3135-3139;

(b) Wu, H.; Zhuo, D.; Kong, D. S.; Cui, Y., Improving battery safety by early detection of internal shorting with a bifunctional separator. *Nature Communications* **2014**, *5*.

16. Zhang, S. S., A review on the separators of liquid electrolyte Li-ion batteries. *Journal of Power Sources* **2007**, *164* (1), 351-364.

17. Kim, C. S.; Yoo, J. S.; Jeong, K. M.; Kim, K.; Yi, C. W., Investigation on internal short circuits of lithium polymer batteries with a ceramic-coated separator during nail penetration. *Journal of Power Sources* **2015**, *289*, 41-49.

18. Kalhoff, J.; Eshetu, G. G.; Bresser, D.; Passerini, S., Safer Electrolytes for Lithium-Ion Batteries: State of the Art and Perspectives (vol 8, pg 2154, 2015). *Chemsuschem* **2015**, *8* (17), 2765-2765.

19. (a) JoW, R., *Electrolytes for lithium and lithium-ion batteries*. Springer: New York, 2014; p pages cm; (b) Aurbach, D.; Granot, E., The study of electrolyte solutions based on solvents from the "glyme" family (linear polyethers) for secondary Li battery systems. *Electrochimica Acta* **1997**, *42* (4), 697-718.

20. Whittingham, M. S., Lithium batteries and cathode materials. *Chemical Reviews* **2004**, *104* (10), 4271-4301.

21. (a) Scrosati, B.; Garche, J., Lithium batteries: Status, prospects and future. *Journal of Power Sources* **2010**, *195* (9), 2419-2430; (b) Xiao, Y., Model-Based Virtual Thermal

Sensors for Lithium-Ion Battery in EV Applications. *Ieee Transactions on Industrial Electronics* **2015**, 62 (5), 3112-3122.

22. (a) Sharma, S.; Pollet, B. G., Support materials for PEMFC and DMFC electrocatalysts-A review. *Journal of Power Sources* **2012**, 208, 96-119; (b) Neburchilov, V.; Wang, H. J.; Martin, J. J.; Qu, W., A review on air cathodes for zinc-air fuel cells. *Journal of Power Sources* **2010**, 195 (5), 1271-1291; (c) Papageorgopoulos, D. C.; de Heer, M. P.; Keijzer, M.; Pieterse, J. A. Z.; de Bruijn, F. A., Nonalloyed carbon-supported PtRu catalysts for PEMFC applications. *Journal of the Electrochemical Society* **2004**, 151 (5), A763-A768.

23. Blurton, K. F.; Sammells, A. F., Metal-Air Batteries - Their Status and Potential - Review. *Journal of Power Sources* **1979**, 4 (4), 263-279.

24. (a) Serov, A.; Kwak, C., Review of non-platinum anode catalysts for DMFC and PEMFC application. *Applied Catalysis B-Environmental* **2009**, 90 (3-4), 313-320; (b) Sarakonsri, T.; Suthirakun, S.; Charojrochkul, S.; Vilaithong, T., Preparation of non-noble metal based catalysts supported on carbon for PEMFC cathodes. *Journal of Ceramic Processing Research* **2009**, 10 (5), 589-594.

25. Brankovic, S. R.; Wang, J. X.; Adzic, R. R., Pt submonolayers on Ru nanoparticles - A novel low Pt loading, high CO tolerance fuel cell electrocatalyst. *Electrochemical and Solid State Letters* **2001**, 4 (12), A217-A220.

26. *Electrochemical methods*. J. Wiley: New York, 1986; p xi, 904 p.

27. (a) Reeve, R. W.; Burstein, G. T.; Williams, K. R., Characteristics of a direct methanol fuel cell based on a novel electrode assembly using microporous polymer membranes. *Journal of Power Sources* **2004**, 128 (1), 1-12; (b) Parthasarathy, A.; Srinivasan, S.; Appleby, A. J.; Martin, C. R., Temperature-Dependence of the Electrode-Kinetics of Oxygen Reduction at the Platinum Nafion(R) Interface - a Microelectrode Investigation. *Journal of the Electrochemical Society* **1992**, 139 (9), 2530-2537; (c) Gonzalez-Huerta, R. G.; Chavez-Carvayar, J. A.; Solorza-Feria, O., Electrocatalysis of oxygen reduction on carbon supported Ru-based catalysts in a polymer electrolyte fuel cell. *Journal of Power Sources* **2006**, 153 (1), 11-17.

28. Hoare, J. P., *The electrochemistry of oxygen*. Interscience Publishers: New York,, 1968; p xiv, 423 p.

29. Jaksic, M. M., Volcano plots along the periodic table, their causes and consequences on electrocatalysis for hydrogen electrode reactions. *Journal of New Materials for Electrochemical Systems* **2000**, 3 (2), 153-168.

30. (a) Trasatti, S., Electrocatalysis in the Anodic Evolution of Oxygen and Chlorine.

- Electrochimica Acta* **1984**, 29 (11), 1503-1512; (b) Iwakura, C.; Tada, H.; Tamura, H., Anodic Evolution of Oxygen on Iridium Oxide Electrode. *Denki Kagaku* **1977**, 45 (4), 202-207.
31. (a) Yegnaraman, V.; Basha, C. A.; Rao, G. P., Application of the Accelerated Tafel Plot Technique to Corrosion Kinetics - Role of Double-Layer through Simulation. *Journal of Applied Electrochemistry* **1988**, 18 (6), 869-875; (b) El-Sayed, A. R.; Mohran, H. S.; Abd El-Lateef, H. M., Corrosion Study of Zinc, Nickel, and Zinc-Nickel Alloys in Alkaline Solutions by Tafel Plot and Impedance Techniques. *Metallurgical and Materials Transactions a-Physical Metallurgy and Materials Science* **2012**, 43A (2), 619-632.
32. (a) Wang, H.; Xie, K.; Wang, L. Y.; Han, Y., N-methyl-2-pyrrolidone as a solvent for the non-aqueous electrolyte of rechargeable Li-air batteries. *Journal of Power Sources* **2012**, 219, 263-271; (b) Reichardt, C.; Welton, T., *Solvents and solvent effects in organic chemistry*. John Wiley & Sons: 2011; (c) McCloskey, B. D.; Bethune, D. S.; Shelby, R. M.; Girishkumar, G.; Luntz, A. C., Solvents' Critical Role in Nonaqueous Lithium-Oxygen Battery Electrochemistry. *Journal of Physical Chemistry Letters* **2011**, 2 (10), 1161-1166.
33. (a) Jo, J. Y.; Wu, M.; Nahm, S.; Kang, Y.; Jung, H. K., Discharge/Charge Characteristics of Li-O₂ Batteries Using Noble Metal Catalyst Supported on a Carbon-Free Al-Doped ZnO Cathode. *Ecs Electrochemistry Letters* **2015**, 4 (10), A115-A118; (b) Peng, Z. Q.; Freunberger, S. A.; Chen, Y. H.; Bruce, P. G., A Reversible and Higher-Rate Li-O₂ Battery. *Science* **2012**, 337 (6094), 563-566; (c) Lu, Y. C.; Gasteiger, H. A.; Parent, M. C.; Chiloyan, V.; Shao-Horn, Y., The Influence of Catalysts on Discharge and Charge Voltages of Rechargeable Li-Oxygen Batteries. *Electrochemical and Solid State Letters* **2010**, 13 (6), A69-A72; (d) Li, F. J.; Chan, K. Y.; Yung, H., Carbonization over PFA-protected dispersed platinum: an effective route to synthesize high performance mesoporous-carbon supported Pt electrocatalysts. *Journal of Materials Chemistry* **2011**, 21 (32), 12139-12144.
34. Lu, Y. C.; Xu, Z. C.; Gasteiger, H. A.; Chen, S.; Hamad-Schifferli, K.; Shao-Horn, Y., Platinum-Gold Nanoparticles: A Highly Active Bifunctional Electrocatalyst for Rechargeable Lithium-Air Batteries. *Journal of the American Chemical Society* **2010**, 132 (35), 12170-12171.
35. McCloskey, B. D.; Scheffler, R.; Speidel, A.; Bethune, D. S.; Shelby, R. M.; Luntz, A. C., On the Efficacy of Electrocatalysis in Nonaqueous Li-O₂ Batteries. *Journal of the American Chemical Society* **2011**, 133 (45), 18038-18041.
36. (a) Chen, Z. W.; Higgins, D.; Yu, A. P.; Zhang, L.; Zhang, J. J., A review on non-precious metal electrocatalysts for PEM fuel cells. *Energy & Environmental Science* **2011**, 4 (9), 3167-3192; (b) Lefevre, M.; Dodelet, J. P., Recent Advances in Non-precious Metal

Electrocatalysts for Oxygen Reduction in PEM Fuel Cells. *Tutorials on Electrocatalysis in Low Temperature Fuel Cells* **2012**, 45 (2), 35-44.

37. (a) Debart, A.; Paterson, A. J.; Bao, J.; Bruce, P. G., alpha-MnO(2) nanowires: A catalyst for the O(2) electrode in rechargeable lithium batteries. *Angewandte Chemie-International Edition* **2008**, 47 (24), 4521-4524; (b) Liang, Y. Y.; Wang, H. L.; Zhou, J. G.; Li, Y. G.; Wang, J.; Regier, T.; Dai, H. J., Covalent Hybrid of Spinel Manganese-Cobalt Oxide and Graphene as Advanced Oxygen Reduction Electrocatalysts. *Journal of the American Chemical Society* **2012**, 134 (7), 3517-3523; (c) Wang, H. L.; Yang, Y.; Liang, Y. Y.; Zheng, G. Y.; Li, Y. G.; Cui, Y.; Dai, H. J., Rechargeable Li-O₂ batteries with a covalently coupled MnCo₂O₄-graphene hybrid as an oxygen cathode catalyst. *Energy & Environmental Science* **2012**, 5 (7), 7931-7935; (d) Zhang, L. L.; Zhang, X. B.; Wang, Z. L.; Xu, J. J.; Xu, D.; Wang, L. M., High aspect ratio gamma-MnOOH nanowires for high performance rechargeable nonaqueous lithium-oxygen batteries. *Chemical Communications* **2012**, 48 (61), 7598-7600; (e) Cui, Y. M.; Wen, Z. Y.; Sun, S. J.; Lu, Y.; Jin, J., Mesoporous Co₃O₄ with different porosities as catalysts for the lithium-oxygen cell. *Solid State Ionics* **2012**, 225, 598-603; (f) Lee, D. U.; Kim, B. J.; Chen, Z. W., One-pot synthesis of a mesoporous NiCo₂O₄ nanoplatelet and graphene hybrid and its oxygen reduction and evolution activities as an efficient bi-functional electrocatalyst. *Journal of Materials Chemistry A* **2013**, 1 (15), 4754-4762.
38. Ma, S. C.; Sun, L. Q.; Cong, L. N.; Gao, X. G.; Yao, C.; Guo, X.; Tai, L. H.; Mei, P.; Zeng, Y. P.; Xie, H. M.; Wang, R. S., Multiporous MnCo₂O₄ Microspheres as an Efficient Bifunctional Catalyst for Nonaqueous Li-O₂ Batteries. *Journal of Physical Chemistry C* **2013**, 117 (49), 25890-25897.
39. Debart, A.; Bao, J.; Armstrong, G.; Bruce, P. G., An O₂ cathode for rechargeable lithium batteries: The effect of a catalyst. *Journal of Power Sources* **2007**, 174 (2), 1177-1182.
40. Cheng, F. Y.; Shen, J. A.; Peng, B.; Pan, Y. D.; Tao, Z. L.; Chen, J., Rapid room-temperature synthesis of nanocrystalline spinels as oxygen reduction and evolution electrocatalysts. *Nature Chemistry* **2011**, 3 (1), 79-84.
41. Hummelshoj, J. S.; Blomqvist, J.; Datta, S.; Vegge, T.; Rossmeisl, J.; Thygesen, K. S.; Luntz, A. C.; Jacobsen, K. W.; Nørskov, J. K., Communications: Elementary oxygen electrode reactions in the aprotic Li-air battery. *Journal of Chemical Physics* **2010**, 132 (7).
42. Wu, G.; Mack, N. H.; Gao, W.; Ma, S. G.; Zhong, R. Q.; Han, J. T.; Baldwin, J. K.; Zelenay, P., Nitrogen Doped Graphene-Rich Catalysts Derived from Heteroatom Polymers for Oxygen Reduction in Nonaqueous Lithium-O₂ Battery Cathodes. *Acs Nano* **2012**, 6 (11),

9764-9776.

43. Qin, Y.; Lu, J.; Du, P.; Chen, Z. H.; Ren, Y.; Wu, T. P.; Miller, J. T.; Wen, J. G.; Miller, D. J.; Zhang, Z. C.; Amine, K., In situ fabrication of porous-carbon-supported alpha-MnO₂ nanorods at room temperature: application for rechargeable Li-O₂ batteries. *Energy & Environmental Science* **2013**, *6* (2), 519-531.
44. (a) Laoire, C. O.; Mukerjee, S.; Abraham, K. M.; Plichta, E. J.; Hendrickson, M. A., Elucidating the Mechanism of Oxygen Reduction for Lithium-Air Battery Applications. *Journal of Physical Chemistry C* **2009**, *113* (46), 20127-20134; (b) Beattie, S. D.; Manolescu, D. M.; Blair, S. L., High-Capacity Lithium-Air Cathodes. *Journal of the Electrochemical Society* **2009**, *156* (1), A44-A47.
45. Xiao, J.; Mei, D. H.; Li, X. L.; Xu, W.; Wang, D. Y.; Graff, G. L.; Bennett, W. D.; Nie, Z. M.; Saraf, L. V.; Aksay, I. A.; Liu, J.; Zhang, J. G., Hierarchically Porous Graphene as a Lithium-Air Battery Electrode. *Nano Letters* **2011**, *11* (11), 5071-5078.
46. Wang, Y. G.; Zhou, H. S., To draw an air electrode of a Li-air battery by pencil. *Energy & Environmental Science* **2011**, *4* (5), 1704-1707.
47. (a) Mi, R.; Liu, H.; Wang, H.; Wong, K. W.; Mei, J.; Chen, Y. G.; Lau, W. M.; Yan, H., Effects of nitrogen-doped carbon nanotubes on the discharge performance of Li-air batteries. *Carbon* **2014**, *67*, 744-752; (b) Nie, H. J.; Zhang, H. M.; Zhang, Y. N.; Liu, T.; Li, J.; Lai, Q. Z., Nitrogen enriched mesoporous carbon as a high capacity cathode in lithium-oxygen batteries. *Nanoscale* **2013**, *5* (18), 8484-8487.
48. (a) Girishkumar, G.; McCloskey, B.; Luntz, A. C.; Swanson, S.; Wilcke, W., Lithium - Air Battery: Promise and Challenges. *Journal of Physical Chemistry Letters* **2010**, *1* (14), 2193-2203; (b) Laoire, C. O.; Mukerjee, S.; Plichta, E. J.; Hendrickson, M. A.; Abraham, K. M., Rechargeable Lithium/TEGDME-LiPF₆/O₂ Battery. *Journal of the Electrochemical Society* **2011**, *158* (3), A302-A308.
49. McCloskey, B. D.; Speidel, A.; Scheffler, R.; Miller, D. C.; Viswanathan, V.; Hummelshoj, J. S.; Nørskov, J. K.; Luntz, A. C., Twin Problems of Interfacial Carbonate Formation in Nonaqueous Li-O₂ Batteries. *Journal of Physical Chemistry Letters* **2012**, *3* (8), 997-1001.
50. Xu, W.; Hu, J. Z.; Engelhard, M. H.; Towne, S. A.; Hardy, J. S.; Xiao, J.; Feng, J.; Hu, M. Y.; Zhang, J.; Ding, F.; Gross, M. E.; Zhang, J. G., The stability of organic solvents and carbon electrode in nonaqueous Li-O₂ batteries. *Journal of Power Sources* **2012**, *215*, 240-247.
51. (a) Thotiyl, M. M. O.; Freunberger, S. A.; Peng, Z. Q.; Bruce, P. G., The Carbon

- Electrode in Nonaqueous Li-O₂ Cells. *Journal of the American Chemical Society* **2013**, *135* (1), 494-500; (b) Meng, W.; Liu, S. W.; Wen, L. N.; Qin, X., Carbon microspheres air electrode for rechargeable Li-O₂ batteries. *Rsc Advances* **2015**, *5* (64), 52206-52209.
52. Kim, J.; Lee, J.; Tak, Y., Relationship between carbon corrosion and positive electrode potential in a proton-exchange membrane fuel cell during start/stop operation. *Journal of Power Sources* **2009**, *192* (2), 674-678.
53. (a) Freunberger, S. A.; Chen, Y. H.; Drewett, N. E.; Hardwick, L. J.; Barde, F.; Bruce, P. G., The Lithium-Oxygen Battery with Ether-Based Electrolytes. *Angewandte Chemie-International Edition* **2011**, *50* (37), 8609-8613; (b) Zhang, Z. C.; Lu, J.; Assary, R. S.; Du, P.; Wang, H. H.; Sun, Y. K.; Qin, Y.; Lau, K. C.; Greeley, J.; Redfern, P. C.; Iddir, H.; Curtiss, L. A.; Amine, K., Increased Stability Toward Oxygen Reduction Products for Lithium-Air Batteries with Oligoether-Functionalized Silane Electrolytes. *Journal of Physical Chemistry C* **2011**, *115* (51), 25535-25542.
54. Thotiyl, M. M. O.; Freunberger, S. A.; Peng, Z. Q.; Chen, Y. H.; Liu, Z.; Bruce, P. G., A stable cathode for the aprotic Li-O₂ battery. *Nature Materials* **2013**, *12* (11), 1049-1055.
55. Li, F. J.; Tang, D. M.; Chen, Y.; Golberg, D.; Kitaura, H.; Zhang, T.; Yamada, A.; Zhou, H. S., Ru/ITO: A Carbon-Free Cathode for Nonaqueous Li-O₂ Battery. *Nano Letters* **2013**, *13* (10), 4702-4707.
56. Li, F. J.; Tang, D. M.; Jian, Z. L.; Liu, D. Q.; Golberg, D.; Yamada, A.; Zhou, H. S., Li-O₂ Battery Based on Highly Efficient Sb-Doped Tin Oxide Supported Ru Nanoparticles. *Advanced Materials* **2014**, *26* (27), 4659-+.
57. Kalubarme, R. S.; Jadhav, H. S.; Ngo, D. T.; Park, G. E.; Fisher, J. G.; Choi, Y. I.; Ryu, W. H.; Park, C. J., Simple synthesis of highly catalytic carbon-free MnCo₂O₄@Ni as an oxygen electrode for rechargeable Li-O₂ batteries with long-term stability. *Scientific Reports* **2015**, *5*.
58. (a) Sieminski, D., Recent advances in rechargeable zinc-air battery technology. *Twelfth Annual Battery Conference on Applications and Advances* **1997**, 171-180; (b) Chodos, S. M.; Katsouli, E.; Rosansky, M. G., A High Energy Density Zinc/Oxygen Battery System. *Journal of Spacecraft and Rockets* **1967**, *4* (5), 680-684; (c) Lan, C. J.; Chin, T. S.; Lin, P. H.; Perng, T. P., Zn-Al alloy as a new anode-metal of a zinc-air battery. *Journal of New Materials for Electrochemical Systems* **2006**, *9* (1), 27-32.
59. (a) Rao, C. S.; Gunasekaran, G., Cobalt-Lead-Manganese oxides combined cathode catalyst for air electrode in Zinc -air battery. *Electrochimica Acta* **2015**, *176*, 649-656; (b)

- Chen, Z.; Yu, A. P.; Ahmed, R.; Wang, H. J.; Li, H.; Chen, Z. W., Manganese dioxide nanotube and nitrogen-doped carbon nanotube based composite bifunctional catalyst for rechargeable zinc-air battery. *Electrochimica Acta* **2012**, *69*, 295-300; (c) Wang, X. Y.; Sebastian, P. J.; Smit, M. A.; Yang, H. P.; Gamboa, S. A., Studies on the oxygen reduction catalyst for zinc-air battery electrode. *Journal of Power Sources* **2003**, *124* (1), 278-284.
60. Lee, D. U.; Park, H. W.; Park, M. G.; Ismayilov, V.; Chen, Z. W., Synergistic Bifunctional Catalyst Design based on Perovskite Oxide Nanoparticles and Intertwined Carbon Nanotubes for Rechargeable Zinc-Air Battery Applications. *Acs Applied Materials & Interfaces* **2015**, *7* (1), 902-910.
61. Hilder, M.; Winther-Jensen, B.; Clark, N. B., The effect of binder and electrolyte on the performance of thin zinc-air battery. *Electrochimica Acta* **2012**, *69*, 308-314.
62. Zhu, W. H.; Poole, B. A.; Cahela, D. R.; Tatarchuk, B. J., New structures of thin air cathodes for zinc-air batteries. *Journal of Applied Electrochemistry* **2003**, *33* (1), 29-36.
63. (a) Cheng, F. Y.; Chen, J., Metal-air batteries: from oxygen reduction electrochemistry to cathode catalysts. *Chemical Society Reviews* **2012**, *41* (6), 2172-2192; (b) Spendelow, J. S.; Wieckowski, A., Electrocatalysis of oxygen reduction and small alcohol oxidation in alkaline media. *Physical Chemistry Chemical Physics* **2007**, *9* (21), 2654-2675.
64. Kim, H.; Jeong, G.; Kim, Y. U.; Kim, J. H.; Park, C. M.; Sohn, H. J., Metallic anodes for next generation secondary batteries. *Chemical Society Reviews* **2013**, *42* (23), 9011-9034.
65. (a) Foller, P. C., Improved Slurry Zinc Air Systems as Batteries for Urban Vehicle Propulsion. *Journal of Applied Electrochemistry* **1986**, *16* (4), 527-543; (b) Thacker, R., Use of Palladium-Catalyzed Air Cathodes in a Secondary Zinc-Air Cell. *Energy Conversion* **1972**, *12* (1), 17-&.
66. (a) Gorlin, Y.; Chung, C. J.; Nordlund, D.; Clemens, B. M.; Jaramillo, T. F., Mn₃O₄ Supported on Glassy Carbon: An Active Non-Precious Metal Catalyst for the Oxygen Reduction Reaction. *Acs Catalysis* **2012**, *2* (12), 2687-2694; (b) Cheng, F. Y.; Zhang, T. R.; Zhang, Y.; Du, J.; Han, X. P.; Chen, J., Enhancing Electrocatalytic Oxygen Reduction on MnO₂ with Vacancies. *Angewandte Chemie-International Edition* **2013**, *52* (9), 2474-2477.
67. (a) Gong, K. P.; Du, F.; Xia, Z. H.; Durstock, M.; Dai, L. M., Nitrogen-Doped Carbon Nanotube Arrays with High Electrocatalytic Activity for Oxygen Reduction. *Science* **2009**, *323* (5915), 760-764; (b) Liu, R. L.; Wu, D. Q.; Feng, X. L.; Mullen, K., Nitrogen-Doped Ordered Mesoporous Graphitic Arrays with High Electrocatalytic Activity for Oxygen Reduction. *Angewandte Chemie-International Edition* **2010**, *49* (14), 2565-2569; (c) Geng, D. S.; Chen, Y.; Chen, Y. G.; Li, Y. L.; Li, R. Y.; Sun, X. L.; Ye, S. Y.; Knights, S., High

- oxygen-reduction activity and durability of nitrogen-doped graphene. *Energy & Environmental Science* **2011**, *4* (3), 760-764; (d) Du, R.; Zhang, N.; Zhu, J. H.; Wang, Y.; Xu, C. Y.; Hu, Y.; Mao, N. N.; Xu, H.; Duan, W. J.; Zhuang, L.; Qu, L. T.; Hou, Y. L.; Zhang, J., Nitrogen-Doped Carbon Nanotube Aerogels for High-Performance ORR Catalysts. *Small* **2015**, *11* (32), 3903-3908; (e) Li, J. S.; Li, S. L.; Tang, Y. J.; Han, M.; Dai, Z. H.; Bao, J. C.; Lan, Y. Q., Nitrogen-doped Fe/Fe₃C@graphitic layer/carbon nanotube hybrids derived from MOFs: efficient bifunctional electrocatalysts for ORR and OER. *Chemical Communications* **2015**, *51* (13), 2710-2713; (f) Shrestha, S.; Asheghi, S.; Timbro, J.; Mustain, W. E., Temperature controlled surface chemistry of nitrogen-doped mesoporous carbon and its influence on Pt ORR activity. *Applied Catalysis a-General* **2013**, *464*, 233-242.
68. Zhou, M.; Chan, K. Y., Highly active iron and nitrogen doped carbon catalyst with hollow core mesoporous shell structure toward oxygen reduction reaction (ORR). *Abstracts of Papers of the American Chemical Society* **2014**, 248.
69. (a) Daems, N.; Sheng, X.; Vankelecom, I. F. J.; Pescarmona, P. P., Metal-free doped carbon materials as electrocatalysts for the oxygen reduction reaction. *Journal of Materials Chemistry A* **2014**, *2* (12), 4085-4110; (b) Liu, Y. L.; Shi, C. X.; Xu, X. Y.; Sun, P. C.; Chen, T. H., Nitrogen-doped hierarchically porous carbon spheres as efficient metal-free electrocatalysts for an oxygen reduction reaction. *Journal of Power Sources* **2015**, *283*, 389-396.
70. Zhang, X. G., Fibrous zinc anodes for high power batteries. *Journal of Power Sources* **2006**, *163* (1), 591-597.
71. (a) Ma, H.; Li, C. S.; Su, Y.; Chen, J., Studies on the vapour-transport synthesis and electrochemical properties of zinc micro-, meso- and nanoscale structures. *Journal of Materials Chemistry* **2007**, *17* (7), 684-691; (b) Yang, C. C.; Lin, S. J., Improvement of high-rate capability of alkaline Zn-MnO₂ battery. *Journal of Power Sources* **2002**, *112* (1), 174-183.
72. See, D. M.; White, R. E., Temperature and concentration dependence of the specific conductivity of concentrated solutions of potassium hydroxide. *Journal of Chemical and Engineering Data* **1997**, *42* (6), 1266-1268.
73. Li, Y. G.; Dai, H. J., Recent advances in zinc-air batteries. *Chemical Society Reviews* **2014**, *43* (15), 5257-5275.
74. Lee, J. S.; Kim, S. T.; Cao, R.; Choi, N. S.; Liu, M.; Lee, K. T.; Cho, J., Metal-Air Batteries with High Energy Density: Li-Air versus Zn-Air. *Advanced Energy Materials* **2011**, *1* (1), 34-50.

75. (a) Albertus, P.; Girishkumar, G.; McCloskey, B.; Sanchez-Carrera, R. S.; Kozinsky, B.; Christensen, J.; Luntz, A. C., Identifying Capacity Limitations in the Li/Oxygen Battery Using Experiments and Modeling. *Journal of the Electrochemical Society* **2011**, *158* (3), A343-A351; (b) Peng, Z. Q.; Freunberger, S. A.; Chen, Y. H.; Bruce, P. G., Oxygen reactions in the non-aqueous rechargeable Li-O₂ battery. *Abstracts of Papers of the American Chemical Society* **2012**, *243*; (c) Zhu, J. Z.; Ren, X. D.; Liu, J. J.; Zhang, W. Q.; Wen, Z. Y., Unraveling the Catalytic Mechanism of Co₃O₄ for the Oxygen Evolution Reaction in a Li-O₂ Battery. *Acs Catalysis* **2015**, *5* (1), 73-81.
76. Abraham, K. M.; Jiang, Z., A polymer electrolyte-based rechargeable lithium/oxygen battery. *Journal of the Electrochemical Society* **1996**, *143* (1), 1-5.
77. Laoire, C. O.; Mukerjee, S.; Abraham, K. M.; Plichta, E. J.; Hendrickson, M. A., Influence of Nonaqueous Solvents on the Electrochemistry of Oxygen in the Rechargeable Lithium-Air Battery. *Journal of Physical Chemistry C* **2010**, *114* (19), 9178-9186.
78. (a) Shao, Y. Y.; Park, S.; Xiao, J.; Zhang, J. G.; Wang, Y.; Liu, J., Electrocatalysts for Nonaqueous Lithium-Air Batteries: Status, Challenges, and Perspective. *Acs Catalysis* **2012**, *2* (5), 844-857; (b) Cao, R.; Lee, J. S.; Liu, M. L.; Cho, J., Recent Progress in Non-Precious Catalysts for Metal-Air Batteries. *Advanced Energy Materials* **2012**, *2* (7), 816-829.
79. (a) Marinaro, M.; Riek, U.; Moorthy, S. K. E.; Bernhard, J.; Kaiser, U.; Wohlfahrt-Mehrens, M.; Jorissen, L., Au-coated carbon cathodes for improved oxygen reduction and evolution kinetics in aprotic Li-O₂ batteries. *Electrochemistry Communications* **2013**, *37*, 53-56; (b) Zhou, W.; Li, J.; Nie, H. J.; Zhang, Y. N.; Xi, X. L.; Zhang, H. M., Carbon Electrode for Nonaqueous Li-O₂ Battery: the Influence of Surface Oxygen Species. *Electrochimica Acta* **2014**, *138*, 410-416; (c) Zhao, G. Y.; Zhang, L.; Pan, T.; Sun, K. N., Preparation of NiO/multiwalled carbon nanotube nanocomposite for use as the oxygen cathode catalyst in rechargeable Li-O₂ batteries. *Journal of Solid State Electrochemistry* **2013**, *17* (6), 1759-1764.
80. (a) Zhang, S. S.; Foster, D.; Read, J., Discharge characteristic of a non-aqueous electrolyte Li/O₂ battery. *Journal of Power Sources* **2010**, *195* (4), 1235-1240; (b) Mirzaeian, M.; Hall, P. J., Preparation of controlled porosity carbon aerogels for energy storage in rechargeable lithium oxygen batteries. *Electrochimica Acta* **2009**, *54* (28), 7444-7451; (c) Yang, X. H.; He, P.; Xia, Y. Y., Preparation of mesocellular carbon foam and its application for lithium/oxygen battery. *Electrochemistry Communications* **2009**, *11* (6), 1127-1130.
81. (a) Xiao, J.; Wang, D. H.; Xu, W.; Wang, D. Y.; Williford, R. E.; Liu, J.; Zhang, J. G., Optimization of Air Electrode for Li/Air Batteries. *Journal of the Electrochemical Society*

- 2010**, 157 (4), A487-A492; (b) Younesi, S. R.; Urbonaite, S.; Bjorefors, F.; Edstrom, K., Influence of the cathode porosity on the discharge performance of the lithium-oxygen battery. *Journal of Power Sources* **2011**, 196 (22), 9835-9838.
82. Xu, K., Nonaqueous liquid electrolytes for lithium-based rechargeable batteries. *Chemical Reviews* **2004**, 104 (10), 4303-4417.
83. (a) Li, F.; Tang, D.-M.; Chen, Y.; Golberg, D.; Kitaura, H.; Zhang, T.; Yamada, A.; Zhou, H., Ru/ITO: A Carbon-Free Cathode for Nonaqueous Li-O₂ Battery. *Nano letters* **2013**, 13 (10), 4702-4707; (b) Gallant, B. M.; Mitchell, R. R.; Kwabi, D. G.; Zhou, J. G.; Zuin, L.; Thompson, C. V.; Shao-Horn, Y., Chemical and Morphological Changes of Li-O₂ Battery Electrodes upon Cycling. *J Phys Chem C* **2012**, 116 (39), 20800-20805.
84. (a) Li, F. J.; Tang, D. M.; Zhang, T.; Liao, K. M.; He, P.; Golberg, D.; Yamada, A.; Zhou, H. S., Superior Performance of a Li-O₂ Battery with Metallic RuO₂ Hollow Spheres as the Carbon-Free Cathode. *Advanced Energy Materials* **2015**, 5 (13); (b) Zhao, G. Y.; Lv, J. X.; Xu, Z. M.; Zhang, L.; Sun, K. N., Carbon and binder free rechargeable Li-O₂ battery cathode with Pt/Co₃O₄ flake arrays as catalyst. *Journal of Power Sources* **2014**, 248, 1270-1274.
85. (a) Arruda, T. M.; Kumar, A.; Kalinin, S. V.; Jesse, S., The partially reversible formation of Li-metal particles on a solid Li electrolyte: applications toward nanobatteries. *Nanotechnology* **2012**, 23 (32); (b) Shimonishi, Y.; Zhang, T.; Imanishi, N.; Im, D.; Lee, D. J.; Hirano, A.; Takeda, Y.; Yamamoto, O.; Sammes, N., A study on lithium/air secondary batteries-Stability of the NASICON-type lithium ion conducting solid electrolyte in alkaline aqueous solutions. *Journal of Power Sources* **2011**, 196 (11), 5128-5132; (c) McCloskey, B. D.; Scheffler, R.; Speidel, A.; Girishkumar, G.; Luntz, A. C., On the Mechanism of Nonaqueous Li-O₂ Electrochemistry on C and Its Kinetic Overpotentials: Some Implications for Li-Air Batteries. *Journal of Physical Chemistry C* **2012**, 116 (45), 23897-23905.
86. Younesi, R.; Urbonaite, S.; Edstrom, K.; Hahlin, M., The Cathode Surface Composition of a Cycled Li-O₂ Battery: A Photoelectron Spectroscopy Study. *Journal of Physical Chemistry C* **2012**, 116 (39), 20673-20680.
87. Xu, W.; Xu, K.; Viswanathan, V. V.; Towne, S. A.; Hardy, J. S.; Xiao, J.; Hu, D. H.; Wang, D. Y.; Zhang, J. G., Reaction mechanisms for the limited reversibility of Li-O₂ chemistry in organic carbonate electrolytes. *Journal of Power Sources* **2011**, 196 (22), 9631-9639.
88. Li, Y. L.; Wang, J. J.; Li, X. F.; Geng, D. S.; Banis, M. N.; Tang, Y. J.; Wang, D. N.;

Li, R. Y.; Sham, T. K.; Sun, X. L., Discharge product morphology and increased charge performance of lithium-oxygen batteries with graphene nanosheet electrodes: the effect of sulphur doping. *Journal of Materials Chemistry* **2012**, *22* (38), 20170-20174.

89. (a) Wang, H.; Xie, K., Investigation of oxygen reduction chemistry in ether and carbonate based electrolytes for Li-O₂ batteries. *Electrochimica Acta* **2012**, *64*, 29-34; (b) Younesi, R.; Hahlin, M.; Treskow, M.; Scheers, J.; Johansson, P.; Edstrom, K., Ether Based Electrolyte, LiB(CN)₄ Salt and Binder Degradation in the Li-O₂ Battery Studied by Hard X-ray Photoelectron Spectroscopy (HAXPES). *Journal of Physical Chemistry C* **2012**, *116* (35), 18597-18604.

90. (a) Veith, G. M.; Nanda, J.; Delmau, L. H.; Dudney, N. J., Influence of Lithium Salts on the Discharge Chemistry of Li-Air Cells. *Journal of Physical Chemistry Letters* **2012**, *3* (10), 1242-1247; (b) Oh, S. H.; Yim, T.; Pomerantseva, E.; Nazar, L. F., Decomposition Reaction of Lithium Bis(oxalato)borate in the Rechargeable Lithium-Oxygen Cell. *Electrochemical and Solid State Letters* **2011**, *14* (12), A185-A188.

91. (a) Yang, X.-h.; Xia, Y.-y., The effect of oxygen pressures on the electrochemical profile of lithium/oxygen battery. *Journal of Solid State Electrochemistry* **2009**, *14* (1), 109-114; (b) Freunberger, S. A.; Chen, Y. H.; Peng, Z. Q.; Griffin, J. M.; Hardwick, L. J.; Barde, F.; Novak, P.; Bruce, P. G., Reactions in the Rechargeable Lithium-O₂ Battery with Alkyl Carbonate Electrolytes. *Journal of the American Chemical Society* **2011**, *133* (20), 8040-8047; (c) Nasybulin, E.; Xu, W.; Engelhard, M. H.; Nie, Z. M.; Burton, S. D.; Cosimbescu, L.; Gross, M. E.; Zhang, J. G., Effects of Electrolyte Salts on the Performance of Li-O₂ Batteries. *Journal of Physical Chemistry C* **2013**, *117* (6), 2635-2645; (d) Mitchell, R. R.; Gallant, B. M.; Thompson, C. V.; Shao-Horn, Y., All-carbon-nanofiber electrodes for high-energy rechargeable Li-O₂ batteries. *Energy & Environmental Science* **2011**, *4* (8), 2952.

92. (a) Oh, S. H.; Black, R.; Pomerantseva, E.; Lee, J. H.; Nazar, L. F., Synthesis of a metallic mesoporous pyrochlore as a catalyst for lithium-O₂ batteries. *Nat Chem* **2012**, *4* (12), 1004-1010; (b) Jung, H. G.; Hassoun, J.; Park, J. B.; Sun, Y. K.; Scrosati, B., An improved high-performance lithium-air battery. *Nat Chem* **2012**, *4* (7), 579-585.

93. (a) Mizuno, F.; Nakanishi, S.; Kotani, Y.; Yokoishi, S.; Iba, H., Rechargeable Li-Air Batteries with Carbonate-Based Liquid Electrolytes. *Electrochemistry* **2010**, *78* (5), 403-405; (b) Yang, W.; Salim, J.; Ma, C.; Ma, Z. H.; Sun, C. W.; Li, J. Q.; Chen, L. Q.; Kim, Y., Flowerlike Co₃O₄ microspheres loaded with copper nanoparticle as an efficient bifunctional catalyst for lithium-air batteries. *Electrochemistry Communications* **2013**, *28*, 13-16; (c) Jung, K. N.; Riaz, A.; Lee, S. B.; Lim, T. H.; Park, S. J.; Song, R. H.; Yoon, S.; Shin, K. H.; Lee, J.

W., Urchin-like alpha-MnO₂ decorated with Au and Pd as a bi-functional catalyst for rechargeable lithium-oxygen batteries. *Journal of Power Sources* **2013**, *244*, 328-335; (d) Yilmaz, E.; Yogi, C.; Yamanaka, K.; Ohta, T.; Byon, H. R., Promoting Formation of Noncrystalline Li₂O₂ in the Li-O₂ Battery with RuO₂ Nanoparticles. *Nano letters* **2013**, *13* (10), 4679-84.

94. (a) Oh, S. H.; Nazar, L. F., Oxide Catalysts for Rechargeable High-Capacity Li-O₂ Batteries. *Advanced Energy Materials* **2012**, *2* (7), 903-910; (b) Black, R.; Lee, J. H.; Adams, B.; Mims, C. A.; Nazar, L. F., The Role of Catalysts and Peroxide Oxidation in Lithium-Oxygen Batteries. *Angew Chem Int Edit* **2013**, *52* (1), 392-396; (c) Etacheri, V.; Sharon, D.; Garsuch, A.; Afri, M.; Frimer, A. A.; Aurbach, D., Hierarchical activated carbon microfiber (ACM) electrodes for rechargeable Li-O₂ batteries. *J Mater Chem A* **2013**, *1* (16), 5021-5030; (d) Lim, H. D.; Park, K. Y.; Song, H.; Jang, E. Y.; Gwon, H.; Kim, J.; Kim, Y. H.; Lima, M. D.; Robles, R. O.; Lepro, X.; Baughman, R. H.; Kang, K., Enhanced Power and Rechargeability of a LiO₂ Battery Based on a Hierarchical-Fibril CNT Electrode. *Advanced Materials* **2013**, *25* (9), 1348-1352; (e) Yang, Y.; Shi, M.; Zhou, Q. F.; Li, Y. S.; Fu, Z. W., Platinum nanoparticle-graphene hybrids synthesized by liquid phase pulsed laser ablation as cathode catalysts for Li-air batteries. *Electrochemistry Communications* **2012**, *20*, 11-14; (f) Shui, J. L.; Du, F.; Xue, C. M.; Li, Q.; Dai, L. M., Vertically Aligned N-Doped Coral-like Carbon Fiber Arrays as Efficient Air Electrodes for High-Performance Nonaqueous Li-O₂ Batteries. *Acs Nano* **2014**, *8* (3), 3015-3022.

95. Lim, H. D.; Song, H.; Kim, J.; Gwon, H.; Bae, Y.; Park, K. Y.; Hong, J.; Kim, H.; Kim, T.; Kim, Y. H.; Lepro, X.; Ovalle-Robles, R.; Baughman, R. H.; Kang, K., Superior Rechargeability and Efficiency of Lithium-Oxygen Batteries: Hierarchical Air Electrode Architecture Combined with a Soluble Catalyst. *Angew Chem Int Edit* **2014**, *53* (15), 3926-3931.

96. Black, R.; Oh, S. H.; Lee, J. H.; Yim, T.; Adams, B.; Nazar, L. F., Screening for superoxide reactivity in Li-O₂ batteries: effect on Li₂O₂/LiOH crystallization. *Journal of the American Chemical Society* **2012**, *134* (6), 2902-5.

97. Younesi, R.; Hahlin, M.; Bjorefors, F.; Johansson, P.; Edstrom, K., Li-O₂ Battery Degradation by Lithium Peroxide (Li₂O₂): A Model Study. *Chem Mater* **2013**, *25* (1), 77-84.

98. Lu, Y. C.; Gallant, B. M.; Kwabi, D. G.; Harding, J. R.; Mitchell, R. R.; Whittingham, M. S.; Shao-Horn, Y., Lithium-oxygen batteries: bridging mechanistic understanding and battery performance. *Energy & Environmental Science* **2013**, *6* (3), 750-768.

99. (a) Peng, Z.; Freunberger, S. A.; Chen, Y.; Bruce, P. G., A reversible and higher-rate

- Li-O₂ battery. *Science* **2012**, 337 (6094), 563-6; (b) Ottakam Thotiyl, M. M.; Freunberger, S. A.; Peng, Z.; Chen, Y.; Liu, Z.; Bruce, P. G., A stable cathode for the aprotic Li-O₂ battery. *Nat Mater* **2013**, 12 (11), 1050-6.
100. (a) Lu, Y.-C.; Gasteiger, H. A.; Shao-Horn, Y., Method Development to Evaluate the Oxygen Reduction Activity of High-Surface-Area Catalysts for Li-Air Batteries. *Electrochemical and Solid-State Letters* **2011**, 14 (5), A70; (b) Lu, Y. C.; Gasteiger, H. A.; Shao-Horn, Y., Catalytic Activity Trends of Oxygen Reduction Reaction for Nonaqueous Li-Air Batteries. *Journal of the American Chemical Society* **2011**, 133 (47), 19048-19051.
101. (a) Zhang, D.; Fu, Z. H.; Wei, Z.; Huang, T.; Yu, A. S., Polarization of Oxygen Electrode in Rechargeable Lithium Oxygen Batteries. *Journal of the Electrochemical Society* **2010**, 157 (3), A362-A365; (b) Beattie, S. D.; Manolescu, D. M.; Blair, S. L., High-Capacity Lithium–Air Cathodes. *Journal of The Electrochemical Society* **2009**, 156 (1), A44; (c) Cui, Y.; Wen, Z.; Liu, Y., A free-standing-type design for cathodes of rechargeable Li–O₂ batteries. *Energy & Environmental Science* **2011**, 4 (11), 4727.
102. Xu, J. J.; Wang, Z. L.; Xu, D.; Zhang, L. L.; Zhang, X. B., Tailoring deposition and morphology of discharge products towards high-rate and long-life lithium-oxygen batteries. *Nat Commun* **2013**, 4.
103. Shui, J. L.; Okasinski, J. S.; Kenesei, P.; Dobbs, H. A.; Zhao, D.; Almer, J. D.; Liu, D. J., Reversibility of anodic lithium in rechargeable lithium-oxygen batteries. *Nat Commun* **2013**, 4.
104. Aurbach, D.; Daroux, M.; Faguy, P.; Yeager, E., The Electrochemistry of Noble-Metal Electrodes in Aprotic Organic-Solvents Containing Lithium-Salts. *Journal of Electroanalytical Chemistry* **1991**, 297 (1), 225-244.
105. Hummelshoj, J. S.; Luntz, A. C.; Nørskov, J. K., Theoretical evidence for low kinetic overpotentials in Li-O₂ electrochemistry. *J Chem Phys* **2013**, 138 (3).
106. Chen, Y.; Freunberger, S. A.; Peng, Z.; Barde, F.; Bruce, P. G., Li-O₂ Battery with a Dimethylformamide Electrolyte. *Journal of the American Chemical Society* **2012**, 134 (18), 7952-7957.
107. (a) Kim, S. T.; Choi, N. S.; Park, S.; Cho, J., Optimization of Carbon- and Binder-Free Au Nanoparticle-Coated Ni Nanowire Electrodes for Lithium-Oxygen Batteries. *Adv Energy Mater* **2015**, 5 (3); (b) Riaz, A.; Jung, K. N.; Chang, W.; Lee, S. B.; Lim, T. H.; Park, S. J.; Song, R. H.; Yoon, S.; Shin, K. H.; Lee, J. W., Carbon-free cobalt oxide cathodes with tunable nanoarchitectures for rechargeable lithium-oxygen batteries. *Chem Commun* **2013**, 49 (53), 5984-5986.

108. (a) Singh, P.; Buttry, D. A., Comparison of Oxygen Reduction Reaction at Silver Nanoparticles and Polycrystalline Silver Electrodes in Alkaline Solution. *J Phys Chem C* **2012**, *116* (19), 10656-10663; (b) Chatenet, M.; Genies-Bultel, L.; Aurousseau, M.; Durand, R.; Andolfatto, F., Oxygen reduction on silver catalysts in solutions containing various concentrations of sodium hydroxide - comparison with platinum. *J Appl Electrochem* **2002**, *32* (10), 1131-1140; (c) Blizanac, B. B.; Ross, P. N.; Markovic, N. M., Oxygen reduction on silver low-index single-crystal surfaces in alkaline solution: Rotating ring Disk(Ag(hkl)) studies. *J Phys Chem B* **2006**, *110* (10), 4735-4741; (d) Kostowskyj, M. A.; Gilliam, R. J.; Kirk, D. W.; Thorpe, S. J., Silver nanowire catalysts for alkaline fuel cells. *Int J Hydrogen Energ* **2008**, *33* (20), 5773-5778; (e) Davis, D. J.; Raji, A. R. O.; Lambert, T. N.; Vigil, J. A.; Li, L.; Nan, K. W.; Tour, J. M., Silver-Graphene Nanoribbon Composite Catalyst for the Oxygen Reduction Reaction in Alkaline Electrolyte. *Electroanal* **2014**, *26* (1), 164-170; (f) Matula, R. A., Electrical-Resistivity of Copper, Gold, Palladium, and Silver. *J Phys Chem Ref Data* **1979**, *8* (4), 1147-1298.
109. (a) Tammeveski, L.; Erikson, H.; Sarapuu, A.; Kozlova, J.; Ritslaid, P.; Sammelselg, V.; Tammeveski, K., Electrocatalytic oxygen reduction on silver nanoparticle/multi-walled carbon nanotube modified glassy carbon electrodes in alkaline solution. *Electrochem Commun* **2012**, *20*, 15-18; (b) Vinodh, R.; Sangeetha, D., Carbon supported silver (Ag/C) electrocatalysts for alkaline membrane fuel cells. *J Mater Sci* **2012**, *47* (2), 852-859; (c) Braam, K. T.; Volkman, S. K.; Subramanian, V., Characterization and optimization of a printed, primary silver-zinc battery. *J Power Sources* **2012**, *199*, 367-372.
110. (a) Kumar, S.; Selvaraj, C.; Scanlon, L. G.; Munichandraiah, N., Ag nanoparticles-anchored reduced graphene oxide catalyst for oxygen electrode reaction in aqueous electrolytes and also a non-aqueous electrolyte for Li-O₂ cells. *Physical Chemistry Chemical Physics* **2014**, *16* (41), 22830-22840; (b) Lu, M. H.; Qu, J. L.; Yao, Q. F.; Xu, C. H.; Zhan, Y.; Xie, J. P.; Lee, J. Y., Exploring Metal Nanoclusters for Lithium-Oxygen Batteries. *Acs Applied Materials & Interfaces* **2015**, *7* (9), 5488-5496.
111. (a) Black, R.; Oh, S. H.; Lee, J. H.; Yim, T.; Adams, B.; Nazar, L. F., Screening for Superoxide Reactivity in Li-O₂ Batteries: Effect on Li₂O₂/LiOH Crystallization. *J Am Chem Soc* **2012**, *134* (6), 2902-2905; (b) McCloskey, B. D.; Bethune, D. S.; Shelby, R. M.; Mori, T.; Scheffler, R.; Speidel, A.; Sherwood, M.; Luntz, A. C., Limitations in Rechargeability of Li-O₂ Batteries and Possible Origins. *J Phys Chem Lett* **2012**, *3* (20), 3043-3047.
112. Zhu, D.; Zhang, L.; Song, M.; Wang, X.; Mei, J.; Lau, L. W. M.; Chen, Y. G., Solvent

autoxidation, electrolyte decomposition, and performance deterioration of the aprotic Li-O-2 battery. *Journal of Solid State Electrochemistry* **2013**, *17* (11), 2865-2870.

113. Aurbach, D.; Pollak, E.; Elazari, R.; Salitra, G.; Kelley, C. S.; Affinito, J., On the Surface Chemical Aspects of Very High Energy Density, Rechargeable Li-Sulfur Batteries. *Journal of the Electrochemical Society* **2009**, *156* (8), A694-A702.

114. Younesi, R.; Norby, P.; Vegge, T., A New Look at the Stability of Dimethyl Sulfoxide and Acetonitrile in Li-O-2 Batteries. *Ecs Electrochem Lett* **2014**, *3* (3), A15-A18.

115. Sharon, D.; Afri, M.; Noked, M.; Garsuch, A.; Frimer, A. A.; Aurbach, D., Oxidation of Dimethyl Sulfoxide Solutions by Electrochemical Reduction of Oxygen. *Journal of Physical Chemistry Letters* **2013**, *4* (18), 3115-3119.

116. Marinaro, M.; Balasubramanian, P.; Gucciardi, E.; Theil, S.; Jorissen, L.; Wohlfahrt-Mehrens, M., Importance of Reaction Kinetics and Oxygen Crossover in aprotic Li-O-2 Batteries Based on a Dimethyl Sulfoxide Electrolyte. *Chemsuschem* **2015**, *8* (18), 3139-3145.

117. McCloskey, B. D.; Valery, A.; Luntz, A. C.; Gowda, S. R.; Wallraff, G. M.; Garcia, J. M.; Mori, T.; Krupp, L. E., Combining Accurate O-2 and Li2O2 Assays to Separate Discharge and Charge Stability Limitations in Nonaqueous Li-O-2 Batteries. *J Phys Chem Lett* **2013**, *4* (17), 2989-2993.

118. (a) Sinha, A.; Thomson, M. J., The chemical structures of opposed flow diffusion flames of C3 oxygenated hydrocarbons (isopropanol, dimethoxy methane, and dimethyl carbonate) and their mixtures. *Combustion and Flame* **2004**, *136* (4), 548-556; (b) Atkinson, R., Atmospheric reactions of alkoxy and beta-hydroxyalkoxy radicals. *International Journal of Chemical Kinetics* **1997**, *29* (2), 99-111.

Acknowledgement

First of all, I would like to express my appreciation to Prof. Jaephil Cho about all his supports and sincere guidances. He always try to guide me to right way as an advisor and as an elder. Because of him, I can have an objective sight not only to the academic thing, but also to an attitude for my life. And second of all, I would like to give my sincere respect to Prof. Soojin Park and Prof. Nam-Soon Choi. They have given me many advices and counsel when I stuck in reverse. Without their helps, I can't complete this thesis. Thirdly, I would say thank you all to our group members. Lastly, I would like to express my thoughts about "how to live" in this writing. This will be a little letter to me. I think life is a journey to find happiness. During my Master's and Ph.D period, I have experienced so much including a macular hole surgery at Jun. 2. 2011. After that I realized I can do anything because basically I am an owner of my life. And integrating the whole choices I have made make my current status so I can do everything with my responsibility. After all, everything will be changed naturally in everywhere. But one thing is never changed that my love for my family.

I loved them all, I am, and I will.

I dedicated this humble and miserable thesis to

To all the people who struggle for the equality of opportunity of everyone.

To all the people who try to make a better world.

To those people who I love.